INFORMATION TO USERS

Functional Stabilization of Unstable Systems

by

Patrick S. Foo

A Dissertation Submitted to the Faculty

of the Charles E. Schmidt College of Science

in Partial Fulfillment of the Requirements for the Degree of

Doctor of Philosophy

Florida Atlantic University

Boca Raton, Florida

December 2000

UMI Number: 9988027

Copyright 2000 by
Foo, Patrick Stephen

All rights reserved.

UMI®

UMI Microform 9988027

Copyright 2001 by Bell & Howell Information and Learning Company.
All rights reserved. This microform edition is protected against
unauthorized copying under Title 17, United States Code.

Functional Stabilization of Unstable Systems

by
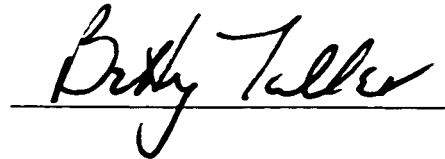
Patrick S. Foo

This dissertation was prepared under the direction of the candidate's dissertation advisor, Dr. J. A. Scott Kelso, Program in Complex Systems and Brain Sciences, and has been approved by the members of his supervisory committee. It was submitted to the faculty of The Charles E. Schmidt College of Science and was accepted in partial fulfillment of the requirements for the degree of Doctor of Philosophy.

SUPERVISORY COMMITTEE

_____
Dissertation Advisor.

_____

_____
Chairperson, Program in Complex
Systems and Brain Sciences

_____
Dean, Charles E. Schmidt College of Science

_____
Dean of Graduate Studies and Research

_____

_____

8 Sept 2000
_____
Date

iii

iv

help in the Coordination Lab, "the lung", Hopsing's wilderness laundry, keeping the Panzer organized, and now, Lawn Boy II. To Wilson Truccolo, who is now climbing the Grandest of Canyons, I say check your pack for extraneous rocks. Good luck to the California couple Fred and Priscilla Carver who braved the pygmy forest. Taube, I'm sending you a set of auto jacks in case you need to bring Gwen back down to Earth. My best wishes to Tim and Kaleigh and Connie, who are close to the finish line. As I write this I know the late night shift is probably in full swing at the Center: Collins, Chris, Cheng, Dinesh, and Gautam are probably cranking up the heat and getting it done right now. A big hello to my Triathlon buds: Viktor, KJ, Rob, Jeff, Pris, Ed, Kari and Susan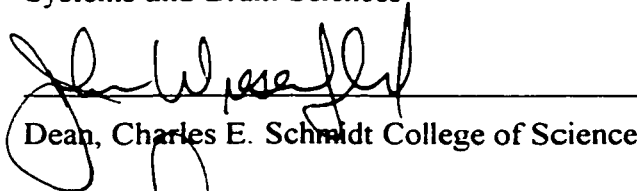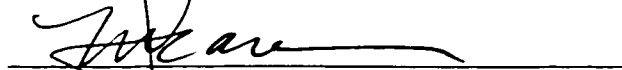. Good luck to Subterranean-Tim, Shelrie, and Debbie and the rest of the yellow lines. If I can do it, so can you! I wish long life, prosperity, and fertility to Dr. Chen and Mrs. Chen, who endured 5 years of Pat Foo and survived! I wish a big, Kmart hello to Tom Ditzinger, the nicest guy I have ever met. Thank you Armin "T-shirt skiing" Fuchs, for your support and hospitality in those final weeks. Finally, I would like to express my affection, admiration and gratitude for my best friend and cartel-mate, Justine Mayville, with whom I had the honor of finishing this degree. I would never have been able to survive the last months of this work without you.

I thank my great friend John Heiland for carrying my pack down Niwot Ridge and for always welcoming me back to the mountains. Peace and happiness to Joe "my hair is my hat" Sears and Grant "can we just start at the beginning" Hendren for getting me interested in brain research. Finally, I dedicate this thesis to my parents, Robert and Agnes Foo, for encouraging me to follow my dreams, and teaching me how to work hard and make those dreams come to be. I am indebted to my brothers, Gabriel and Francis, who always supported me, and are the best friends any man could wish for. I thank my extended family for being so patient and putting up with me missing so many holidays! All my love to Scarlet, my little snow-widow, for giving her support and companionship while traveling this long road. Finally, I recall a sunset walk at Goat Rock beach 10 years ago and would like to warn Gary Brandt that I am coming for my bet money!

ABSTRACT

Author: Patrick S. Foo

Title: Functional Stabilization of Unstable Systems

Institution: Florida Atlantic University

Dissertation Advisor: Dr. J. A. Scott Kelso

Degree: Doctor of Philosophy

Year: 2000

Humans are often faced with tasks that require stabilizing inherently unstable situations. We performed four experiments to explore the nature of functional stabilization. In Experiment 1 participants balanced a pole until a time criterion was reached. The geometry, mass, and characteristic "fall time" of the pole were manipulated. Distributions of timing between pole and hand velocities showed strong action-perception coupling. When actions demonstrated a potential for failure, the period of hand oscillation correlated significantly with the "time to balance" ($\tau_{bal} \equiv \theta/\dot{\theta}$), where θ is pole angle re: the vertical balance point, but not other quantities such as θ and $\dot{\theta}$ alone. This suggested that participants were attending to available τ_{bal} information during critical situations. In a model analysis and simulation, we demonstrated how discrete τ_{bal} information may be used to adjust the parameters of a controller to perform this task.

In Experiment 2 participants balanced a virtual inverted pendulum under manipulations designed: 1) to decouple the mechanics of the system from its visual image; 2) to alter the mapping of perception and action; and 3) to perturb successful balancing. A replication of the correlation analysis of Experiment 1 revealed that across all conditions, significant relationships existed between visually specified τ-variables and hand oscillation during critical motions of the pole. These results suggested that participants use the same τ_{bal} information to successfully stabilize both virtual and physical unstable systems, despite quite dramatic visual and mechanical transformations.

In Experiments 3 and 4 we investigated how parts of the body, or individuals in a social dyad cooperate to perform a functional stabilization task. Participants balanced a pole either intermanually (using 2 separate hands) or interpersonally (2 persons each using their preferred right hand) until a time criterion was reached. Although the magnitudes of the forces exerted by each hand were different, an analysis of the timing of the forces revealed that intermanual (interpersonal) participants developed a consistent antiphase (inphase) coordination pattern. These different coordination patterns allowed for the recruitment of previously unavailable efferent and afferent connections to produce the net forces that served to stabilize the pole via $\dot{\theta}$ (see Experiment 1).

Table of Contents

Table List

Figure List

Relationship between the shape of the curve τ_{bal} vs. t and pole trajectory. When the pole is confined to the region $-\frac{\pi}{2} < \theta < \frac{\pi}{2}$ so that it does not dip below the horizontal, the time series plot of τ_{bal} is composed of four basic shapes: (a) sigmoid: τ_{bal} goes through the sequence $-\infty \rightarrow 0 \rightarrow +\infty$ in a reverse S-shape fashion and occurs when the pole starts from one side, overshoots the vertical, and ends up on the other side; (b) Inverted-U, which occurs as the pole moves up but undershoots the vertical, (c) U-curve, which occurs when the pole drifts away from vertical after an undershoot; Incomplete-U curve, which occurs during a catastrophic fall of the pole. These τ_{bal} vs. t curves are the same regardless of which side of vertical the pole resides in. Note that when the pole does not dip below the horizontal, plots (b) and (c) always occur together.

during non-periodic pole motions. This implies a k value that is not constant, and that exhibits a complex dynamics (see text for discussion).

Representative time series of experimental (a) and simulated (b) k_1 values obtained from the ratio $-\dfrac{\ddot{\theta}}{\theta}$.

Simulation of (a) hand (solid lines) and pole velocities (dashed lines), (b) τ_{bal}, and (c) $\dot{\tau}_{bal}$. The parameters used were: $\beta = 4.6$, $\varepsilon = .75$, $\alpha_0 = 2.8$ for the initial value of α, $\mu = 0.4$, $\omega = \sqrt{9.8}$, noise standard deviation of 0.001, and a simulation run-time of 100 sec. Initial conditions were: $\theta_0 = 28 \deg$, $\dot{\theta}_0 = -11.5 \deg/\sec$, $x_0 = -50 cm$, $\dot{x}_0 = 4.1 cm/\sec$.

Phase portrait of $\dot{\tau}_{bal}$ vs. τ_{bal} using the simulation of Fig. 2.13.

Chapter 3
(a) The experimental setup consisting of a personal computer and a digitizing tablet over which a linear track with an aluminum cart holds a digitizing pen and an accelerometer. A custom-built simulation program generates a virtual inverted pendulum, which is controlled by the inputs of the digitizing pen and accelerometer. This experiment was designed to simulate the inverted pendulum apparatus that was used in previous experiments (see Foo et al., 2000; Treffner & Kelso, 1995, 1999). (b) Schematic of an inverted pendulum pivoting on a cart that is affixed to a horizontal linear track. The convention used is: θ is positive (negative) when the pole is right (left) of the vertical; M = mass of the cart, L = pole length, m = pole mass, F = force applied by moving the cart and pen over the digitizing tablet.

An illustration of the nine experimental conditions used in the present experiment. In all of the figures one can see the horizontal linear track, the cart, and the straight pendulum. The arrow at the bottom of each figure represents the direction of the cart moves when the participant moves the digitizing pen to the right. The top row (Figures 3.2a-d) exhibits the details of the first four experimental conditions, and the bottom row (Figures 3.2e-h) indicates the complementary conditions that included a computer-generated angular velocity perturbation (averaging once every 2 s, see the

lightning icons). The first column Figures 3.2a and 3.2e, shows the control condition of a simulated inverted pendulum, and it's perturbed counterpart. The next three columns describe the vertically flipped pole (Figures 3.2b and 3.2f), the action-mapped pole (Figures 3.2c and 3.2g), and the occluded pole (Figures 3.2d and 3.2h), respectively. In Figure 3.2i, the pole parameter alteration is shown. Detailed descriptions of these conditions can be found in the text.

(a) Time series plots of the hand velocity (solid lines) and pole velocity (dashed lines) showing tight anti-phase coordination. (b)-(c) Plots of τ_{bal} and $\dot{\tau}_{bal}$ computed from the same data source as in (a). Note that at hand velocity extrema, the value of τ_{bal} is conserved near $\tau_{bal} = 0$ s and $\dot{\tau}_{bal}$ around $\dot{\tau}_{bal} = 1$. Here the participant undershoots and drifts the pole for the first 5 cycles, then overshoots the vertical for the remaining 2 cycles of pole motion. The classification and investigation of the stereotypical motions of τ_{bal} has revealed that participants use τ_{bal} information to gear hand motions during certain critical pole motions (see also Table 2.2).

Classification system based upon two successive cycles of *successful* balancing behavior. Here the six different paths that are seen in the experimental data and their corresponding τ_{bal} vs. t curves (see Figures 2.5a-c) are enumerated. Paths 1-3 represent situations where the participant successfully avoided a catastrophic fall of the pole from either instability of the pole (Path 2: a failure to reverse, see Foo et al., 2000), or from running out of track with which to correct the fall (or perturbation) of the pole and are of special import during the present correlation analysis (see Tables 3.1-3.5).

Chapter 4

The experimental setup consisting of an inverted pendulum pivoting on a cart with two pull cords affixed to a horizontal linear track. The convention used is: θ is positive (negative) when the pole is right (left) of the vertical; M = mass of θ the cart, L = pole length, m = pole mass, F = force applied by pulling the (right hand) cord at the base; g = acceleration due to gravity. Strain gauges recorded the horizontal components of each force applied with the pull cords. Note the apparatus was designed so the

hands must collaborate to produce the bi-directional motions required for successful completion of the task.

(a) Representative time series of cart position (x: solid line) and the pole angle (θ: dashed line) during successful intermanual balancing. (b) Time series plots of the cart velocity ($\dot{x}$: solid line) and pole angular velocity ($\dot{\theta}$: dashed line) showing tight antiphase coupling during successful balancing. (c) Plots of the force exerted by the right (solid line) and left (dashed line) hands showing the hands alternating their pulling on the cart so as to produce the resulting pole oscillations. These kinematic data are essentially identical to data from the interpersonal (Experiment 4) conditions, and previous unimanual balancing (compare with Figures 2.2 and 2.4), thus only intermanual behavior is shown here.

Distribution of continuous relative phase Φ values during successful intermanual balancing. The mean continuous relative phase for the eight participants (-147.8 deg) denotes on average, an antiphase coordination pattern with the right hand leading the left (~180 deg, see also Table 4.4).

Representative time series of the alternation (left column, figures a, c) and co-contraction (right column, figures b, d) balancing strategies and their corresponding continuous relative phase values. The topmost figures (a, b) plot the time series of the forces exerted by the right (solid line) and left (dashed line) hands on the cart, while the bottommost figures (c, d) show the commensurate continuous relative phase values. Note that during alternation, relative phase Φ values are centered around 180 deg (c), whilst in co-contraction the coordination pattern shows a relative phase Φ centered around 0 deg (d).

(a). Demonstration of the alternation strategy used to balance and control the pole. Here the hand on the left is pulling and the right hand is not. The net effect on the cart is to move it to the left. This corresponds to an antiphase coordination pattern (180 deg) between the forces from the hands, and was observed for the intermanual conditions in Experiments 3 and 4 (see also Tables 4.4 and 4.8). (b). Schematic of two hands using the co-contraction strategy to balance the pole. Both hands exert simultaneous tension on the pull cords, although here the right hand is pulling harder, and the net effect moves the cart to the right. This balancing strategy was

seen during interpersonal balancing (Experiment 4), and corresponds to an inphase (0 deg) coordination pattern between the forces from the hands (see also Table 4.12).

(a) Distribution of continuous relative phase Φ values during successful intermanual balancing. The mean continuous relative phase denotes on average, an antiphase coordination pattern with the right hand leading the left (~180 deg, see also Table 4.8). (b) Distribution of continuous relative phase Φ values during successful interpersonal balancing. Here the mean continuous relative phase describes an inphase coordination pattern (~0 deg, see also Table 4.12).

1.0 Introduction

1.1 Functional Stabilization of Unstable Systems

In the previous several decades, a research paradigm that is known as *coordination dynamics* has shown that biological coordination may be governed by generic processes of self-organization (see Kelso, 1995, for an extensive review). Beginning with experiments of biological coordination that employed the model system of bimanual finger oscillation (see Kelso, 1981, 1984), a strong theoretical base has been established (Haken, Kelso, & Bunz, 1985; Schöner, Haken, & Kelso, 1986). Using the concepts of self-organization from Synergetics, this paradigm has successfully characterized and predicted biological coordination in terms of the dynamical behavior of attractors and repellors of nonlinear dynamical systems.

These original findings have been generalized to many other experimental situations (Haken, 1996; Kelso, 1995 for reviews). Quantitative predictions of coordination dynamics have captured the interactive coupling between participants and the environment (Kelso, Delcolle, & Schöner, 1990; Kelso, Fuchs, & Jirsa, 1998; Wimmers, Beek, & van Wieringen, 1992). With minor changes, these same dynamics have accurately predicted the global coordination observed when individual effectors of a system are asymmetric (see Treffner & Turvey, 1996). Moreover, social coordination between persons can also be accounted for in this approach (Amazeen, Schmidt, & Turvey, 1995; Schmidt, Bienvenu, Fitzpatrick, & Amazeen, 1998; Schmidt, Carello, &

1

Turvey, 1990). Recently, these concepts and experimental designs have been used to understand the functioning of the brain (Kelso, 1992). Aided by improvements in noninvasive functional neuroimaging, coordination dynamics has shown that underlying neural activity is also self-organized (Fuchs, Kelso, & Haken, 1992; Fuchs, Deecke, Kelso, 2000; Wallenstein, Kelso, & Bressler, 1995; Fuchs, Deeke, & Kelso, 2000; Kelso, Bressler, Buchanan, de Guzman, Ding, Fuchs, & Holroyd, 1991; 1992; Mayville, Bressler, Fuchs, Kelso, 1999).

More recently, we have examined a complimentary set of questions in coordination dynamics. In addition to investigating self-organized behavior during episodes of spontaneous pattern switching due to dynamic instability, we have sought to understand how biological systems *stabilize* behaviors. Two branches of this approach have developed. The first aims to discover what the factors are that stabilize *stable* coordination patterns during situations that would *typically render them unstable*. These factors have come to include learning and intentional processes (Foo & Kelso, 2000; Kelso, Scholz, & Schöner, 1988; Lee, Craig, & Grealy, 1999; Zanone & Kelso, 1992, 1997), the recruitment of additional degrees of freedom (Buchanan, & Kelso, 1999; Fink, Kelso, Jirsa, & de Guzman, 2000), and the use of specific information in the environment (Fink, Foo, Jirsa, & Kelso, 2000; Jirsa, Fink, Foo, Kelso, 2000). These influences stabilize coordination states under conditions in which they would otherwise become unstable (e.g. past critical movement frequencies) and switch. The work presented in this dissertation represents the other line of investigation, asking, how do biological systems functionally stabilize an *inherently* unstable system? Studies of posture have shown that

2

entraining to an external oscillating perceptual stimulus can help stabilize the postural system (Jeka, Schöner, Dijkstra, Ribeiro, & Lackner, 1997; Lee & Aronson, 1974; Thelen, 1990). Note that in these posture and locomotion systems the action system was observed to entrain to an external stimulus. In Experiments 1, 3 & 4 we investigated what the characteristics of action-perception coupling revealed when an external entraining stimulus was not available for the pole balancing system (Foo et al., 2000; Treffner & Kelso, 1995; 1999).

1.2 Intrinsic Dynamics of Unstable Systems

One task that may serve as a window into this type of emerging coordination is the stabilization of an inherently unstable system, such as balancing a broomstick on the end of one's finger (e.g. Foo, Kelso, & de Guzman, 2000; Treffner & Kelso, 1995). In contrast to other tasks used in the study of coordination that exhibit the dynamics of an attractor, or a stable fixed point, here an inverted pendulum shows the characteristics of an *unstable* fixed point or a repellor (e.g. Strogatz, 1994). The intrinsic dynamics of a repellor system dictate that after any infinitesimal deviation from its balance point, the system will asymptotically move toward a fall of the pendulum. Because of these intrinsic failure-seeking tendencies, when participants simply react to the motions of the pole, they inevitably do so (within the range of typical reaction times) too slowly and the pole falls (see Foo et al., 2000). If participants over-anticipate the pole's motion, equally dire consequences result. Moreover, at every point in time, the participant is actually perturbing the very system he or she is trying to stabilize: the task/environment affects the participant and vice versa. Thus the task of balancing an inverted pendulum presents

participants with a singularly difficult coordination challenge: a mechanical system that tends toward destabilization where the human controller must exert a mixed "reaction-anticipation" active control, and where his or her own motions destabilize the very system they are trying to stabilize.

1.3 Stabilization of Unstable Systems by Artificial Controllers

The study of stabilization of inherently unstable systems has received much attention within the domain of control theory. Here, the task of balancing an inverted pendulum has been used to illustrate basic control concepts as well as to motivate various control design techniques (see Geva & Sitte, 1993 for a review; Kwakernaak & Sivan, 1972). The inverted pendulum configuration in our experiment is based on the commonly employed cartpole design of Barto, Sutton, and Anderson (1983). Linear control, in which the force used to balance the pole F is linear with respect to the pole angle θ (i.e. $F = k\theta$, k constant), has been widely used to balance an inverted pendulum successfully when the angle of the pole remains within a small range near vertical (Kwakernaak & Sivan, 1972). Systems have also been designed that successfully balance the pendulum by monitoring only the direction of the angle (without magnitude) the so-called "bang-bang" control (Schaefer, 1965). Artificial neural networks that employ movement data (such as cart position and pole angle) or images of the cart-pole system in action as learning templates, have successfully balanced the inverted pendulum (Guez & Selinsky, 1988; Tolat and Widrow, 1988), and have often been claimed to provide possible insights into how biological systems may accomplish this task.

4

Importantly, these engineered systems typically exhibit behaviors that are totally unlike those observed when humans perform this task (Foo et al., 2000), suggesting some limitations to control-theoretic views, at least with respect to the issue of functional stabilization in biological systems. Artificial controllers usually develop a uniform oscillation of the pole around its balance point, with ever decreasing magnitudes that one may term *asymptotic balancing*. Also of note, the goal of most of these engineering approaches is to determine the control force F that is necessary to maintain upright balance of the pendulum without regard to how these forces are generated. While this is our focus in Experiments 1 and 2, in Experiments 3 and 4 we are interested in exactly the opposite, namely how participants successfully coordinate the necessary control forces that balance the pole.

1.4 Visual Information Used in Functional Stabilization: Experiment and Modeling

In typical situations, humans rely on both haptic and visual information, the latter being very much affected by the relative motion of the human-pole system. The goal of Experiments 1 and 2 was to identify the nature of visual information used to balance an inverted pendulum. While previous research has identified a time-to-fall (τ_{fall}) variable as having the least variation prior to the onset of hand deceleration (see Treffner & Kelso, 1995), in the first two experiments we examined the role of a perceptual quantity, time-to-balance (τ_{bal}) in functional stabilization. Time-to-balance (τ_{bal}) is defined as the ratio of the angle of the pole with the vertical and its instantaneous rate of change:

$$\tau_{bal} = \frac{\theta}{\dot{\theta}} \tag{1.1}$$

5

When τ_{bal} is negative its magnitude is an approximate measure of the time to upright the pole. Optical variables similar to τ_{bal} have been shown to elicit avoidance, defensive, or interceptive behaviors in animals and humans (Lee & Reddish, 1981; Schiff, 1965; Savelsbergh, Whiting, & Bootsma, 1991; Schiff, Caviness, & Gibson, 1962), although there is some question as to what extent the empirical data support the use of optic-τ versus alternative possibilities (Bootsma, Fayt, Zaal, & Laurent, 1997; Bootsma & Oudejans, 1993; Savelsbergh, 1995; Tresilian, 1994, 1995;Wann, 1996). In Experiment 1 and 2 we aim to identify biologically relevant perceptual variables, and then formulate a procedure based on these results for adjusting the parameters of a control system. In a model analysis, we show how such information may govern the dynamics of perceptual-action coupling in this task. While this is not exactly a formulation of a control law, it follows the spirit of Warren (e.g. Warren, 1988; 1998; Warren & Kelso, 1985) in that we aim to specify how perceptually available information constrains action, and vice-versa.

1.5 Virtual Reality as an Experimental Platform

In Experiment 2 we asked if the information used to balance a real inverted pendulum was the same as that employed to control a virtual simulation of that mechanical system. Do participants use different perceptual quantities when the mechanics of an unstable system are systematically decoupled from the visual information about that system? When one is forced to map a transformed action onto visual stimuli, what deviations from the foregoing normal relationships may be seen? If essential elements of this visual information are withheld from participants, can one still

successfully balance the pole? Do these types of visual information provide robust support for functional stabilization in the presence of perturbations?

To these ends we employed a virtual computer simulation of the inverted pole balancing task from Experiment 1. We began with a control condition that simulated a typical cart-pole system. This control tests if utilizing the presented (visual) information in the real situation transfers to the simulation. Next we introduced manipulations designed to: 1) decouple mechanics and visual information of pole motion; 2) alter mapping of hand action; 3) remove visual information; and 4) introduce a perturbation. A replication of the correlation analysis of Foo et al. (2000) was employed to confirm and extend previous findings that showed during critical motions of the pole, the visually specified time-to-balance was used to gear the corrective actions of the pole. It was hypothesized that regardless of the conditions, participants would use the same visually specified "time-to-balance" information (i.e. τ balance) to stabilize this inherently unstable inverted pendulum.

1.6 Intermanual and Interpersonal Stabilization

In Experiments 3 and 4 the goal was to discover how actions are coordinated by two independent effectors to produce the appropriate forces necessary to stabilize an unstable system. Here we designed the task so that both effectors must *collaborate* to produce the appropriate forces *necessary before any successful coordination with the pole was possible*, a criticism of prior interpersonal work (Ingham, Levinger, Graves, & Packham, 1974; Schmidt et al., 1990). In these experiments we introduced new conditions into the functional stabilization paradigm: an intermanual and an

7

interpersonal balancing requirement. In the intermanual condition (Experiment 3 and 4) participants controlled *two potentially independent* hands to perform functional stabilization, a coordination task that was markedly more difficult than previous experiments where the only goal was to produce a required pattern (e.g. the bimanual drawing task of Preilowski, 1972; and the aforementioned coordination experiments in Section 1.2). Intermanual coordination was also more difficult than unimanual pendulum balancing (Foo et al., 2000; Treffner & Kelso, 1995, 1999) where the participant can move the cart in both directions with a single effector. In Experiment 4 we required pairs of participants to balance the pendulum (interpersonal balancing) in addition to intermanual balancing. During interpersonal coordination each participant was required to develop coupling with the environment *and* with another person for success.

1.7 Organization of This Dissertation

In the first of four experiments we have used the model task of inverted pendulum balancing to determine what visual information is used to perform functional stabilization, and to use the aforementioned empirical results to develop a model of stabilization that more accurately reflects the behavior of biological systems. In Experiment 2 we asked whether the same visual information is used when stabilizing a virtual simulation of pole balancing, introducing drastic manipulations and perturbations designed to test the generalizability of the results of Experiment 1. In Experiments 3 and 4, we utilized the pole balancing paradigm to examine the nature of bimanual coordination when performing functional stabilization, a heretofore under-investigated line of research. Here we compared the behavior seen when the two separate hands of an

8

individual or two individuals of a social system must cooperate to succeed at the task, and showed that participants generated coordination patterns that may be used to recruit additional afferent and efferent information (e.g. haptic) to stabilize an unstable system. Thus our research program was threefold: to understand which perceptual information is used in functional stabilization and to model these findings; to examine how action and perception are coupled in this paradigm, and to characterize the coordination of appropriate actions in successful stabilization.

2.0 Functional Stabilization of Unstable Fixed Points:

Human Pole Balancing Using Time-to-Balance Information

2.1 Experiment 1: Introduction

Biologically significant activities such as the maintenance of posture (e.g. Jeka &

Lackner, 1994, 1995), the development of posture and locomotion (e.g. Lee & Aronson,

1974; Thelen, 1990), and the learning of new motor skills (Zanone & Kelso, 1992, 1997),

may be viewed as involving active stabilization of inherently unstable fixed points of a

dynamical system. In each of these cases, participants use relevant perceptual

information to stabilize an unstable system. In quiet standing posture, light fingertip

contact with a touch bar that is too weak to provide physical support can reduce the mean

sway amplitude, or entrain the motion of the body if the touch bar oscillates (Jeka &

Lackner, 1994, 1995; Jeka et al., 1997). In the moving room paradigm, postural

compensations to changes in optical flow (stemming from the motion of the room) can be

demonstrated across a range of ages and motor developmental stages (Bertenthal & Bai,

1989; Bertenthal, Rose, & Bai, 1997; Lee & Aronson, 1974). Information about the

relative phase between rhythmically moving limbs may be used to stabilize previously

unstable, to-be-learned patterns of coordination (Zanone & Kelso, 1992, 1997). The

present work explores functional stabilization through the model task of humans

balancing an inverted pendulum along a linear track (Treffner & Kelso, 1995; 1997;

1999). Note that unlike the foregoing posture and locomotion paradigms where a sensory modality drives or entrains an action system, in pole balancing the system perturbs itself: at each instant the participants' own actions directly influence the perceptual information that guides action. To date, detailed kinematic studies of human pole balancing have been largely absent (see however, Treffner & Kelso, 1995), although a similar balancing task has been used as an interference task during studies of hemispheric cerebral function (see Kinsbourne & Hicks, 1978).

The study of stabilization of inherently unstable systems has received much attention within the domain of control theory. Here, the textbook example of balancing an inverted pendulum has played a key role in elucidating basic control concepts as well as motivating various control design techniques (see e.g. Kwakernaak & Sivan, 1972). The inverted pendulum configuration in our experiment (see Figure 2.1a) is based on the often-used cart and pole design by Barto et al. (1983). As in most theoretical considerations, we focus on the nature of the control force F and bypass the details of its delivery. Linear control, in which F is a linear function of the state space variables has been widely used to balance an inverted pendulum successfully (see Geva & Sitte, 1993 for a review). Here state-space variables are defined as those quantities such as positions and velocities used to describe the state of the system. We distinguish these from parameters, those quantities that are externally determined and typically used to specify the overall strength of the control signal given the form of F. For example, if the force F is linear with respect to the pole angle ($F = k\theta$), then k is a parameter while θ is a state-space variable. By linearizing the equations for the motion of the cartpole system, it is

possible to extract the parameter range that results in successful balancing in the region of small pole angles.

Neuromorphic linear controllers whose parameters (sometimes also called weights in the neural network literature) are determined using artificial neural networks provide not only effective solutions but also possible insights into how biological systems may accomplish the balancing task (e.g. Anderson, 1989). Using actual movement data (the state space variables) from balancing experiments, neural network controllers can learn how to mimic humans accurately (Guez & Selinsky, 1988). Along the same line but using time varying digitized images of the cart-pole system instead as inputs, Tolat and Widrow (1988) constructed a pattern recognizing system that mastered the balancing task well enough to keep the pole from falling.

A central problem in neural network design in which no teacher is available (unsupervised learning) is how to adjust future control actions based on the outcome of a sequence of actions. This is known as the credit assignment problem and is usually addressed by imposing a suitable constraint such as maximizing the balance time or minimizing excursions from the vertical. As noted emphatically by Geva and Sitte (1993), a random search in parameter space can produce outcomes that in many respects are not significantly different from those resulting from a more systematic search. In the present paper, we explore the idea that in addition to the kinematic variables (e.g. hand position and velocity), human controllers also use direct perceptual information to solve the balancing task. Clearly, a key question is which perceptual variables the human controller employs.

In typical situations, humans rely on both haptic and visual information, the latter being very much affected by the relative motion of the human-pole system. This paper examines the role of a perceptual quantity, time to balance (τ_{bal}), defined as the ratio of the angle of the pole with the vertical (θ in Figure 2.1) to its rate of change:

$$\tau_{bal} = \frac{\theta}{\dot{\theta}} \tag{2.1}$$

When τ_{bal} is negative its magnitude is an approximate measure of the time to upright the pole. Only in the case when the angular velocity is constant is τ_{bal} the actual time to upright. In the present work, we show that participants are more attuned to the temporal behavior of the pole and produce more consistent values of τ_{bal} and $\dot{\tau}_{bal}$ when there is a potential for failure compared to when the pole is near balanced conditions. These suggest that participants are using available τ_{bal} information, especially near critical conditions. During typical (non-critical) motions of successful performance, wider variation in these quantities is observed, suggesting that participants may not be attending to this type of perceptual information. In a model analysis, we show how such information may govern the dynamics of perceptual-action coupling in this task.

The main goals of the present research are to identify biologically relevant perceptual variables in successful balancing and the nature of the perception-action coupling that supports functional stabilization. Once these variables are identified experimentally, we may then formulate a procedure for adjusting the parameters of the control system. While this is not exactly a formulation of a control law, it follows the

spirit of Warren (e.g. Warren, 1988; 1998) in that we aim to specify how perceptually available information constrains action, and vice-versa.

2.2 Method

2.2.1 Participants

Thirty-six right-handed students between the ages 17-30, served as participants (n=18 males; n=18 females). All participants completed an informed consent form prior to data collection and received course credit for participating. All participants were treated in accordance with the ethical standards of the APA.

2.2.2 Apparatus

The apparatus consisted of a pole configuration attached via a metal bearing to a cart (mass = 388.0 g) such that the pole only pivoted in the XY- plane (Figure 2.1). The cart was constrained to slide along a 180 cm linear track, oriented parallel to the X-axis. The track rested securely on a table approximately waist-level height for adult participants (92 cm). Three different poles of varying length, mass and configuration (one straight pole, two L-shaped poles) were used. The L-poles were designed so that the center of mass did not coincide with any portion of the pole: here the simplistic strategy of aligning the pole with vertical (which stabilizes the straight pole) was ineffective.

In the straight pole condition (Figure 2.1a), the pole was made from a single aluminum dowel (length = 108.0 cm, diameter = 1.0 cm, mass = 207.4 g, and moment of inertia I = 0.07 kg/m^2). In the L-pole conditions, the configurations had identical appearances but different material compositions, moments of inertia, total masses, and balance points. The steel L-pole (Figure 2.1b) had the same moment of inertia as the
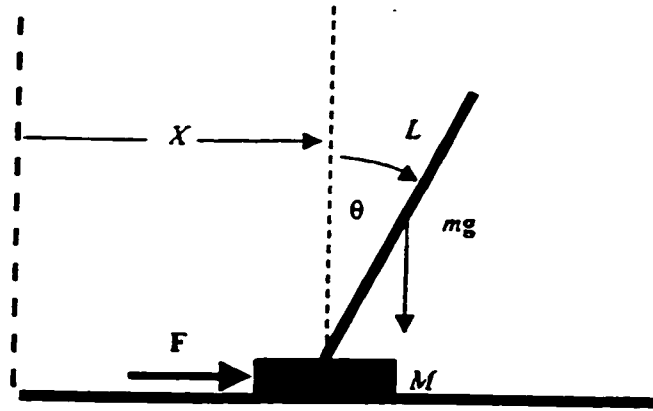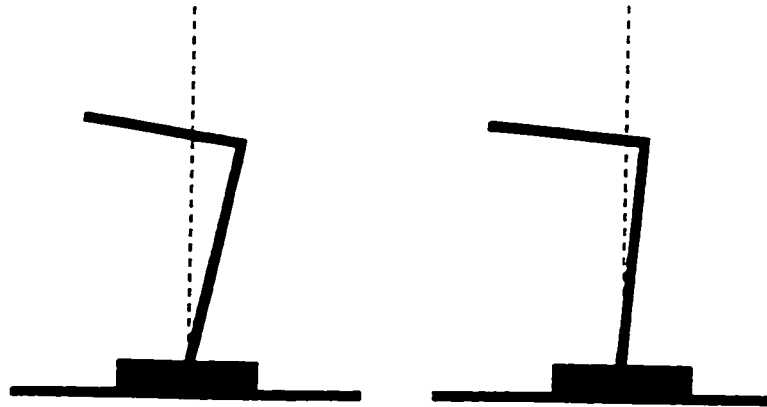
Figure 2.1a-c. The experimental setup consisting of a pole configuration, a cart, and a horizontal linear track. (a) Straight pole configuration and the relevant physical parameters and variables used in the analysis. The convention used is: θ is positive (negative) when the pole is right (left) of the vertical; M = mass of the cart, L = pole length, m = pole mass, F = force applied by the hand to the base; g = acceleration due to gravity; (b) Steel L-pole configuration shown at its balance point (the base rod inclined 11.4 degrees from the vertical). (c) Wood L-pole configuration at its balance point (the base rod inclined 4 degrees from the vertical). For the L-poles, the angles were adjusted by subtracting the appropriate balance point value.

straight pole (I=0.07 kg/m^2) but a greater total mass (279.0 g). This pole was constructed by attaching a steel rod (length=29.4 cm, mass = 163.8 g) perpendicular to and on top of an aluminum rod (length = 60.0 cm, mass = 115.2 g) acting as the base. The 90-degree bend extended to either the left or right side of the participant. When this pole was balanced so that the center of mass lay directly on top of the pivot point, the base aluminum rod was displaced approximately 11.4 degrees from vertical. The wood L-pole (Figure 2.1c) was constructed similarly, but with the steel portion replaced by a 15.9g wooden rod of the same length. The total mass and moment of inertia of the wood L-pole configuration were 131.1 g and 0.02 kg/m^2, respectively. When balanced, the base aluminum rod was displaced approximately 4.0 degrees from vertical. For the three pole systems, the surfaces of the rods were covered to mask their textures and material compositions.

To monitor movements of the hand and pole, five infrared-emitting diodes (IREDs) were affixed to strategic locations. IREDs #1 and #2 were attached to the base of the track and the adjoining line defined the horizontal reference. IRED #3, placed on the pivot point of the cart was used to monitor the hand displacements that were restricted to horizontal movements. IREDs #4 and #5 were placed on the pole in such a way as to permit measurement of its angular orientation (in either the straight or L-shape conditions). Signals from the five IREDs were sampled at 100 Hz using an OPTOTRAK 3010 system, and later filtered with a low-pass (set at 8 Hz) second order Butterworth filter. The basic kinematic data thus consisted of horizontal hand position (X) and the angle (θ) from the pole's balance point.

2.2.3 Procedure

The task was to balance the pole by moving the cart with the right hand along the linear track (the X-axis). Haptic information from the cart, but not directly from the pole itself was thus available to the participant. The goal was to balance the pole for 30 seconds without allowing it to fall and make contact with the track. Failure to complete 30 continuous seconds of balancing constituted an unsuccessful trial. Obviously, participants received visual feedback about success or failure of their performance on each trial. Each participant performed blocks of ten experimental trials followed by a one-minute rest period. Moreover, during the rest period participants were given Knowledge of Results in the form of total time of balance for each trial in the previous block. In addition to inter-block rests, participants were provided 5-minute rest periods at trials 40 and 70.

2.2.4 Design

Participants were placed via matched (by sex) random assignment into one of six experimental groups ($n = 6$ for each group; $n = 3$ males, $n = 3$ females), and asked to perform *all three* testing sessions (acquisition, transfer, and retention; see Table 2.1) until they could reach a performance criterion. Participants were required to perform a given balancing task until they could complete 3 successful attempts out of 5 consecutive, successful trials for *each* of the three testing sessions.

Each group was assigned a criterion task during the acquisition session that was to successfully balance one of the three pole configurations: straight, L-steel, and L-wood. Upon completing the acquisition session, the participant attempted the transfer task,

17

which was to balance a different pole. One week later, the participant was asked to balance the original pole in a retention test.

Table 2.1: Experiment Design

	Day 1: Acquisition	Day 1: Transfer	Day 8: Retention
Group Number	**Session 1**	**Session 2**	**Session 3**
1	Straight Pole	L-Steel Pole	Straight Pole
2	Straight Pole	L-Wood Pole	Straight Pole
3	L-Steel Pole	Straight Pole	L-Steel Pole
4	L-Steel Pole	L-Wood Pole	L-Steel Pole
5	L-Wood Pole	Straight Pole	L-Wood Pole
6	L-Wood Pole	L-Steel Pole	L-Wood Pole

2.2.5 Data Analysis

If a participant did not successfully balance the first pole after 99 trials, and also did not successfully complete the transfer task after 50 trials, he/she was rejected and their data excluded from the final data analysis. For each participant who reached criterion, the number of trials executed to meet the criterion level of performance (Nc) was noted.

For the kinematic analysis that follows, all trials showing continuous pole balancing lasting longer than 3 seconds were included in the final data set. This set included 339 trials meeting the original 30-second criterion as well as 1,935 additional

trials. For each trial, all cycles of contiguous balancing were included except the last cycle that preceded a failure. Each cycle was defined as one half-period of the continuous hand velocity time series. Thus 76,637 cycles of 2,274 individual trials were included in the analysis of continuous balancing. Note that even for unsuccessful *trials*, successful *cycles* of balancing were included in our analysis.

2.3 Results and Discussion

2.3.1 Learning Results

Did participants significantly improve their balancing performance by the end of the experiment for any of the poles? A mixed 6 (groups) X 3 (testing sessions) ANOVA with group as a between participants factor and testing session as a within participants factor was performed on the dependent variable (Nc) to assess differences in performance between acquisition and retention tests. A significant interaction, $F(10, 60) = 3.59$, $p < .01$, revealed that practice led to a significant improvement in performance for the four L-pole groups (groups 3-6, see Table 2.1) between acquisition and retention. However, excellent performance of the straight pole groups (groups 1-2) in acquisition limited the amount of improvement available upon retention testing, and no significant change in performance was seen.

Which pole was easiest to balance during the acquisition session? A Tukey post-hoc analysis revealed that during acquisition, the straight pole was significantly easier to balance than the steel L-shaped pole and the wood L-shaped pole ($p < .05$). The significant difference in performance between the straight pole and the steel L-pole ($I=0.07$ kg/m^2 for both poles) suggests that the moment of inertia manipulation was not

19

effective. The similar performance of the L-steel and L-wood poles indicated that the pole configuration manipulation (compared to the straight pole) depressed acquisition performance.

Did practice with *different* poles during acquisition improve performance (proactive transfer) during the transfer session? A Tukey post-hoc analysis of the previous 6 (groups) X 3 (sessions) mixed ANOVA revealed that participants who practiced with either L-shaped pole in acquisition (e.g. group 4 which balanced the L-steel pole in acquisition and transferred to the L-wood pole) showed a significant performance improvement in the transfer session when compared to participants balancing the same (transfer) pole in acquisition (and did not receive any previous practice, e.g. groups 5 and 6). Participants who balanced the easier straight pole in acquisition (e.g. group 2) did not receive the benefit of transfer, and their performance was comparable to participants who did not have any previous practice at all (e.g. groups 5 and 6 in acquisition). Additionally, no performance *improvement* was seen in the straight pole transfer session groups (e.g. groups 3 and 5) because of the exceptional performance of participants who balanced the straight pole in the acquisition session (e.g. groups 1 and 2). Thus, when improvement was possible, practice with the more difficult balancing poles during acquisition ameliorated performance in the transfer session. These results differ from Bachman (1961) who found no evidence for transfer of learning between two gross balancing tasks. It should be noted that Bachman's study was designed to discover a generalized motor ability, and the tasks were designed to be distinctive in execution while retaining the common element of balancing.

20

2.3.2 Kinematic Analysis: Introduction

Our principal focus is on the quantities that characterize successful balancing behavior, both in acquisition and across differences in the geometrical and physical properties of the balanced object. Data for the hand velocity ($\dot{x}$) and pole angular velocity ($\dot{\theta}$) were obtained by numerically differentiating the time series data for the hand position (x) and the pole angle (θ). Figure 2.2 shows representative time-series of the hand position (solid lines) and pole angle (dashed lines) for one participant balancing a straight pole (Figures 2.2a,b) and one participant balancing an L-shaped pole (Figures 2.2c,d). The plots on the left side show balancing behavior early in acquisition; plots on the right side show successful performance late in retention testing. The straight pole participant is able to develop and maintain successful balancing in both acquisition and retention. Note that the peaks (valleys) of the hand position coincide with valleys (peaks) of the pole angle, indicating an anti-phase coordination between the hand and the pole.

In contrast, early in the acquisition session, the participant using the wood L-pole (Figure 2.2c) fails to develop this anti-phase pattern, and the pole moves to extreme angles followed by failure. Later (Figure 2.2d) this participant successfully balances the pole during the retention phase, and the anti-phase coordination between hand and pole is evident.

2.3.3 Action-Perception Coupling Between Hand and Pole

To explore coordinated behavior beyond that induced by the mechanical coupling of the pole to the cart, we analyzed the timing differences between the hand and pole actions for each cycle (half-period) of the hand velocity trajectory (see Figure 2.4a). As
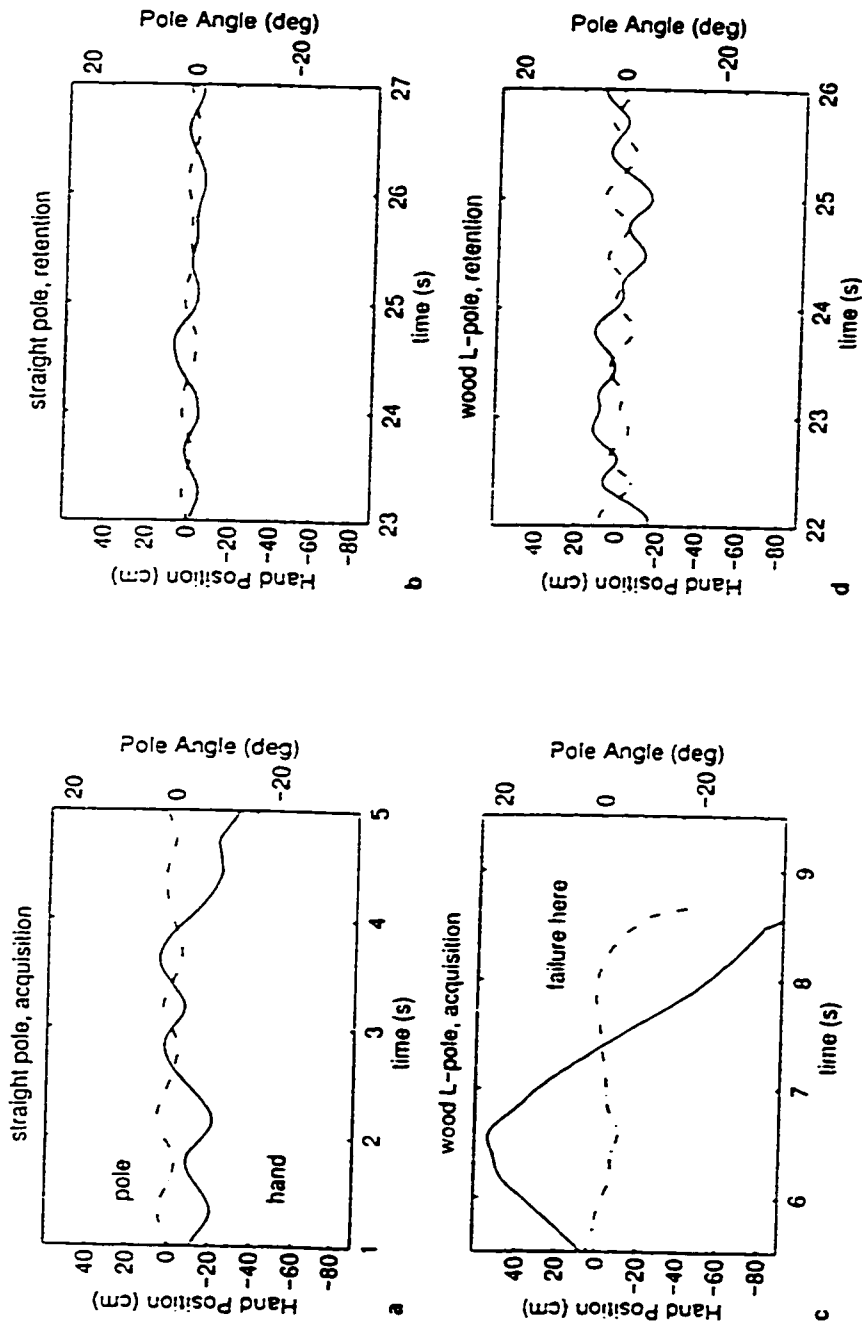
Figure 2.2a-d. Hand Position (solid) and pole angle (dashed) time-series for successful and unsuccessful balancing trials. Shown are timeseries of typical balancing behaviors during acquisition and retention sessions using the straight pole (a, b) and the wood L-pole (c, d). In both cases, hand position is anti-phase with the pole angle. As seen in (c, d), although early balancing using the L-shaped wood pole is unsuccessful, after practice the kinematic behavior takes on the characteristics of the successful trials of the straight pole.

22
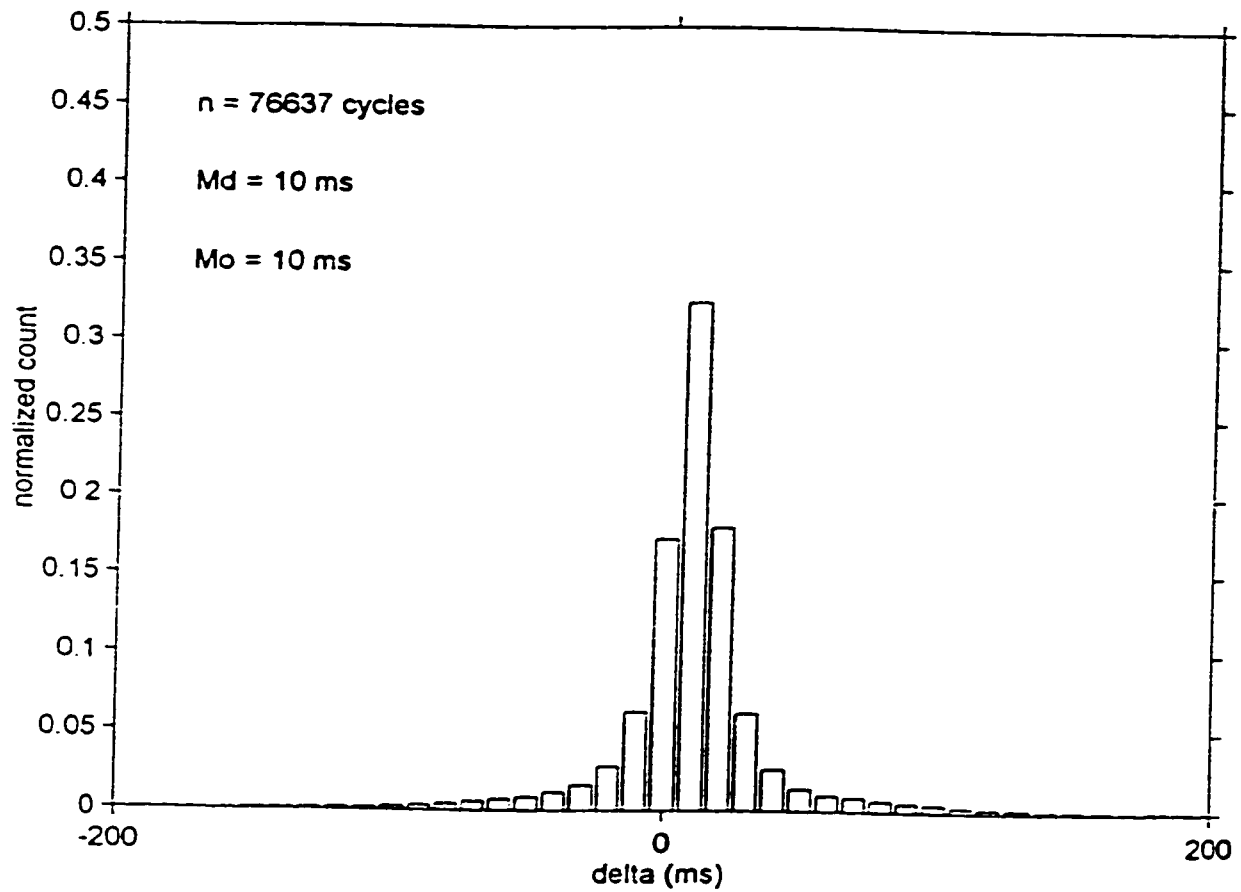
Figure 2.2

Figure 2.3. Distribution of Δ-values collapsed across learning and pole conditions. Md is the median value, and Mo represents the mode.

noted in Figure 2.2, hand position and angle tend to be coordinated when the pole remains upright. However further consideration suggests that the velocity variables might provide more sensitive evidence of coupling behavior (e.g. Jeka & Lackner, 1994, 1995; Kelso, Fuchs, Lancaster, Holroyd, Cheyne, &Weinberg, 1998). A cross correlation was performed between the time series of the hand and pole velocities for each cycle of the hand velocity. The value of Δ was defined as the time difference between the peak of the normalized cross correlation and a zero-lag value (as in simultaneous hand and pole velocity peaks). Over the course of successful balancing, participants develop and maintain a high degree of coupling between the hand and the pole as evidenced by an average Δ-value of 10 ms (hand lagging the pole) across all learning and pole conditions (see Figure 2.3). Of course, this value though impressive is limited by the sampling rate ($\pm$ one sample).

2.3.4 Kinematics of τ_{bal}

When balancing a pole under the current experimental conditions, information about the pole's state is available primarily through vision. Although, in principle, both the angle and angular velocity are available as measures of this information, they may not be the principal sources through which a human controller regulates action. In the following, we present the kinematic behavior of the hand-pole system in terms of the time to balance, τ_{bal}. Recall that τ_{bal} is defined as the ratio of θ over $\dot{\theta}$ (see Equation 2.1). Then, using a model analysis, we will argue that knowledge of τ_{bal} and the hand position (x) is sufficient to implement a more direct control system for balancing the pole.

To familiarize the reader with the typical properties of τ_{bal} and how it behaves in terms of conventional position and velocity measures, we show in Figure 2.4 three time series for the successful balancing data of Figure 2.2d. We will examine the behavior of these perceptual variables at the hand velocity extrema ($\ddot{x}=0$). The rationale for selecting the hand velocity extrema is that they reflect most accurately the onset of interceptive actions such as when the hand starts to reverse its direction of motion, or equivalently, when it starts to recover from a previous action (see also Treffner & Kelso, 1995; Wagner, 1982). Although previous balancing data has shown that the perceptual τ-variable demonstrates the smallest coefficient of variation during successful performance at approximately 170 ms prior to the onset of hand deceleration (Treffner & Kelso, 1995), in the current experiment we explore the possibility that *sufficient* perceptual information may be gleaned by monitoring τ_{bal} and $\dot{\tau}_{bal}$ at the onset of hand deceleration, since these variables appear to be conserved near these time points in the balancing cycle. Note that around the times of hand velocity extrema ($\ddot{x}=0$: see solid lines of Figure 2.4a), the value of τ_{bal} is conserved near $\tau_{bal}=0$ (see Figure 2.4b), and furthermore, at the corresponding time, the value of $\dot{\tau}_{bal}$ is conserved near $\dot{\tau}_{bal}=1$ (see Figure 2.4c). In other words, during the onset of deceleration of the hand, the pole is moving near the vertical ($\tau_{bal}=0$), and is typically overshooting the vertical ($\dot{\tau}_{bal}=1$).

Unlike the continuous and smooth variations of the $\dot{x}$ and $\dot{\theta}$ plots, τ_{bal} exhibits characteristic singularities in an almost regular manner. The divergences occur when $\dot{\theta}$ reaches zero and usually correspond to pole reversals (see Figure 2.4b). The behavior

25
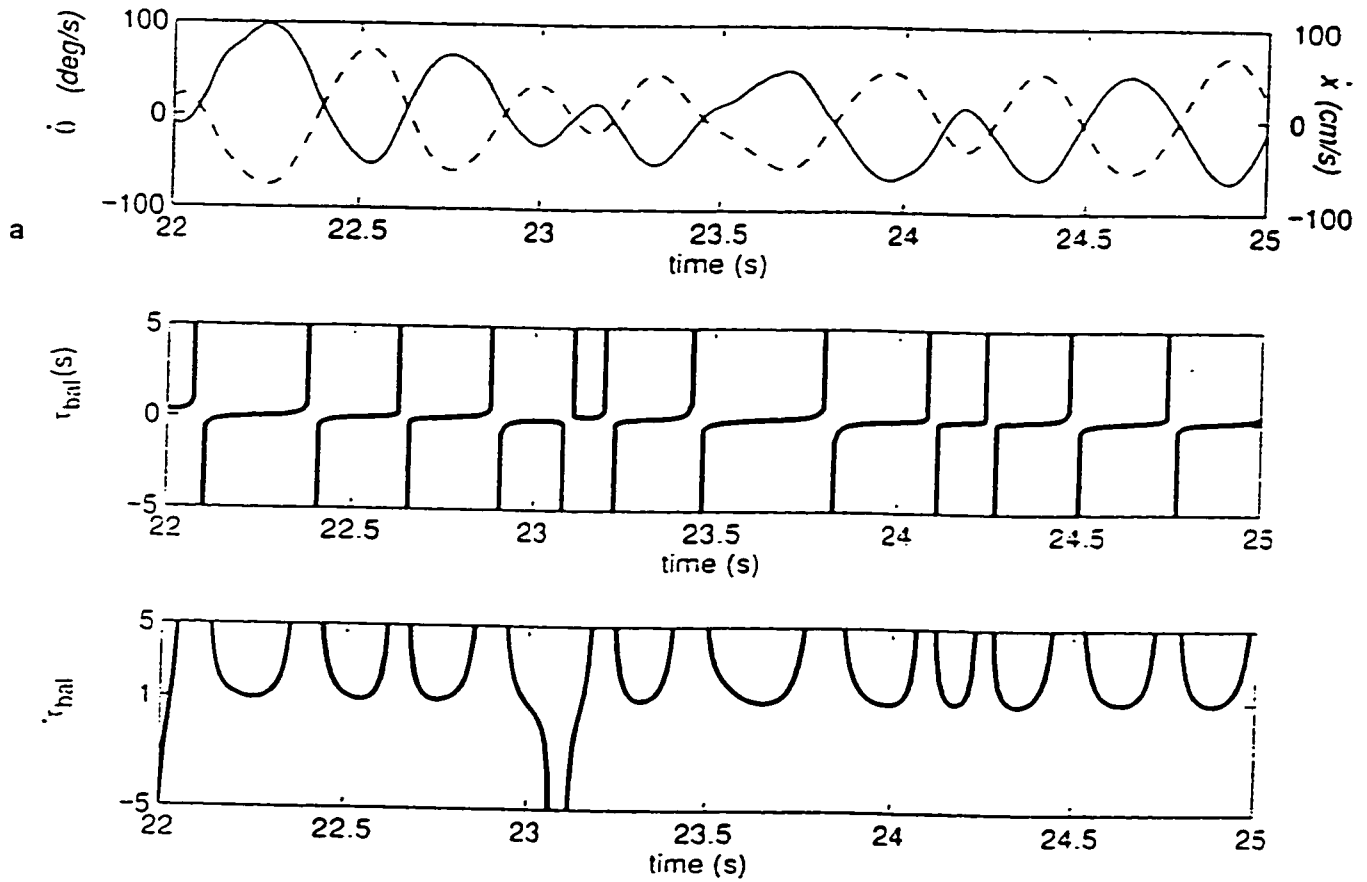
Figure 2.4a-c. (a) Time series plots of the hand velocity (solid lines) and pole velocity (dashed lines) showing tight anti-phase coordination. Data are from the successful trial shown in Figure 2.2d. (b)-(c) Plots of τ_{bal} and $\dot{\tau}_{bal}$ computed from the same data source as in (a).
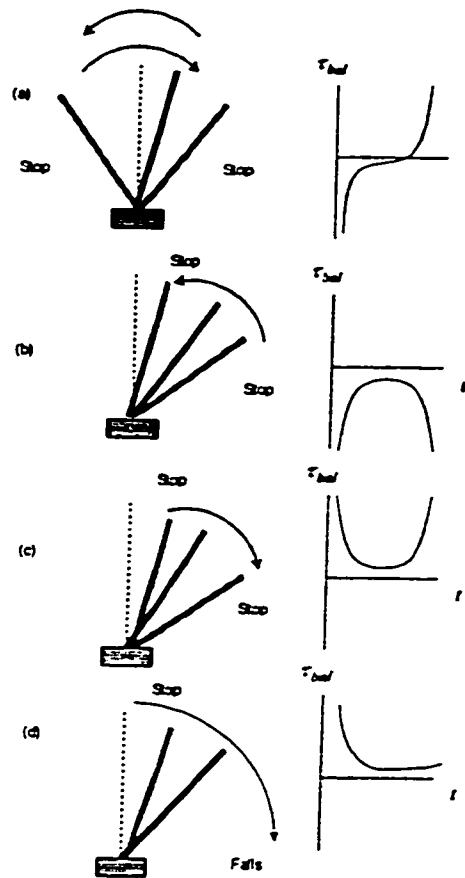
Figure 2.5a-d. Relationship between the shape of the curve τ_{bal} vs. t and the pole trajectory. When the pole is confined to the region $-\frac{\pi}{2} < \theta < \frac{\pi}{2}$ so that it does not dip below the horizontal, the time series plot of τ_{bal} is composed of four basic shapes: (a) sigmoid: τ_{bal} goes through the sequence $-\infty \to 0 \to +\infty$ in a reverse S-shape fashion and occurs when the pole starts from one side, overshoots the vertical, and ends up on the other side; (b) Inverted-U, which occurs as the pole moves up but undershoots the vertical, (c) U-curve, which occurs when the pole drifts away from vertical after an undershoot; (d) Incomplete-U curve, which occurs during a catastrophic fall of the pole. These τ_{bal} vs. t curves are the same regardless of which side of vertical the pole resides in. Note that when the pole does not dip below the horizontal, plots (b) and (c) always occur together.

27

between reversals is schematically illustrated in Figure 2.5. To understand the figure, we note first that because of the symmetry of θ and $\dot{\theta}$ with respect to left-right exchange, τ_{bal} has corresponding sign symmetry. Regardless of which side of vertical the pole is, $\tau_{bal} > 0$ means that the pole is moving away from the vertical while $\tau_{bal} < 0$ means the pole is moving toward the vertical.

Consider now Figure 2.5a, which shows a typical movement consisting of the pole crossing the vertical as it goes from one side to the other. This means τ_{bal} changes from negative (moving toward the vertical) to zero (exactly at the balance point) to positive (moving away from the vertical) values, traversing a sigmoid path. If, during a restoring motion, the pole undershoots the vertical (Figure 2.5b), τ_{bal} is always negative but its absolute value initially decreases, then diverges. The result is an inverted U-shaped curve. After an undershoot, the pole reverses direction and drifts away from the vertical ($\tau_{bal} > 0$ and large). As the pole falls, its angular velocity increases and τ_{bal} decreases. Subsequent deceleration of the pole then increases τ_{bal} again to ∞. This produces the U-shaped plot in Figure 2.5c. When participants fail to recover the pole, the positive τ_{bal} value increases without return until failure: this corresponds to an incomplete U-curve (see Figure 2.5d and Figure 2.2d). Note that because of the symmetry mentioned earlier, the same scenarios occur irrespective of which side of the vertical the pole resides. In Figure 2.6, we show the phase portrait of $(\tau_{bal}, \dot{\tau}_{bal})$ for a section of the time series data in Figure 2.4.
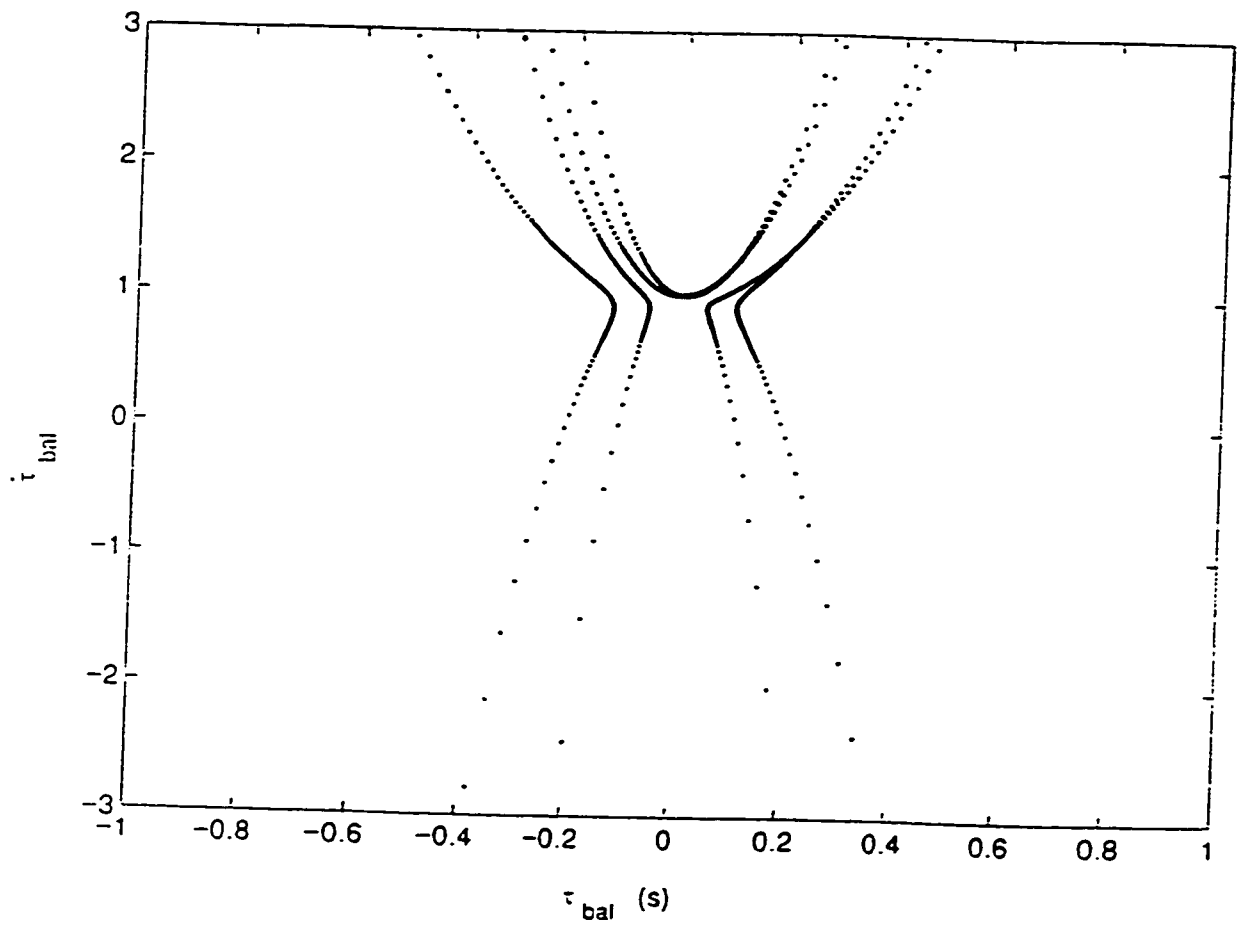
Figure 2.6. An example of a phase portrait, $\dot{\tau}_{bal}$ vs. τ_{bal} using the data from the successful trial of Figure 2.2d.

Except for the negative $\dot{\tau}_{bal}$ region, the shape of the curve suggests quadratic dependence of $\dot{\tau}_{bal}$ with τ_{bal} but with variable curvature at the origin. Note that the instances of pole crossover (which correspond to the sigmoid trajectory in Figure 2.4b and 2.5a) describe a curve like the two quadratic curves in the inner part of the phase portrait of Figure 2.6. Instances of pole undershoots, corresponding to inverted-U curves in Figure 2.4b and 2.5b, are represented by the two trajectories in Figure 2.6 where the τ_{bal} values remain negative. Conversely, drifts of the pole away from vertical (see U-shaped curves of Figure 2.4b and 2.5c) describe the two trajectories in the phase portrait where τ_{bal} remains positive. Note that $\dot{\tau}_{bal}$ values cluster around 1 for small values of τ_{bal}, indicating that as noted previously, during the onset of deceleration of the hand, the pole is moving near the vertical ($\tau_{bal} = 0$), and is typically overshooting the vertical ($\dot{\tau}_{bal} = 1$). Thus, one expects the variability of $\dot{\tau}_{bal}$ to be minimal at $\tau_{bal} = 0$. Does this prediction hold true in general? An analysis was performed on all successful cycles of balancing motion, across pole and learning conditions to determine the values of τ_{bal} and $\dot{\tau}_{bal}$ at the onset of hand deceleration (see Figure 2.7 and Figure 2.8). Participants produce an average τ_{bal} of 0, and $\dot{\tau}_{bal}$ of 1 across all successful balancing cycles, regardless of pole or learning conditions. The robust conservation of these perceptually based variables, across manipulations of pole and learning conditions, suggests that τ_{bal} may provide the informational support for successful completion of this task.
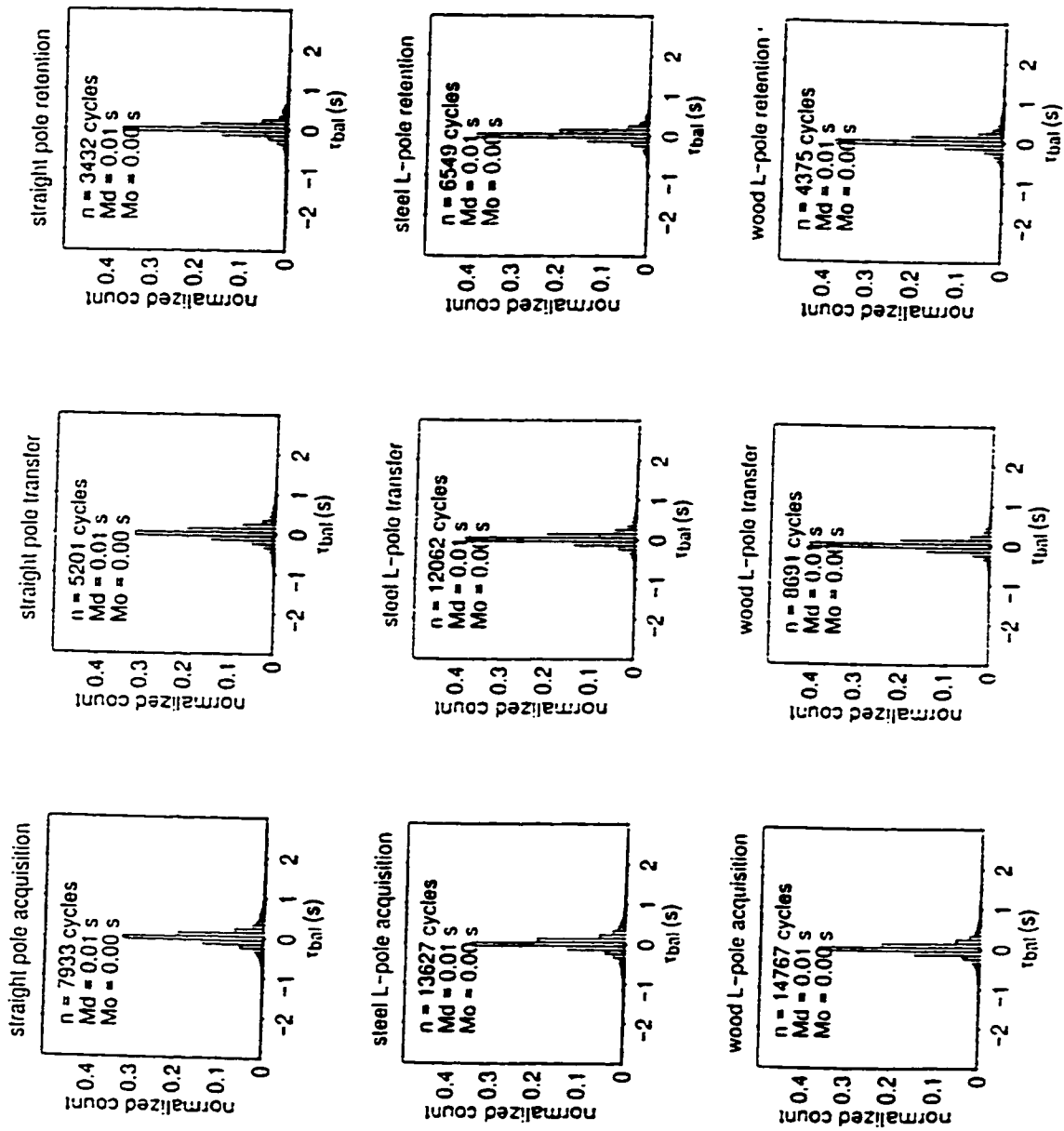
Figure 2.7 Distribution of τ_{bal}-values according to experimental conditions.

31
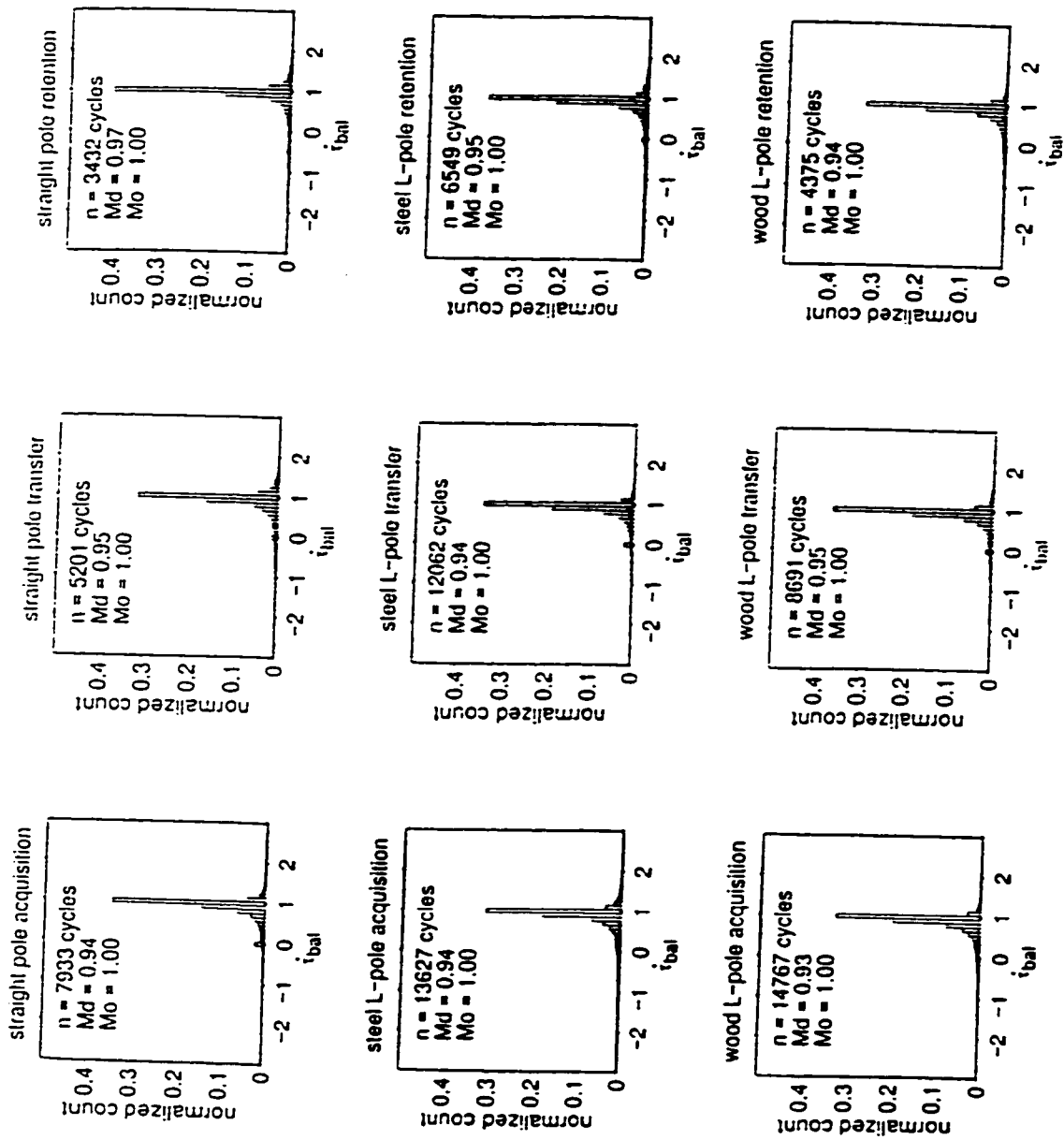
Figure 2.7

Figure 2.8 Distribution of r_{bal}-values according to experimental conditions.

Figure 2.8

2.3.5 Classification of Balancing Strategies: Routes to Failure

There were four classes of failures in the present data set. The first class of failures occurred when the pole was balanced for less than 3 seconds. These "short trials" consisted of an immediate catastrophic fall, and did not have enough kinematic data to be reliably analyzed. In the second type of failure the participant allowed the base of the cart to contact the edges of our linear track, followed by a catastrophic fall. In these "spatial boundary errors" the participant simply ran out of room with which to maneuver the base and change the direction of the pole. In contrast to these types of errors, participants also produced two classes of failures characterized by a loss of perception-action coupling, and after some successful balancing had been completed. In order to discriminate the specific routes to failure for the third and fourth failure types, the balancing behavior of the pole was classified based on a local examination of two successive cycles of τ_{bal} behaviors.

Upon close examination of the experimental time series, it was apparent that the different pole motions (crossing the vertical, undershooting, and drifting) occurred in definite sequences in successful balancing. In Figure 2.9 the observed sequences of τ_{bal} behaviors are shown. From the three pole behaviors seen in successful balancing, here denoted by the boxes, the six paths (shown by arrows) describe the observed sequences between these behaviors. Beginning with the lower box that symbolizes a crossover of vertical (and a sigmoid τ_{bal} curve), it is apparent that three possible paths exist to the next successful cycle. The participant may continue with another crossover as in path number

ı
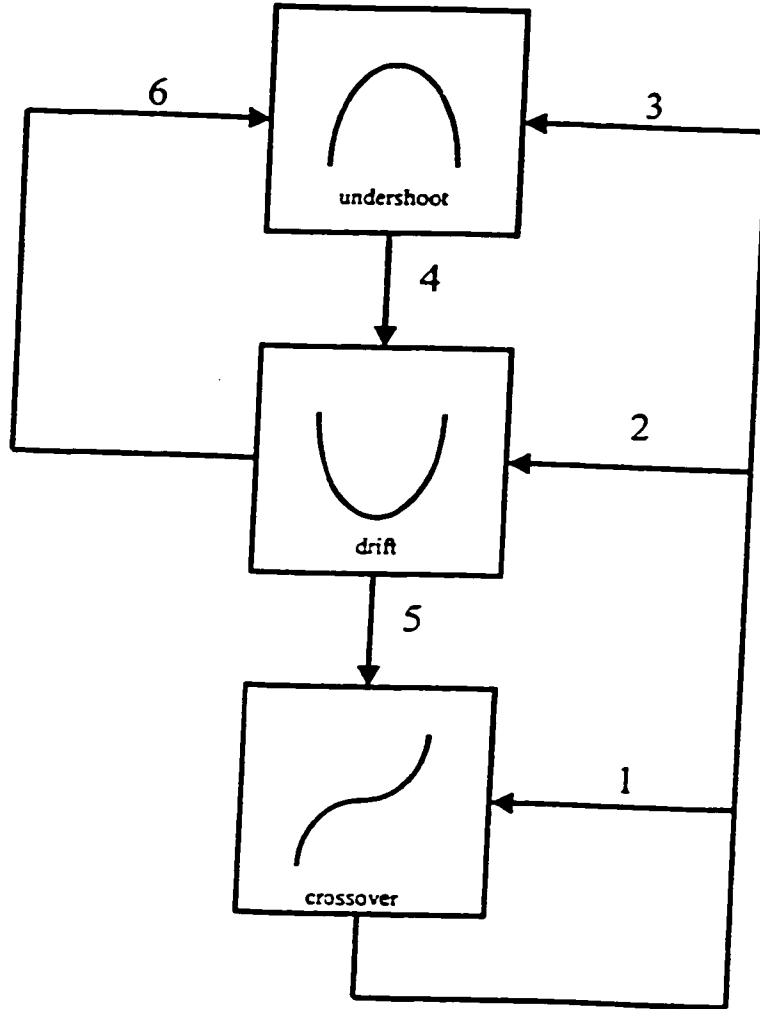
Figure 2.9. Classification system based upon two successive cycles of successful balancing behavior. Here the six different paths that are seen in the experimental data and their corresponding τ_{bal} vs. t curves (see Figures 2.5a-c) are enumerated.

1, or, if the participant follows path number 2 then the crossover of the current cycle will be followed by a drift (the middle box and a U-shaped τ_{bal} curve). When the crossover is followed by an undershoot (the inverted U τ_{bal} curve in the upper box), the participant traverses path number 3.

What happened after a participant performed an undershoot? In all the trials of the experimental data set, undershoot was followed by drift, shown here as path number 4. Once a successful drift was reversed, the participant either returned to a crossover, path number 5, or undershot again (path 6). How did pole falls fit into the classification scheme of τ_{bal} behaviors? The fall of the pole resulted in an incomplete-U τ_{bal} curve (see Figure 2.5d), or a drift that was not reversed. If one substitutes this unreversed drift into the present τ_{bal} behavior classification, making a diagram of unsuccessful balancing cycles, it is apparent that there exists two different routes to failure. Replace the successful drift (middle box) of Figure 2.9 with the incomplete-U curve of a falling pole in Figure 2.10.

What transpired when the participant allowed the pole to fall after a crossover movement (analogous to path 2 in the successful balancing)? Here the participant performed a successful crossover, and decelerated the hand at the base of the pole such that the velocity of the pole approached zero. The pole had not reversed directions, however, and moved away from vertical in the same direction that it crossed the vertical. In order to continue with successful balancing, the participant must now accelerate the pole in the direction opposite to the pole's falling motion, and in the *opposite direction* to

the previous hand movement (see Figure 2.2c). If the participant failed to make this successful reversal of the hand, the pole fell catastrophically. We characterized these cases of failure as a *failure-to-reverse* the hand.

Conversely, consider the participant failing to balance the pole immediately following an undershoot (analogous to path 4 in the successful balancing). Here, the participant undershot the vertical, and then moved his/her hand in the direction of the pole's fall enough to decelerate the pole to a near-zero velocity. As the pole moved away from vertical the participant did not make a successful acceleration of the hand in the *same direction* as the fall of the pole (and the current direction of the hand). We classified this type of failure as a *failure-to-continue* the hand.

From this classification, it is clear that while traversing paths 2 and 4 (see Figure 2.9) the participant must perform an active intervention to prevent a failure. One may thus classify paths 2 and 4 as instances of successfully preventing a failure-to-reverse and failure-to-continue, respectively. Similar to the approach taken by others (e.g. Savelsbergh et al., 1991), we focus on critical situations where an active intervention is needed by the participant to prevent the irreversible fall of the pole. During these two pole sequences (path 2 and 4) it is postulated that the participant must pay special attention to the motions of the pole in order to sustain successful balancing. It was especially during these situations then, that we chose to examine the relation between perceptual variables and pole motions in greater detail.
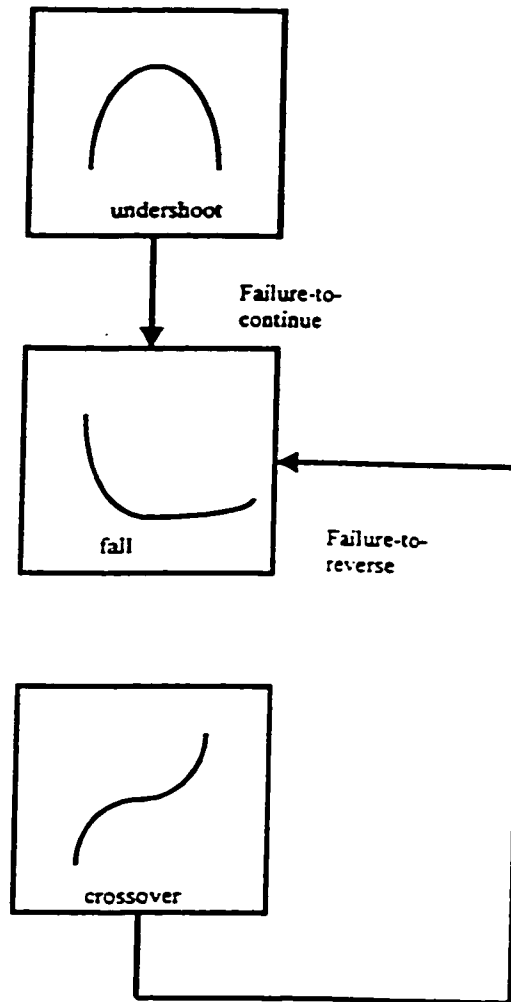
Figure 2.10. Classification system based upon two successive cycles of pole trajectories immediately preceding a catastrophic fall of the pole. Here the incomplete U-curve (τ_{bal} vs. t, see Figure 2.5d) of a pole fall replaces the U-curve found during successful balancing. Two different routes to failure, the failure-to-reverse and failure-to-continue are seen (compare with paths 2 and 4 in Figure 2.9).

2.3.6 Correlational Analysis of Hand and Pole Kinematic Variables

Can one find a strong relationship between a measure of the oscillations of the pole with the perceptual variables identified in this experiment? A correlation analysis was performed on all successful cycles of balancing behavior (see also Wagner, 1982). The half-period of hand velocity ($\dot{x}$, an approximation of the "time to upright" the pole) was correlated with the magnitudes of τ_{bal}, $\dot{\tau}_{bal}$, $\dot{x}$, θ, and $\dot{\theta}$ sampled at the onset of hand deceleration. Also included in this analysis were the complements of τ_{bal} and $\dot{\tau}_{bal}$, specifically τ_{fall} and $\dot{\tau}_{fall}$, which are defined in the following discussion as well as in Treffner and Kelso (1995).

In Table 2.2 the correlation coefficients are reported. The first sets of analyses (first column of Table 2.2) were performed on the kinematic data collapsed across all cycles. No significant relationships were found. In contrast, when partitioned with respect to the τ_{bal} path classification scheme (see Figure 2.9, and columns 2-7 of Table 2.2), a highly significant inverse correlation (r = -0.96) was found between the τ_{bal} values and $\dot{x}$ period during the cycles of path 2 (crossover to drift). Furthermore, during the same pole sequences, relationships that approached significance were seen between the $\dot{x}$ period, $\dot{\tau}_{bal}$, τ_{fall}, and $\dot{\tau}_{fall}$. No similar strength relationship between τ_{bal} and $\dot{x}$ period was found in undershoot to drift (path 4) cycles (note however the relationships with $\dot{\tau}_{bal}$ and $\dot{\tau}_{fall}$). The presence of the significant τ_{bal} and $\dot{x}$ period correlation suggests that participants may be sensitive to the perceptual variable τ_{bal} especially during the critical

situation of avoiding a failure-to-reverse. Note that our experimental data do not show a relationship between τ_{bal} and the period of the pole during typical motions of successful performance. Participants may not be attending to this type of perceptual information during these non-critical situations.

Table 2.2: Correlations Between Hand Motions and Perceptual Variables

| Perceptual Variables | All Cycles | Categorized by τ_{bal} Paths | | | | |
		Path 1	Path 2	Path 3	Path 4	Path 5	Path 6
τ_{bal}	-0.01	-0.33	-0.96	-0.40	0.13	-0.03	-0.04
$\dot{\tau}_{bal}$	0.09	-0.06	0.38	-0.18	0.26	-0.14	-0.08
τ_{fall}	0.01	-0.18	-0.29	-0.26	0.07	-0.02	-0.02
$\dot{\tau}_{fall}$	0.05	-0.13	0.26	-0.17	0.25	-0.17	-0.12
$\dot{x}$	0.04	0.06	0.14	0.07	0.08	-0.02	-0.02
θ	0.03	0.10	0.19	0.02	0.13	-0.01	-0.06
$\dot{\theta}$	-0.04	-0.05	-0.11	-0.07	-0.07	0.01	-0.01

Note. The correlation value in the box represents a highly significant inverse relationship between τ_{bal} and the oscillation of the pole when participants successfully avoid a failure-to-reverse.

2.3.7 $\dot{\tau}_{bal}$ Values Across τ_{bal} Sequence Classification

What are the typical values of $\dot{\tau}_{bal}$ during the onset of hand deceleration? Although $\dot{\tau}_{bal}$ was found to be relatively invariant across learning and pole conditions in the previously presented kinematic analysis (see Figure 2.8), the present classification system allows us to perform an analysis based upon local cycle kinematics that describe *qualitatively distinct* pole motions. Specifically, given the 6 different sequences used in successful balancing (see Figure 2.9), and 2 additional sequences seen during failure (Figure 2.10), one may partition the kinematic data among these 8 categories and examine the values of the perceptual variable $\dot{\tau}_{bal}$ at the onset of hand deceleration. A $(0 < \dot{\tau}_{bal} < 0.5)$ value would predict a decreasing deceleration and an undershoot of the target and $(0.5 < \dot{\tau}_{bal} < 1)$ would predict an overshoot of the target in a "hard collision."

An 8 (τ_{bal} paths) X 36 (participants) ANOVA with $\dot{\tau}_{bal}$ as the dependent variable was performed on all successful balancing cycles, *as well as* those final cycles that denoted a failure. The significant main effect of τ_{bal} paths, $F(7,184) = 6.20$, $p < 0.05$. and post-hoc Tukey tests revealed that the cycles of crossover to crossover (Path 1) had a statistically similar $\dot{\tau}_{bal}$ mean as the crossover to drift cycles, the crossover to undershoot cycles, and the failure-to-reverse cycles. The undershoot to drift cycles, and the drift to crossover cycles had significantly different $\dot{\tau}_{bal}$ means from each other and from the rest of the categories, as did the drift to undershoot and failure-to-continue cycles. Importantly, when the different pole sequences were compared according to whether the

pole overshot the balance point (second column of Table 2.3), or undershot the balance point (third column of Table 2.3), good agreement was found in accordance with previous predictions (see Lee, 1976; Lee, Young, & Rewt, 1992). Note that the mean value in the failure-to-continue sequence may be due to outliers in these particularly noisy data, and that the median value is τ_{bal} = 0.12. These results suggest that functional stabilization may be considered as a collision problem with respect to the balance point on a cycle to cycle time scale.

Table 2.3 Comparison of Mean τ_{bal} Values Across τ_{bal} Path Classification

Sequence	Path	Undershoot $(0 < \tau_{bal} \le 0.5)$	Overshoot $(0.5 < \tau_{bal} \le 1.0)$
Crossover to crossover	1		0.96 (0.07)
Crossover to drift	2		0.87 (0.12)
Crossover to undershoot	3		0.97 (0.08)
Undershoot to drift	4	0.24 (1.77)	
Drift to crossover	5	0.18 (1.66)	
Drift to undershoot	6	0.36 (1.82)	
Failure to reverse	7		0.94 (0.12)
Failure to continue	8	-2.26 (7.72)	

Note. Path refers to τ_{bal} vs. t trajectories shown in Figures 2.9 and 2.10. The τ_{bal} mean of −2.26 in the failure to continue sequence may be due to outlier values. The median value in this sequence is 0.12. Values enclosed in parentheses represent standard deviations.

2.3.8 Functional Stabilization: Modeling Considerations

Figure 2.1 shows a schematic of the cart-pole system used in our analysis of functional stabilization. For the straight pole condition, the mass m is distributed uniformly over the pole length. The angle of the pole is indirectly controlled through an external applied force F acting horizontally on a cart of mass M. For a given F, the equations of motion for cart position X and the pole angle θ may be derived using physical principles and are given in the Appendix A (see e.g. Elgerd, 1967; Ogata, 1978). When formulated as such, the problem of pole balancing often reduces to resolving two key questions: (1) what is the "state" dependence of the function F, and (2) how are the parameters in F modulated to effect a suitable controlled condition. The first question concerns the choice of available kinematic measures (e.g. pole angle and hand position) used to assess the state of the pole. The second question involves the algorithm (and operationally, its physical instantiation) used to implement control. From a control theoretic viewpoint, the variables of choice have always been the canonical ones of pole angle and hand position and their velocities. For the control strategy, linear control in these variables has been successfully applied even outside the linearized regime of the cart-pole system. In explicit form, linear control means

$$F = \alpha_1 \theta + \alpha_2 \dot{\theta} + \beta_1 x + \beta_2 \dot{x} \qquad (2.2)$$

where $\alpha_1, \alpha_2, \beta_1, \beta_2$ are constants. If the unstable system to be controlled has known mechanics, these coefficients may be determined without much difficulty and usually are

specified as a range of parameter values. For systems whose intrinsic dynamics are not a priori well established, neuromorphic controllers (controllers based on artificial neural networks) are often used. The determination of the coefficients (weights in neural network parlance) then defines the control problem. Consider now the specific cart-pole system of Figure 2.1 in which F is implemented by a human controller. In Figure 2.11 we plot the experimental time series of the hand and pole velocities (a), pole angle (b), and the inferred external force F for a representative time interval (c).

To compute F, kinematic information and experimental pole-cart parameters were used as inputs to the equations of motion, which were then inverted to compute the force. Note that pole angle (and to a certain degree, pole and hand velocities) follows F in time, which suggests a strategy based on proportionate or linear control. Note that the control scheme we are proposing asserts the functional form $F = \alpha\theta$, where the determination of the effective coefficient α (possibly non-constant) is the problem. We propose that the perceptual variables τ_{bal} and $\dot{\tau}_{bal}$ are used to evaluate and sometimes adjust the weightings of the linear control function, on a cycle-by-cycle basis, during critical actions where the participant must actively intervene in order to prevent a failure. To see how this may be done, we assume the following equations for the pole angle and cart position

$$\ddot{\theta} = -k_1\theta \qquad \ddot{x} = +k_2\theta \qquad (2.3)$$

where $x = L^{-1}X$ is the hand position normalized with respect to the pole length, and the coefficients k_1 and k_2 are non-linear and possibly discontinuous functions of $x, \dot{x}, \theta, \dot{\theta}$.

Note that this is a perfectly legitimate formulation since no restrictions on k_1 and k_2 are made at this point.

It is helpful to discuss the special case when these functions (k_1 and k_2) are constant. If the controller maintains constant and positive k_1 and k_2 at all times, the pole oscillates about the vertical with a frequency $\Omega = \sqrt{k_1}$ and an amplitude that depends on the initial conditions. From Equation (2.3) we see that the motion of the cart also oscillates at the same frequency. In addition, depending on the initial conditions, the center of oscillation of the cart moves at a constant velocity. On the other hand, if $k_1 < 0$ and constant (k_2 constant, any sign), then, except under very special initial conditions, the pole falls at an exponential rate away from its starting position. The hand executes similar (exponential) behavior plus some constant velocity motion. Plots of the experimental values of k_1 (computed from $-\frac{\ddot{\theta}}{\theta}$) over time, however, show that k_1 may be positive and negative depending on the situation, and varies smoothly except at certain discrete points (see Figure 2.12a for a representative experimental time series). These singularities occur when the θ value approaches zero.
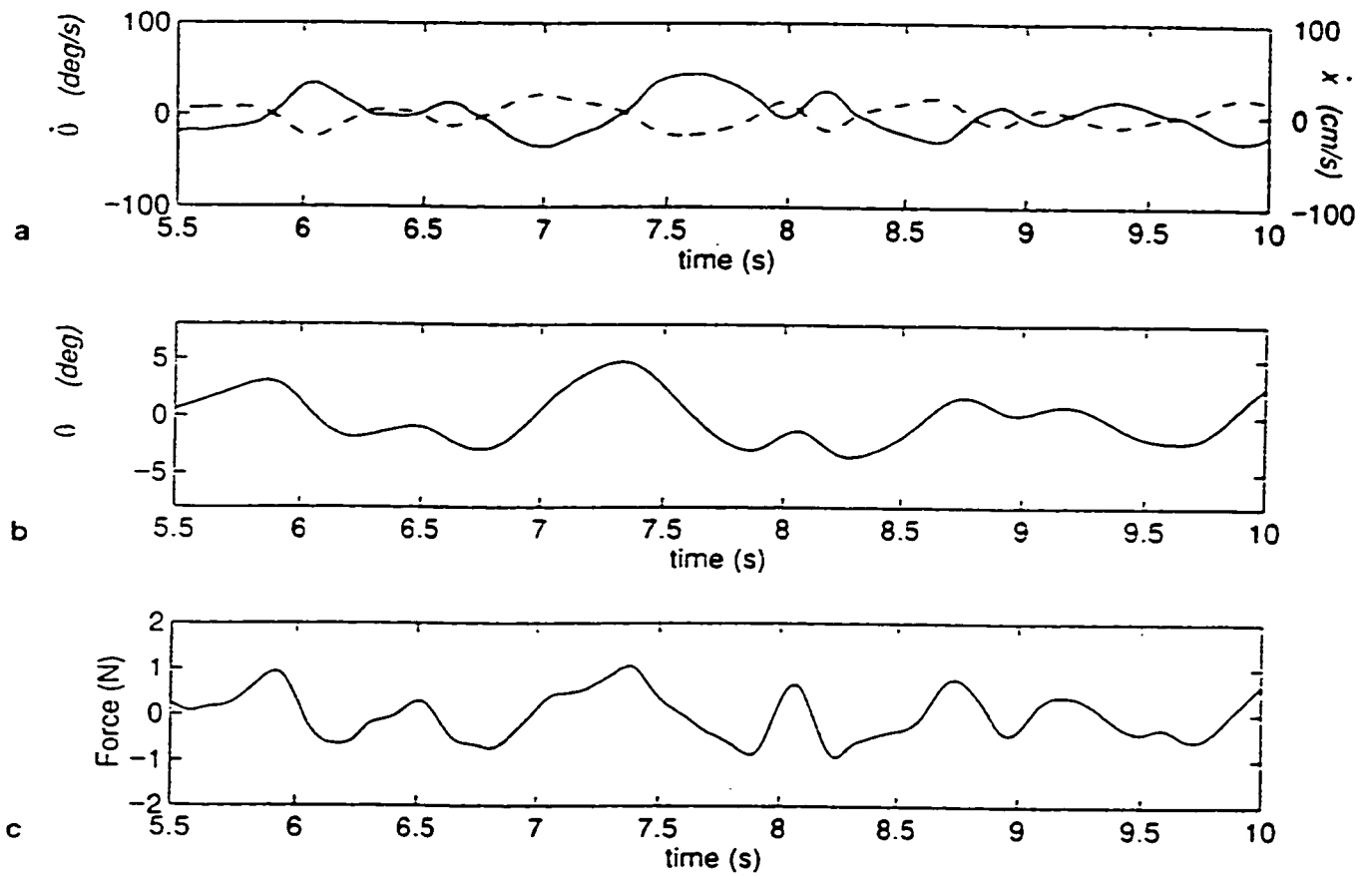
Figure 2.11. Time series of hand velocity (solid lines) versus pole (dashed lines) velocity (a), pole angle (b), and force (c), as computed from equations (A1 and A2). Note the close relationship between the force and the angle during non-periodic pole motions. This implies a k value that is not constant, and that exhibits a complex dynamics (see text for discussion).
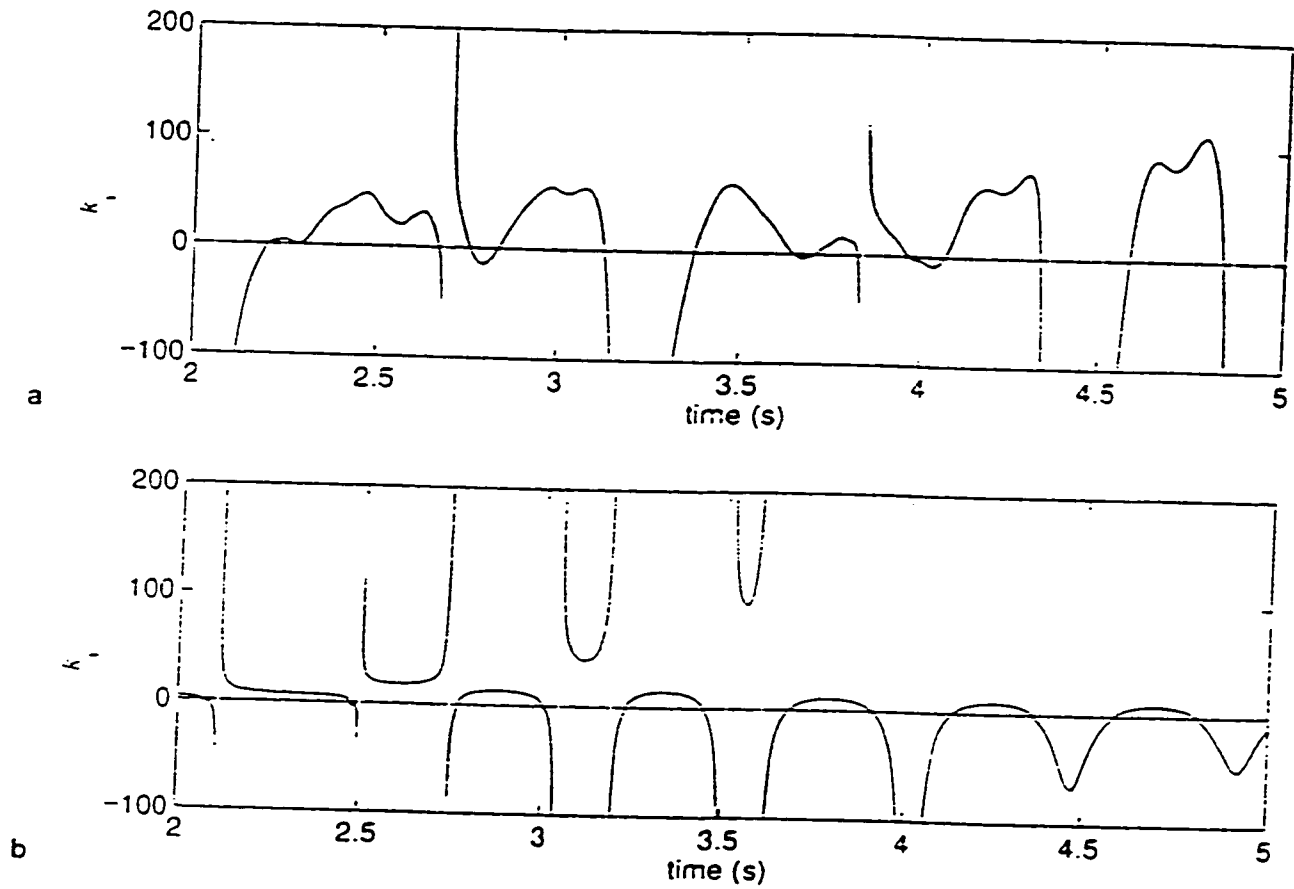
Figure 2.12a-b. Representative time series of experimental (a) and simulated (b) k_1 values obtained from the ratio $-\dfrac{\ddot{\theta}}{\theta}$.

We now consider how the k_1-coefficient relates to the perceptual variables. Differentiating the expression for τ_{bal} with respect to time,

$$\dot{\tau}_{bal} = 1 - \frac{\theta \ddot{\theta}}{\dot{\theta}^2}$$ (2.4)

which, together with Equation (2.3), can be rewritten as $\dot{\tau}_{bal} = 1 + k_1 \tau_{bal}^2$. Upon solving for k_1, this yields

(2.5)

$$k_1 = \frac{\dot{\tau}_{bal} - 1}{\tau_{bal}^2}$$

the relationship we are looking for. Note that the sign of k_1 depends only on $\dot{\tau}_{bal}$

$$k_1 = \begin{cases} < 0, & \dot{\tau}_{bal} < 1 \\ > 0, & \dot{\tau}_{bal} > 1 \end{cases}$$ (2.6)

From the preceding discussions, we saw that for $k_1 > 0$ and constant, the pole oscillates with a fixed frequency and amplitude. Relaxing now this constraint of regular motion, a simple strategy to keep the pole oscillating about the vertical is to keep $k_1 > 0$ at all times. This means maintaining the condition $\dot{\tau}_{bal} > 1$ regardless of the state of the pole and hand. The action of the controller is such that it aims to always overshoot the vertical without considering the consequence for the next cycle. Because of its open-ended nature, this strategy suffers from the undesirable consequences that even though the restoring

47

feature (since $k_1 > 0$) may control the initial oscillations, subsequent motion may lead to increasing excursions in the pole angle and therefore a possible failure.

2.3.9 Possible Control Strategy

In the previous discussion, we explored a simple strategy for pole balancing without specifying exactly how the internal mechanisms of the controller are modified contingent on the perceived state of the pole. To be able to do more, one must incorporate some physical aspects of the problem as well as a model of the control mechanism. For the moment, we disregard the effect of the horizontal velocity and assume that the force is dependent only on $\theta, \dot{\theta}$, and x. Just as we have expressed the motion of the pole angle using a harmonic-like equation, we now assume that the physical force applied by the hand to the cart can be expressed in the form $f = \alpha_1\theta + \alpha_2\dot{\theta} + \beta x$, where β is a constant and α_1, α_2 are functions whose variations will be specified shortly. Here, we have used the reduced form of the force, $f = L^{-1}m^{-1}(m+M)^{-1}F$ as given in the Appendix A. The control force can be rewritten as $f = (\alpha_1 + \alpha_2\tau_{bal}^{-1})\cdot\theta + \beta x = \alpha(\tau_{bal})\cdot\theta + \beta\cdot x$ where τ_{bal} is as defined in Equation (2.1). For the purpose of easing the discussion, we consider the linearized form of the full equations of motion (Equations A3 and A4 of the Appendix A). In the linear region, the functions k_1, k_2 in Equation (2.3) are given by

$$k_1 = \frac{\alpha - \omega^2 + \beta\cdot x/\theta}{\frac{4}{3} - \mu} \tag{2.7}$$

$$k_2 = \frac{\frac{4}{3}\alpha - \mu\omega^2 + \frac{4}{3}\beta\cdot x/\theta}{\frac{4}{3} - \mu} \tag{2.8}$$

(see Appendix A). Since the principal stimulus is the visually specified pole angle, we assume that the variation of the parameters is implemented principally through the α, and keep the x coefficient β constant (note that μ is the normalized mass). We recall from a previous discussion that keeping $\dot{\tau}_{bal} > 1$ at all times means $k_1 > 0$ so that, although there is always a restoring force on the angle, there is a possibility for failure due to uncontrolled oscillation amplitude. Instead of this open-ended condition, consider the case when the controller tries to maintain the condition $\dot{\tau}_{bal} = 1$. When imposed at all times t, this also leads to the unrealistic situation of no oscillation at all (i.e. the frequency $\Omega = \sqrt{k_1} = 0$, identically). For successful balancing, $\dot{\tau}_{bal}$ need only to be kept within the range from 0.5 to 1. Additionally, $\dot{\tau}_{bal}$ need not be restricted as such all the time, but only at time points T_n of peak hand velocity or onset of deceleration (see Table 2.3). In contrast, movement cycles that lead to pole undershoots and sometimes failure yield $\dot{\tau}_{bal}$ below 0.5 at the same time points T_n (Note that by Lee's (1976) analysis, a pole moving upright and maintaining $\dot{\tau}_{bal} = 0.5$ *at all times* reaches the vertical with zero velocity and acceleration). This suggests a control strategy that keeps $\dot{\tau}_{bal}$ between 0.5 to 1.0. Assume that before the application of the control action, $\dot{\tau}_{bal} < 0.5$, and thus there is a potential for undershooting the vertical. Then, at the next time instant in order to increase $\dot{\tau}_{bal}$ to 0.5, a controller must increase k_1 at least by an amount, δk_1, where

$$\delta k_1 = \left| \frac{\dot{\tau}_{bal} - 0.5}{\tau_{bal}^2} \right|$$

(2.9)

49

From Equation (7), this can be implemented by incrementing α by an amount

$\delta\alpha = \left(\frac{4}{3} - \mu\right) \cdot \delta k_1$. In the opposite case of $\dot{\tau}_{bal} > 1$, the controller must decrease k_1 by the

same amount above to reduce $\dot{\tau}_{bal}$ to 0.5, or alternatively, by an amount

$$\delta k_1^{\bullet} = \left| \frac{\dot{\tau}_{bal} - 1}{\tau_{bal}^2} \right| \qquad (2.10)$$

(i.e., $\delta\alpha = \left(\frac{4}{3} - \mu\right) \cdot \delta k_1^{\bullet}$) to bring down the value of $\dot{\tau}_{bal}$ to 1, To test the suitability of the

above strategy, we simulated the hand and pole motion using a simple update rule. The

parameter α was incremented or decremented by a small amount $\Delta\alpha = \varepsilon \cdot \left(\frac{4}{3} - \mu\right) \cdot \delta k_1$ or

$\Delta\alpha = \varepsilon \cdot \left(\frac{4}{3} - \mu\right) \cdot \delta k_1^{\bullet}$, $0 < \varepsilon < 1$, depending on whether $\dot{\tau}_{bal}$ was less than 0.5 or greater

than 1 at time points when the hand velocity reached an extremum. After changing α, its

value was fixed for the duration of the movement cycle (i.e. until the next peak hand

velocity was again encountered). After a few iterations, $\dot{\tau}_{bal}$ was expected to stabilize to

either 0.5 or 1 at peak hand velocity positions. Note that k_1 is a function not just of α but

also of the other state variables. Setting $k_1 = 0$ or, equivalently, $\dot{\tau}_{bal}$ to 1 at peak velocity

maxima does not mean k_1 is zero at all times. In fact, k_1 may be positive or negative

depending on the state of the pole. In Figures 2.12b and Figure 2.13 are shown the results

of a simulation using the above-mentioned strategy. Plots of the time series of $\dot{x}$ (solid

lines) and $\dot{\theta}$ (dashed lines) are shown in Figures 2.13a. The corresponding simulation for

τ_{bal} and $\dot{\tau}_{bal}$ are shown next in Figures 2.13b and 2.13c. Notice that these plots

correspond to time series of the same variables from the experimental data shown in Figures 2.4a to 2.4c. Initially the pole exhibits essentially periodic oscillations. After some iteration however, undershoots occur in which the pole does not quite reach the vertical. The simulation shows qualitative agreement with our experimental data (compare with Figure 2.4). The phase portrait τ_{bal} vs. $\dot{\tau}_{bal}$, plotted in Figure 2.14, also compares quite favorably with the experimental phase portrait of Figure 2.6. Parabolic curves correspond to successful crossing of the vertical. The outermost curves result from undershoots and drifts (see discussion of Figure 2.6). Apparent gaps in the trajectories are due to the discrete nature of the updates of the α parameter in our model.
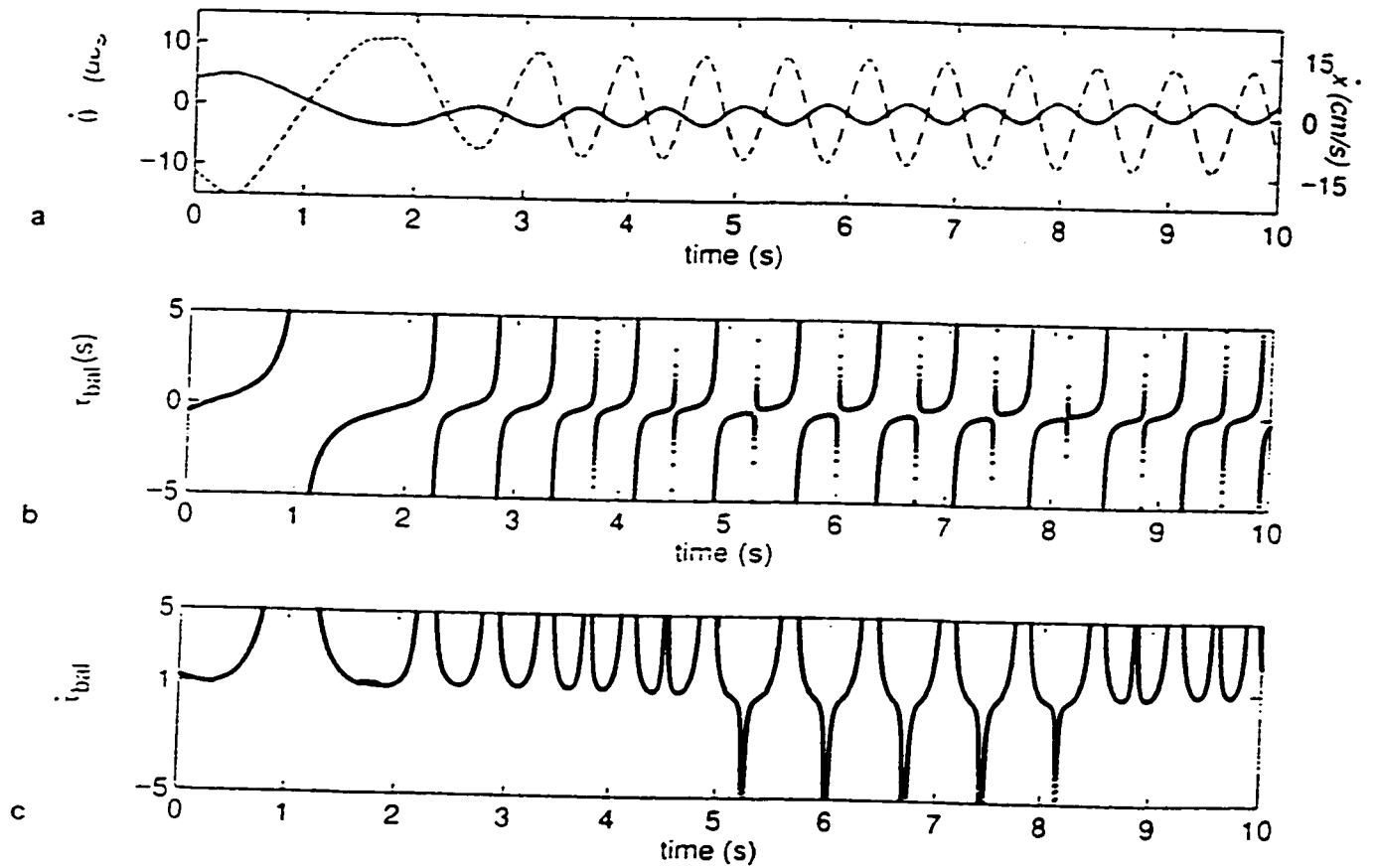
Figure 2.13a-c. Simulation of (a) hand (solid lines) and pole velocities (dashed lines), (b) τ_{bal}, and (c) $\dot{\tau}_{bal}$. The parameters used were: $\beta = 4.6$, $\varepsilon = .75$, $\alpha_0 = 2.8$ for the initial value of α, $\mu = 0.4$, $\omega = \sqrt{9.8}$, noise standard deviation of 0.001, and a simulation run-time of 100 sec. Initial conditions were: $\theta_0 = 28\deg$, $\dot{\theta}_0 = -11.5\deg/\sec$, $x_0 = -50cm$, $\dot{x}_0 = 4.1cm/\sec$.

52
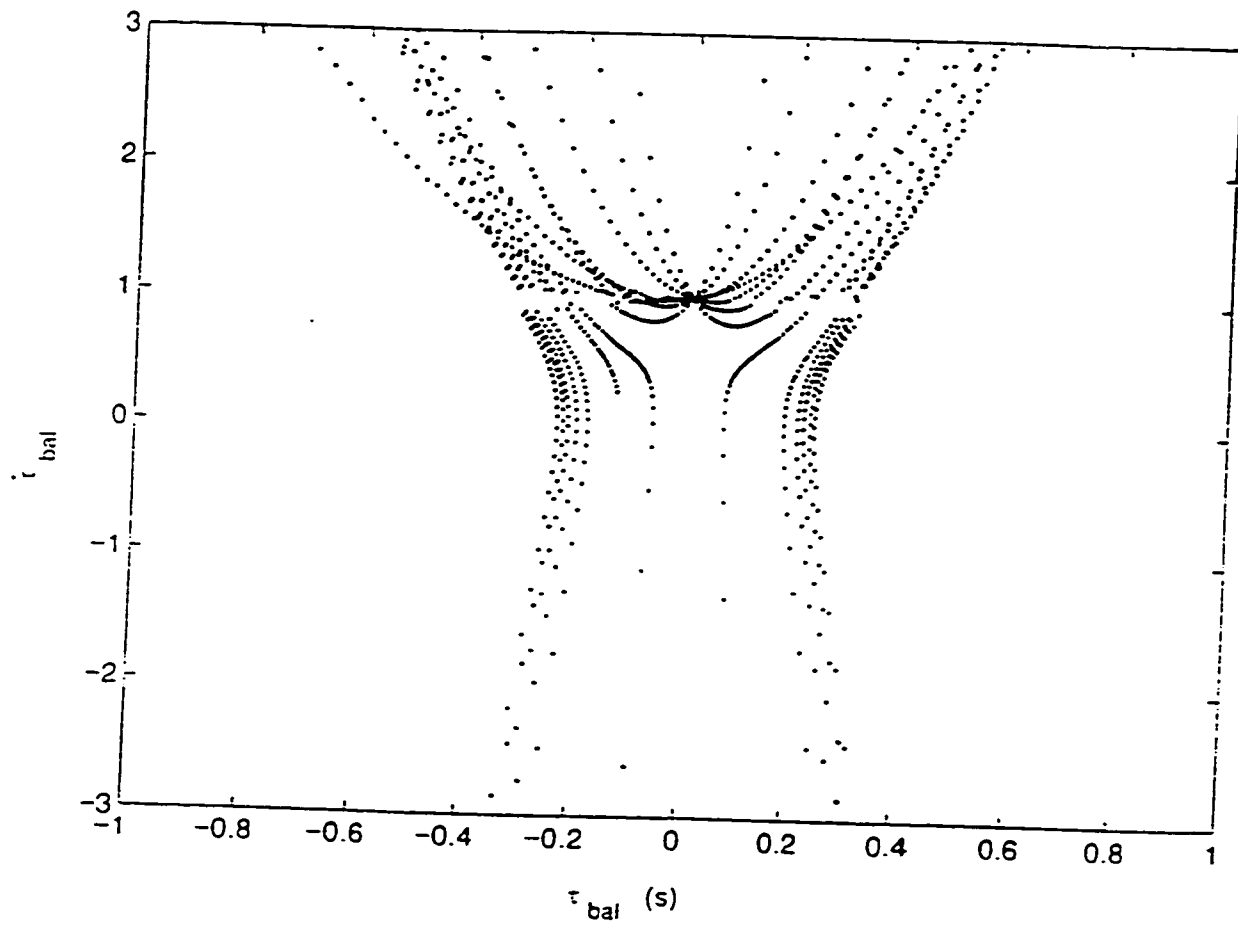
Figure 2.14. Phase portrait of $\dot{\tau}_{bal}$ vs. τ_{bal} using the simulation of Fig. 2.13.

2.4 General Discussion

Similar optical variables (to τ_{bal}) have been shown to be available to human observers through changes in retinal flow fields. Early works showed that ambient optic arrays which produce retinal expansion patterns provide important information about approaching objects and can elicit avoidance or defensive behaviors in animals and infants (Schiff, 1965; Schiff et al., 1962). Manipulations of the incident optic array have also provided evidence that when catching oncoming objects, participants gear their actions to optic-τ rather than to separate distance and velocity information. For example, Savelsbergh et al. (1991) showed that the time of appearance of the maximal closing velocity (and opening velocity, see Savelsbergh, 1995) of the hand was significantly later for an oncoming ball presented as progressively deflating than for a ball of constant size. This suggests that participants geared their actions to the characteristics of the deflating ball and not solely to its time of arrival based on computations involving position and velocity attributes.

For the current experimental research, τ_{bal} specifies the relative rate of constriction of the angle the pole makes with the vertical. There has been controversy in the literature concerning the types of perceptual information (e.g. visual and auditory) that are available to observers (e.g. Lee & Reddish, 1981; Shaw, McGowan, & Turvey, 1991; Tresilian, 1994; Wagner, 1982), how these different modalities may be combined (Savelsbergh, Whiting, & Pepers, 1992; Tresilian, 1994), and to what extent the empirical

54

data support the optic-τ versus alternative possibilities (Bootsma et al., 1997; Bootsma & Oudejans, 1993; Savelsbergh, 1995; Tresilian, 1994, 1995;Wann, 1996).

Our results show that, while there are differences in the initial performance between balancing a straight versus an L-pole (e.g. Figure 2.3a and 2c), these differences become insignificant as the participants become more skilled at the task (e.g. Figure 2.3b and 2d). This indicates that participants eventually learn the balance position of the L-poles and adapt such that the resulting behavior is indistinguishable from that of a straight pole task. One crucial component of the process of learning to balance the L-pole, seems to be in the initial act of setting up the pole. Since the balance position does not manifest itself until after the participant has moved the pole or manipulated the initial conditions, this suggests that the perception of this physical attribute (equilibrium position) is acquired dynamically. If the participants had aligned the L-shaped pole with an absolute reference (the vertical position) instead of the dynamically acquired balance point, the pole would fall in the same direction of the *open end* of the L-shaped pole (e.g. to the left for the L-poles in figure 2.1b-c). In fact the participants that were rejected from this experiment demonstrated significantly more falls in this direction during the failed acquisition trials of the L-shaped poles, χ^2 (1, N = 28) = 182.08, p < .01. These participants did not typically set the initial conditions of the task at this balance point (in contrast to successful participants, especially later in practice), and were not able to identify the balance point of the L-shaped poles during exit interviews. Evidence of perception of physical attributes that are not directly available is also found in other

studies. For example, by actively wagging a non-uniform stick, a person acquires information on essential (with respect to translational and rotational motions) attributes of the object such as its inertia tensor (Pagano & Turvey, 1992; Turvey, Burton, Pagano, Solomon, & Runeson, 1992). Since the present analysis centers on the kinematics of successful balancing, rather than on the participants' acquisition of this skill, the question of how one can adjust his/her action to fit different physical constraints (i.e. different balance points) was not explored in detail. This will be an interesting topic for future research.

The postulated control strategy in balancing may be compared with that used in controlled braking. Although the essence of the controls in both cases is the same, i.e. both use $\dot{\tau} = c$ at some point, the resulting dynamics are, of course, very different. In Lee (1976), it can be shown that the regulated motion is one of constant deceleration caused by a frictional force. Since the effect of friction ends the moment the stop position is reached, there is no need for analysis beyond the goal position. In pole balancing, the destabilizing factor of gravity acts like a reverse spring (at least for small angles) and is balanced by the spring-like mechanism of the controller. Another difference between the two systems is the way τ-information appears to be used. Whereas Lee's (1976) strategy is to modulate continuously action based on the current value of $\dot{\tau}$, here the stiffness parameter is updated only near peaks of hand velocity. Although our data indicate that $\dot{\tau}_{bal}$ was conserved most of the time near such points, it is still unclear whether this is the strategy itself, or a part of, even a consequence of, some other strategy. Previous experiments by Treffner and Kelso (1995) suggest that a more complete description may

have to include another τ-variable, the inverse of the rate of change of the angle with respect to the horizontal. In Treffner and Kelso (1995) this was called τ_{fall} and was found to be nearly conserved at points of maximum hand velocity. It can be shown that the pair $(\tau_{fall}, \tau_{bal})$ can be derived from $(\theta, \dot{\theta})$ and vice versa. Thus, no information is lost. They are just represented and perceived differently.

2.5 Conclusion

To survive in a changing environment, biological systems often must adopt means for quickly and efficiently regulating their actions. An important, but largely unstudied subset of these tasks is functional stabilization in inherently unstable situations, addressed here using the prototypical task of pole balancing. We showed how the task may be accomplished by utilizing visual perceptual information to adjust a parameter of a linear controller. To a certain extent, the control strategy we have presented parallels that used in some artificial neural networks. One key feature of a neuromorphic linear controller is the adjustment of the "weights" using an update rule. In our case, we use constraints on a perceptual variable (τ_{bal}, a temporal measure) to adjust a parameter (here, also a temporal measure related to the fall time of the pole) of a linear controller. We propose that the perceptual variables τ_{bal} and $\dot{\tau}_{bal}$ are used to monitor and sometimes adjust the weightings of this linear control function, on a cycle-by-cycle basis, during critical actions where the participant must actively intervene in order to prevent a failure. We performed a learning and transfer experiment to explore a hypothesized balancing strategy based on the variable τ_{bal}. For successful balancing, regardless of the general configuration and

inertial properties of the pole, participants couple their hand movements to the movements of the pole. These actions are most predictable near regions of hand velocity extrema where participants exhibit quite consistent values of $\dot{\tau}_{bal}$. Successful balancing, in which the pole is maintained upright with some degree of oscillation, yields $\dot{\tau}_{bal}$ ranging from 0.5 to 1.0 at the onset of interceptive hand action. Perceived deviations from the above range may be used prospectively to adjust a future action.

3.0 Functional Stabilization of Virtual Systems

Using Time to Balance Information

3.1 Experiment 2: Introduction

In this experiment we investigate what visually available information is used to perform a functional stabilization task. Is the information that is used to balance a real inverted pendulum the same as employed to control a virtual simulation of that mechanical system? If essential elements of this visual information are withheld from participants, can one still successfully balance the pole? Do participants use different perceptual quantities when the mechanics of an unstable system are systematically decoupled from the visual information about that system? When one is forced to map a transformed action onto visual stimuli, what deviations from the foregoing normal relationships may be seen? Do these types of visual information provide robust support for functional stabilization in the presence of perturbations?

In a series of experiments, we have used the task of balancing an inverted pendulum with the hand as a window into how humans functionally stabilize unstable systems (Foo, de Guzman, & Kelso, in preparation; Foo et al., 2000; see also Treffner & Kelso, 1995; 1997; 1999). The task of balancing an inverted pendulum is an especially challenging stabilization problem because of its intrinsic dynamics. An inverted pendulum possesses the characteristics of an *unstable* fixed point, or a repellor (e.g. Strogatz, 1994). The intrinsic dynamics of a repellor system dictate that after any

infinitesimal deviation from its balance point, the system will asymptotically move toward a fall of the pendulum. Because of these intrinsic failure-seeking dynamics, when participants simply react to the motions of the pole, they inevitably react too slowly and the pole falls to the track (see Foo et al., 2000). If participants over-anticipate the pole's motion, equally dire consequences result. Moreover, at every point in time, the participant is actually perturbing the very system he or she is trying to stabilize: the task/environment affects the participant and vice-versa.

The goal of the present research is to identify the nature of visual information used to balance an inverted pendulum. While previous research has identified a time-to-fall variable as having the least variation prior to the onset of hand deceleration (see Treffner & Kelso, 1995), we have shown that a significant inverse linear relationship exists between a participant's hand oscillation and the visually specified time-to-balance especially during potentially catastrophic situations (Foo et al., 2000). The time-to-balance (τ_{bal}), is defined as the ratio of the angle of the pole with the vertical and its instantaneous rate of change:

$$\tau_{bal} = \frac{\theta}{\dot{\theta}} \tag{3.1}$$

When τ_{bal} is negative its magnitude is an approximate measure of the time to upright the pole. Optical variables similar to τ_{bal} have been shown to elicit avoidance, defensive, or interceptive behaviors in animals and humans (Lee & Reddish, 1981; Schiff, 1965; Savelsbergh et al., 1991; Schiff et al., 1962), although there is some question as to what extent the empirical data support the use of optic-τ versus alternative possibilities

(Bootsma et al., 1997; Bootsma & Oudejans, 1993; Savelsbergh, 1995; Tresilian, 1994, 1995; Wann, 1996). Importantly, we have shown that only during potentially catastrophic situations does the aforementioned relationship exist between the actions of the hand and the time-to-balance. Because of this evidence, we focus the present investigations around critical, potentially catastrophic situations where further evidence of the use of τ_{bal} information may be obtained.

Is the information that is used in balancing a real inverted pendulum the same information that may be employed when controlling a virtual simulation of that mechanical system? Virtual reality environments are under development in many areas including architectural, entertainment, tourism, and sports applications (Hansson, 2000; Morizono & Kawamura, 1998). There is a growing trend toward using virtual reality simulations to save money and time and to increase safety when training pilots, tank crews, and surgeons (Dutta, 1999; Playter &Raibert, 1997). The effectiveness of these training methods is based upon the implicit assumption that skill in utilizing the presented (visual) information in the simulation transfers to the real situation. Here we test that assumption with a control condition that simulates the typical cart-pole system (see also Mehta & Schaal, 1999). We hypothesize that participants will use the same τ_{bal} information (Equation 3.1) to stabilize the simulated balancing pole.

Next we directly test previous findings that time-to-balance information supports functional stabilization by manipulating the visual information available to the participant. In the virtual environment one can occlude the image of the pole and cart system as much as one wants. It is possible even to reduce the visual information such

that even the pole angle is unavailable to the participant. In such situations, do subjects represent an internal model of the angle of the pole (or indeed richer visual variables such as r_{bal}) to successfully complete the task?

Which perceptual quantities are needed to complete the task when the mechanics of an unstable system are systematically decoupled from its corresponding visual image? It is important to separate physically the actor from the object being controlled, since it has been demonstrated that important information (e.g. the inertial tensor or balance point) about the object can be gleaned via hatpic touch (Foo et al., 2000; Treffner & Kelso, 1995; 1997; 1999; Turvey et al., 1992). In a similar task to the one presented here, participants developed a specialized balancing strategy that increased the haptic information about the system, and supported successful balancing (Foo et al., in preparation). Similarly, touch with an object has been shown to aid one's control of a virtual simulation (using force feedback, see Castro, Postigo, & Manzano 2000).

In the virtual world one may effectively perform this decoupling to produce extreme manipulations of the underlying mechanics of the simulated system, both a prioi and as real-time changes. In earlier experiments it was shown that a manipulation of the balance angle or intrinsic frequency of "fall time" of the pole depressed acquisition but not retention performance (Foo et al., 2000), and here we increase the strength of these manipulations. We introduce both a systematic manipulation of the balance angle of the pole as well as an on-line perturbation of the length and intrinsic frequency of the pole.

What visual information is used to stabilize an unstable system when one is forced to map a transformed action onto one's visual inputs? Previous experiments have

altered the mapping between action and perception via mirrored surfaces or prism glasses (McGonigle & Flook, 1978; Redding & Wallace, 2000; in speech, Houde & Jordan, 1998), and a similar condition is included in this experiment. In the action-mapping condition, while the visual information is true to the cart-pole system, the actions of the participant undergo a manipulation.

Do these types of visual information provide robust support for functional stabilization in the presence of perturbations to the apparatus? Another advantage to studying this system in the virtual world is the abi4lity to perturb effectively the system in real time as participants balance the pole. Perturbations can be used as an index into the stability of a dynamical system (see Scholz, Kelso, & Schöner, 1987), but are used here primarily to elicit the types of critical situations that appear to bring out the τ_{bal} relation. These perturbations are used in all of the preceding conditions with the exception of the on-line manipulation of pole frequency, which is in itself, a perturbation.

Thus nine different experimental conditions are tested in the present experiment. To confirm and elaborate upon the previous time-to-balance findings, participants balanced a normal inverted pendulum, an occluded pole, a pole with an altered balance angle. one with a variable intrinsic frequency, a normal pole matched with a transformation of the participants' actions, and all of the preceding conditions with a randomly generated angular velocity perturbation. A replication of the correlational analysis of Foo et al. (2000) was employed to confirm and extend previous findings that showed during critical motions of the pole, the visually specified time-to-balance is used to gear the corrective actions of the pole. It was hypothesized that regardless of the

conditions, participants would use the same visually specified "time-to-balance" information (i.e. τ balance) to stabilize the inherently unstable inverted pendulum.

3.2 Method

3.2.1 Participants

Four right-handed adult volunteers who met a performance criterion (3 consecutive 90 s long trials in the control condition) were used. All subjects signed an informed consent prior to data collection in accordance with APA requirements.

3.2.2 Apparatus

The experimental apparatus consisted of a Dell OptiPlex GxPro personal computer and a (40.64 cm X 40.64 cm) Wacom ArtZII digitizing tablet (see Figure 3.1a). Over the digitizing tablet a custom built linear track (60 cm long) served as the base of support for an aluminium cart (172.5 g) that held a digitizing pen and an accelerometer (Analog Devices ADXL105) constrained to move for 20 cm along the X-axis. Signals from the tablet (accurate to +/- 0.25 mm) and the accelerometer (2 μ g's accuracy) were sampled at 50 Hz. A custom-built simulation program running on Visual C++ generated the virtual inverted pendulum, which was controlled with the inputs of the digitizing pen and accelerometer (see Appendix B). A high-resolution monitor refreshed the screen image at a rate of 75 Hz, producing lifelike motion. There were several pole configurations, outlined in the procedures section, but the basic pole was designed to simulate the inverted pendulum apparatus that was used in previous experiments (see Foo
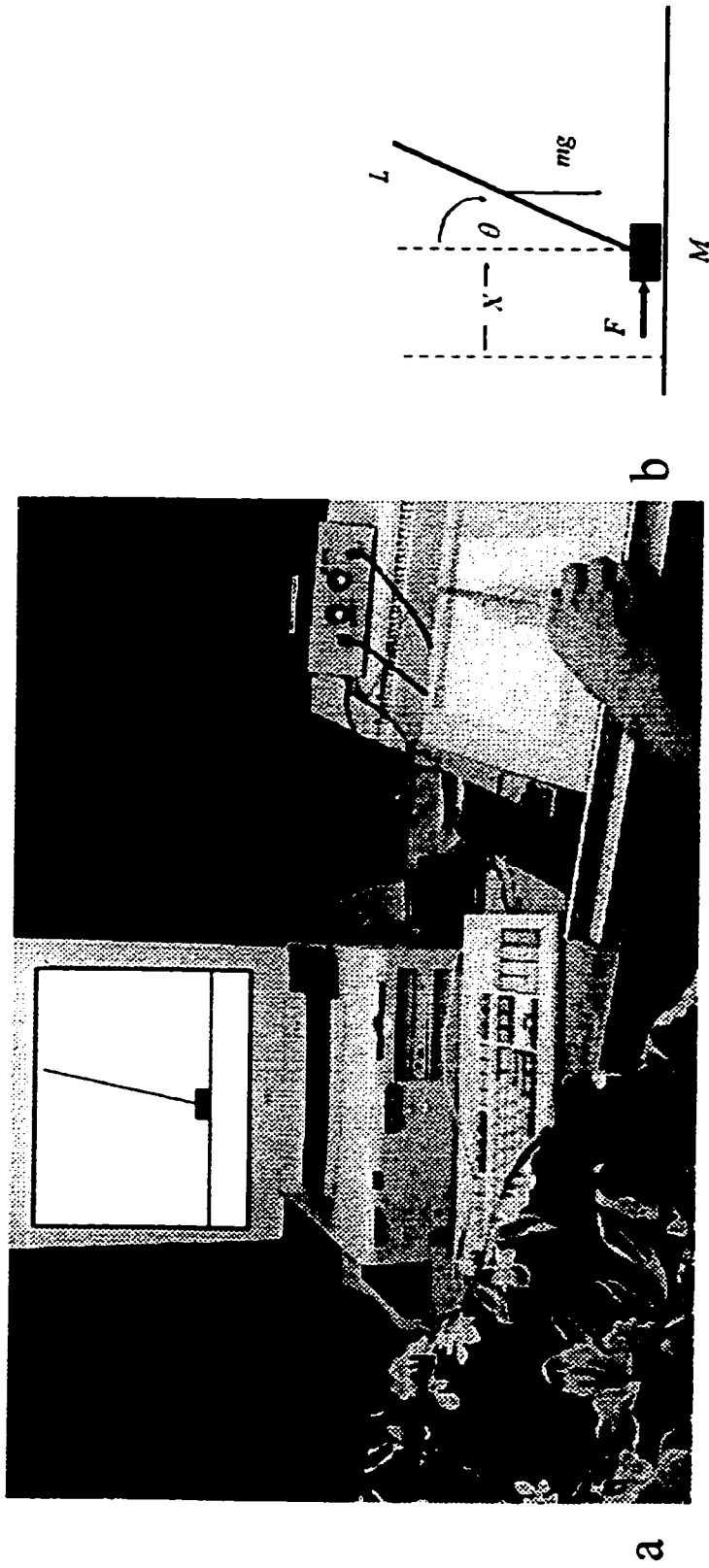
Figure 3.1a-b. (a) The experimental setup consisting of a personal computer and a digitizing tablet over which a linear track with an aluminum cart holds a digitizing pen and an accelerometer. A custom-built simulation program generates a virtual inverted pendulum, which is controlled by the inputs of the digitizing pen and accelerometer. This experiment was designed to simulate the inverted pendulum apparatus that was used in previous experiments (see Foo et al., 2000; Treffner & Kelso, 1995, 1999). (b) Schematic of an inverted pendulum pivoting on a cart that is affixed to a horizontal linear track. The convention used is: θ is positive (negative) when the pole is right (left) of the vertical; M = mass of the cart, L = pole length, m = pole mass, F = force applied by moving the cart and pen over the digitizing tablet.

Figure 3.1

et al., 2000; Treffner & Kelso, 1995, 1999). This virtual pendulum consisted of a straight pole, 14.30 mm long by 2.9 mm wide, and a cart 114.7 mm wide by 57.4 mm tall (see schematic, Figure 3.1b).

3.2.3 Procedures and Design

The task for the subjects was to balance a virtual inverted pendulum for as long as possible during a 90 s testing session. Subjects repeated ten sessions of each of nine conditions, presented randomly. No instruction was given to the participants pertaining to how to balance the pole. However, we note that these participants had already met a performance criterion and were already skilled at the task. Unlike previous experiments, the initial conditions of all trials were set to $\theta = 0$ and $\dot{\theta} = 0$ by the computer (see Foo et al., 2000; Treffner & Kelso, 1995, 1999). Data collection was carried out for each testing session. Within each testing session, subjects performed as many successful trials of balancing as they could. When the participant lost control and the pole fell to the track the individual trial was ended. The display and the pole variables were then reset for the next trial. This was repeated until the entire 90 s testing session was completed.

3.2.4 Experimental Manipulations

Experimental conditions are schematically represented in Figure 3.2a-i. In each figure one can see a cart, a straight pendulum, and a linear track that extends across the figure. The arrow at the bottom of each figure represents the direction of motion of the cart when the hand is moved to the right. In the top row (Figures 2a-d) a schematic representation of the first four experimental conditions are shown, and in the bottom row (Figures 2e-h) the conditions are identical (by columns) with the addition of the computer

generated angular velocity perturbation. On the right in Figure 3.2i is the parametric manipulation of pole length.

Control Condition

The control condition (Figure 3.2a) is how one would normally implement a pole balancing task. Here the whole pole and cart is visible to the participant and the motion of the cart follows that of the hand.

Vertically Flipped Condition

Figure 3.2b shows the vertically flipped manipulation used in the inverted case. The intrinsic balance point of the pole was radically transformed by the following relation (from here on, the prime values denote the transformed variables):

$$\theta' = (180 - \theta) \qquad\qquad (3.2)$$

Because of the magnitude of this transformation (the inverted pendulum system *was itself* inverted), the visual image presented to the subject described a normal pendulum that normally exhibits the properties of an attractor, or stable system, and not the unstable characteristics of a repellor. In this manipulation the unstable dynamics of the upright pole were not affected, thus the visual image was decoupled and transformed whereas the underlying mechanics of the pendulum were unaffected.

Action-Mapped Pole

Figure 3.2c shows a schematic of the action mapping condition. Here the perceptual information about the angle and motion of the pole remained true to the underlying mechanics of the pole, but the mapping between perception and action was
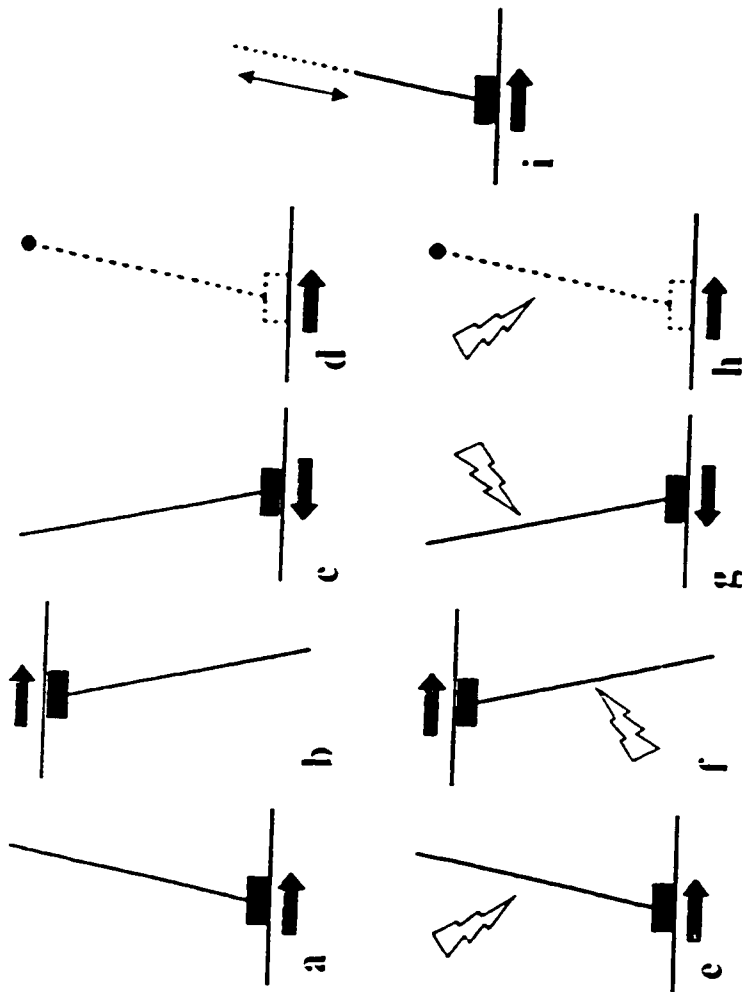
Figure 3.2a-i. An illustration of the nine experimental conditions used in the present experiment. In all of the figures one can see the horizontal linear track, the cart, and the straight pendulum. The arrow at the bottom of each figure represents the direction of the cart moves when the participant moves the digitizing pen to the right. The top row (Figures 3.2a-d) exhibits the details of the first four experimental conditions, and the bottom row (Figures 3.2e-h) indicates the complementary conditions that included a computer-generated angular velocity perturbation (averaging once every 2 s, see the lightning icons). The first column Figures 3.2a and 3.2e, shows the control condition of a simulated inverted pendulum, and it's perturbed counterpart. The next three columns describe the vertically flipped pole (Figures 3.2b and 3.2f), the action-mapped pole (Figures 3.2c and 3.2g), and the occluded pole (Figures 3.2d and 3.2h), respectively. In Figure 3.2i, the pole parameter alteration is shown. Detailed descriptions of these conditions can be found in the text.

68

Figure 3.2

distorted. The cart motion and pole angle were treated to a horizontal symmetry operation:

$$x' = -x \qquad\qquad (3.3)$$

As a result, when the participant moved his or her hand in one direction, the cart moved in the opposite direction. Similarly, the pole angle was transformed to reflect this transformation.

$$\theta' = -\theta \qquad\qquad (3.4)$$

Here the participants were required to perform a mirror movement to the action that the visual information specified.

<u>Occluded Pole</u>

In Figures 2d the occluded pole condition is illustrated. This condition was designed to test directly previous findings that time-to-balance information supports functional stabilization by manipulating the visual information available to the participant. Specifically, since it was shown that the ratio of angle and angular velocity subserved successful pole balancing (see Equation 3.1), we removed visual angle information to determine if participants could still complete the task. Here a small circle (6.3 mm in diameter) was used to mark the top of the inverted pendulum, but no other visual information about the base of the pole or cart was available. Thus although perceptual information was impoverished here, the underlying dynamics of the inverted pendulum remained unchanged.

Pole Parameter Alteration

The parameters of the pole were manipulated online in such a way as to alter the intrinsic dynamics of the system in the virtual simulation (see Figure 3.2i). The computer program was designed to shorten and lengthen repeatedly (average interval of 2000 ms, with a +/- 50 ms random variation) the pole by a factor of two. This manipulation affected the mechanics of the pole, but was not accompanied by a commensurate change in the visual display. The intrinsic pole frequency (ω) of a simple inverted pendulum is a function of its length (L) and the acceleration due to gravity (g):

$$\omega = \sqrt{\frac{g}{L}} \qquad . \qquad (3.5)$$

Thus shortening the length of the pendulum by a factor of two altered its intrinsic frequency or "fall time" by $\sqrt{2}$ in the following manner:

$$\omega' = \sqrt{2}\omega \qquad . \qquad (3.6)$$

Here the mechanics of the upright pole were manipulated in real time, but the visual image was decoupled and remained constant (the pole retained its 14.30 mm length).

Angular Velocity Perturbation

Perturbations to the pole's motion were applied to the four manipulations previously listed (see Figures 2a-d) and are schematically shown in the bottom row of Figure 3.2 (see Figures 2e-h). During a perturbation trial, the computer program generated 45 perturbations of the pole at random intervals (average interval of 2000 ms, with a +/- 50 ms random variation). For each perturbation the angular velocity was

incremented by 30 deg/sec in the direction away from the unstable balance point. These perturbations were designed to induce critical situations, which required more focused attention and corrective actions (Foo et al., 2000).

3.2.5 Data Analysis

The participants balanced the virtual inverted pendulum system as long as possible during ninety testing sessions (10 repeated sessions of 9 experimental conditions per participant). All successful cycles of balancing were included in the analysis, with special attention given to those cycles of balance immediately preceding a potentially catastrophic fall of the pole. Each cycle was defined as one half-period of the continuous hand velocity ($\dot{x}$) time series. Across all nine experimental conditions, this procedure resulted in 25,669 s of 2,797 balancing trials, averaging 9.2 s/trial. Of these 2,797 trials, 51,471 cycles of successful balancing behavior were recorded and included in the final data analysis.

The interactive computer program reported the pole angle (θ), pole angular velocity ($\dot{\theta}$), and the cart acceleration ($\ddot{x}$) directly. Data for the cart velocity ($\dot{x}$) were obtained by numerically differentiating the time series data for the cart position (x). The visually specified time to contact measures of τ_{bal} and τ_{fall} were calculated as the ratio of the angle of the pole (with respect to vertical and horizontal, respectively), and its instantaneous angular velocity (see Equations 3.1 and 3.7).

$$\tau_{fall} \equiv \frac{90 \cdot \text{sgn}\,\theta - \theta}{\dot{\theta}} \qquad (3.7)$$

71

The time derivatives of these measures (i.e. of $\dot{\tau}_{bal}$ and $\dot{\tau}_{fall}$) were calculated by differentiation.

3.2.6 Average Balance Time per Session

The successful balance time for each trial in a testing session was averaged and the mean calculated for each of the nine experimental conditions. The average balance time per session was used as a measure of participant proficiency in performing the task.

3.2.7 Correlation Analysis of Hand and Pole Kinematic Variables

In the present experiment, as in Foo et al. (2000), we compare the relationship between the magnitudes of $\tau_{bal}, \dot{\tau}_{bal}, \tau_{fall}, \dot{\tau}_{fall}, \dot{x}, \theta$, and $\dot{\theta}$ all sampled at the onset of hand deceleration with the period of hand velocity ($\dot{x}$). The onset of hand deceleration (peak velocity) has been shown to be the critical event during each period of hand oscillation, as this is when the participant actively begins to slow the cart in preparation for reversing the direction or minimizing the angular velocity of the pole (see Treffner & Kelso, 1995; Wagner, 1982).

3.3 Results

3.3.1 Average Balance Time per Session

A single factor (nine experimental conditions) repeated measures ANOVA was performed on the average balance time/session, and showed that the control condition was significantly easier to balance than any of the other eight conditions (F (8, 351) = 23.80, $p < .001$). Participants balanced the normal simulated pendulum an average of 61.7 s/session. Tukey post-hoc tests confirmed that the remainder of the experimental conditions fell into two groups, that were significantly different from the other, but not

different within each group. The first group consisted of the three unperturbed poles: vertically flipped, action-mapped, and occluded poles (mean balance times of 35.2 s/session, 31.2 s/session, and 29.8 s/session respectively). Finally, the five perturbed conditions formed the group with the poorest performance. In order, the average balance times for the parametrically altered, perturbed control, perturbed occluded, perturbed vertically flipped, and perturbed and action-mapped conditions were 24.7 s/session, 18.6 s/session, 13.8 s/session, 13.3 s/session, and 11.1 s/session.

3.3.2 Kinematics of τ_{bal}

In Figure 3.3a-c representative timeseries of $\dot{x}, \dot{\theta}, \tau_{bal}, \dot{\tau}_{bal}$ from the control condition are shown. Note the tight anti-phase coupling that exists between hand and pole velocities that supports successful functional stabilization of the pole. Around the times of hand velocity extrema (solid line of Fig. 3a), the value of τ_{bal} is conserved near $\tau_{bal} = 0$ s (Fig. 3b), and $\dot{\tau}_{bal}$ is conserved near $\dot{\tau}_{bal} = 1$ (Fig 3c). In other words, during the onset of deceleration of the hand, the pole is moving near the vertical ($\tau_{bal} = 0$), and is typically overshooting the vertical ($\dot{\tau}_{bal} = 1$).

Note in Figure 3.3b that τ_{bal} exhibits characteristic singularities when θ reaches zero, and usually corresponds to pole reversals. The τ_{bal} behavior between these reversals can be classified into four types according to how the pole approaches the vertical balance point (see Figure 3.4): (a) pole crossover of the balance point (sigmoidal $\dot{\tau}_{bal}$ curve, Figure 3.4 bottom); b) pole undershooting vertical (inverted-U $\dot{\tau}_{bal}$ curve, Figure 3.4 top); (c) pole drifting away from vertical (U-shaped $\dot{\tau}_{bal}$ curve, Figure 3.4

73

Figure 3.3a-c. (a) Time series plots of the hand velocity (solid lines) and pole velocity (dashed lines) showing tight anti-phase coordination. (b)-(c) Plots of τ_{bal} and $\dot{\tau}_{bal}$ computed from the same data source as in (a). Note that at hand velocity extrema, the value of τ_{bal} is conserved near $\tau_{bal} = 0$ s and $\dot{\tau}_{bal}$ around $\dot{\tau}_{bal} = 1$. Here the participant undershoots and drifts the pole for the first 5 cycles, then overshoots the vertical for the remaining 2 cycles of pole motion. The classification and investigation of the stereotypical motions of τ_{bal} has revealed that participants use τ_{bal} information to gear hand motions during certain critical pole motions (see also Table 2.2).

74

Figure 3.4. Classification system based upon two successive cycles of *successful* balancing behavior. Here the six different paths that are seen in the experimental data and their corresponding τ_{bal} vs. t curves (see Figures 2.5a-c) are enumerated. Paths 1-3 represent situations where the participant successfully avoided a catastrophic fall of the pole from either instability of the pole (Path 2: a failure to reverse, see Foo et al., 2000), or from running out of track with which to correct the fall (or perturbation) of the pole and are of special import during the present correlation analysis (see Tables 3.1-3.5).

middle); and (d) a catastrophic fall (not shown here). If one observes the sequences that connect the three motions of the pole that do not result in a fall, six paths between these motions can be classified (see Figure 3.4). Of these six successful paths, paths 2 and 4 represent when participants successfully performed an active intervention that prevented a fall of the pole.

3.3.3 Control Condition

As expected, participants exhibited the best performance when asked to stabilize the normal inverted pendulum (Figure 3.2a). No significant relationships were found between the period of hand velocity and any of the perceptual variables when collapsed across all cycles ($p > .05$, see column 1, Table 3.1). When partitioned with respect to the τ_{bal} path classification scheme (columns 2-4 of Table 3.1, see also Figure 3.4), the correlation values indicated significant linear relationships (at $p < .05$ or better) between the τ-variables and the period of hand velocity during all the pole cycles that immediately followed a crossover of vertical (see Paths 1-3 of Figure 3.4). Specifically, hand velocity period was significantly correlated with τ_{bal} during the 1,026 cycles of path 1, with $\dot{\tau}_{bal}$, and $\dot{\tau}_{fall}$ during the 84 cycles of path 2, and with τ_{bal} during the 596 cycles of path 3. While the strength of these relationships did not match the level of balancing an actual physical pole (Foo et al., 2000), they were still highly significant.

Table 3.1 Correlations Between Hand Motions and Perceptual Variables: Control

	All Cycles	Categorized by τ_{bal} Paths		
Perceptual Variables	Path 1	Path 1	Path 2	Path 3
τ_{bal}	-.13 (-.19)	-.40* (-.43)*	-.24 (-.51)*	- .31* (-.35)*
$\dot{\tau}_{bal}$	-.02 (-.13)	-.21 (-.17)	.51* (.36)*	-.28 (-.32)*
τ_{fall}	-.11 (-.17)	-.25 (-.37)*	-.52* (-.45)*	-.21 (-.30)*
$\dot{\tau}_{fall}$	-.06 (-.08)	-.22 (-.17)	.12* (-.33)*	-.16 (-.14)
$\dot{x}$	.06 (.02)	.05 (-.01)	-.02 (.03)	.06 (-.03)
θ	.03 (-.07)	.22 (.15)	.18 (-.05)	-.04 (-.02)
$\dot{\theta}$	-.06 (-.06)	-.03 (-.02)	-.17 (-.36)*	-.06 (.04)

Note. The correlation values with an asterisk (*) indicate significant ($p < 0.05$) relationships. Values for perturbed trials shown in parentheses.

3.3.4 Vertically Flipped Pole

Significant linear relationships were observed between hand velocity and τ_{bal} and τ_{fall} during the 810 cycles of path 1, and with $\tau_{bal}, \dot{\tau}_{bal}, \tau_{fall}$, and $\dot{\tau}_{fall}$ during the 126 cycles of path 2 (see Table 3.2).

Table 3.2 Correlations Between Hand Motions and Perceptual Variables: Vertically Flipped Pole

Perceptual Variables	All Cycles	Categorized by τ_{bal} Paths		
		Path 1	Path 2	Path 3
τ_{bal}	-.17 (-.18)	-.60* (-.34)*	-.74* (-.33)*	-.23 (-.33)*
$\dot{\tau}_{bal}$	-.02 (-.05)	-.17 (-.14)	.48* (.39)*	-.21 (-.30)*
τ_{fall}	-.17 (-.14)	-.43* (-.30)*	-.50* (-.18)	-.25 (-.26)
$\dot{\tau}_{fall}$	-.03 (-.05)	-.12 (-.14)	-.58* (-.40)*	-.16 (-.11)
$\dot{x}$	.07 (.01)	.16 (-.02)	-.06 (-.02)	.06 (.00)
θ	.01 (.09)	.27 (.16)	.11 (.01)	.07 (.08)
$\dot{\theta}$	-.06 (-.01)	-.06 (-.01)	-.06 (-.23)	-.07 (.02)

Note. The correlation values with an asterisk (*) indicate significant ($p < 0.05$) relationships. Values for perturbed trials shown in parentheses.

3.3.5 Action-Mapped Pole

When participants balanced the pole and their hand motions were required to perform mirror movements, correlation analysis again revealed significant linear relationships between the τ-variables and the period of hand velocity (Table 3.3). During the 855 cycles of path 1 the action of the hand was significantly correlated with τ_{bal} and

τ_{fall}. Similarly, τ_{bal}, $\dot{\tau}_{bal}$, and $\dot{\tau}_{fall}$ were related to the velocity time of hand velocity in the 130 cycles that comprised path 2 ($p < .05$).

Table 3.3 Correlations Between Hand Motions and Perceptual Variables: Action-Mapped Pole

	All Cycles	Categorized by τ_{bal} Paths		
Perceptual Variables	Path 1	Path 1	Path 2	Path 3
τ_{bal}	-.12 (-.20)	-.55* (-.32)*	-.47* (-.05)	-.28 (-.09)
$\dot{\tau}_{bal}$	-.02 (-.07)	-.18 (-.23)	.56* (.16)	-.28 (-.13)
τ_{fall}	-.10 (-.12)	-.36* (-.30)*	-.23 (.08)	-.27 (-.11)
$\dot{\tau}_{fall}$	-.03 (-.08)	-.07 (-.16)	-.38* (-.07)	-.19 (-.17)
$\dot{x}$	-.12 (-.05)	-.21 (-.06)	.25 (.16)	-.14 (.06)
θ	-.03 (-.12)	-.22 (-.13)	-.21 (-.09)	.01 (-.10)
$\dot{\theta}$	.10 (.01)	.15 (.08)	-.05 (.12)	.13 (-.05)

Note. The correlation values with an asterisk (*) indicate significant ($p < 0.05$) relationships. Values for perturbed trials shown in parentheses.

3.3.6 Occluded Pole

Remarkably the successful stabilization of the occluded pole revealed similar results to the vertically flipped and action-mapped conditions. Significant linear

relationships between the τ-variables and the period of hand velocity were observed during two sets of pole cycles (Paths 1-2, see Table 3.4). The period of hand velocity was significantly correlated with τ_{bal} and τ_{fall} and θ during the 1,029 cycles of path 1; with $\dot{\tau}_{bal}$, $\dot{\tau}_{bal}$, and τ_{fall} during the 109 cycles of path 2, and with τ_{bal} and τ_{fall} during the 626 cycles of path 3. Interestingly, there was also a significant, but weaker correlation between hand velocity period and a variable (θ) that was not a τ-variable (see Table 3.1).

Table 3.4 Correlations Between Hand Motions and Perceptual Variables: Occluded Pole

	All Cycles	Categorized by τ_{bal} Paths		
Perceptual Variables		Path 1	Path 2	Path 3
τ_{bal}	-.12 (-.18)	-.62* (-.40)*	-.57* (-.36)*	- .41* (-.33)*
$\dot{\tau}_{bal}$	-.04 (-.11)	-.26 (-.27)	.51* (.38)*	-.22 (-.29)
τ_{fall}	-.12 (-.14)	-.45* (-.30)*	-.46* (-.31)*	-.35* (-.29)
$\dot{\tau}_{fall}$	-.06 (-.07)	-.25 (-.17)	-.25 (-.46)*	-.19 (-.13)
$\dot{x}$	.10 (.03)	.14 (-.04)	-.19 (-.17)	.08 (.01)
θ	.06 (.08)	.35* (.21)	.13 (.14)	.04 (.05)
$\dot{\theta}$	-.08 (-.01)	-.12 (-.07)	-.07 (-.08)	-.06 (.00)

Note. The correlation values with an asterisk (*) indicate significant ($p < 0.05$) relationships. Values for perturbed trials shown in parentheses.

3.3.7 Pole Parameter Alteration

When partitioned with respect to the τ_{bal} path classification scheme the correlation values indicated significant linear relationships between the τ-variables and the period of hand velocity (Table 3.5). Specifically, hand velocity period was significantly correlated with τ_{bal} and τ_{fall} during the 1225 cycles of path 1, with $\tau_{bal}, \dot{\tau}_{bal}$, and τ_{fall} during the 125 cycles of path 2, and with $\dot{\tau}_{bal}$ during path 3 (consisting of 883 cycles of movement).

3.3.8 Perturbed Control

A significant linear relationship was found between the magnitude of θ sampled at the onset of deceleration and the period of that cycle of hand velocity when participants successfully avoided a failure (see values in parentheses of Path 2, Table 3.1). This correlation was accompanied by relationships of similar strength with the magnitudes of $\tau_{bal}, \dot{\tau}_{bal}$, and τ_{fall} during the same 83 cycles of pole motion. Hand velocity period was also significantly correlated with τ_{bal} and τ_{fall} during the 1438 cycles of path 1.

3.3.9 Remaining Perturbed Conditions

The average balance time performance on the remaining perturbed conditions: occluded, vertically flipped and action-mapped were significantly poorer than the preceding conditions and not significantly different from each other. The significant correlations found between τ-variables and the period of hand velocity followed the same trends as seen in the other conditions. The trends in these results replicate the correlation

values reported in Tables 1-6 and will not be fully enumerated here (for full details. see correlation values in parentheses, Tables 2-4).

Table 3.5 Correlations Between Hand Motions and Perceptual Variables: Pole Parameter Alteration

	All Cycles	Categorized by τ_{bal} Paths		
Perceptual Variables		Path 1	Path 2	Path 3
τ_{bal}	-.17	-.59*	-.65*	-.29*
$\dot{\tau}_{bal}$	-.03	-.08	.67*	-.35*
τ_{fall}	-.17	-.44*	-.35*	-.28
$\dot{\tau}_{fall}$	-.04	-.19	-.20	-.21
$\dot{x}$	.03	.03	-.08	.08
θ	.07	.29	.13	.05
$\dot{\theta}$	-.03	-.01	.07	-.11

Note. The correlation values with an asterisk (*) indicate significant ($p < 0.05$) relationships. There were no perturbations of angular velocity in this condition.

82

3.4 Discussion

This experiment extends our previous results on physical pole balancing showing that the time to balance, τ_{bal} was a crucial information variable determining how humans functionally stabilize unstable systems, in particular to avoid catastrophic failures (Foo, de Guzman, & Kelso, in preparation; Foo, Kelso, & de Guzman, 2000; Treffner & Kelso, 1995; 1997; 1999). The key idea was to push the τ_{bal} hypothesis by transforming the task in different ways. We used a virtual computer simulation to manipulate the available visual information and the underlying mechanics of the cart-pole system. These manipulations were designed to: 1) decouple mechanics and visual information of pole motion; 2) alter mapping of hand action; 3) remove visual information; and 4) introduce a perturbation. A first step was to establish that virtual balancing was regulated in the same fashion as the physical situation. Although, not surprisingly, the relationship was not as strong, results clearly indicated that τ_{bal} and τ_{fall} information supported successful balancing, consistent with the same result in the physical version of this task (Foo et al., 2000).

The perturbed version of the control condition was the only angular velocity perturbation condition that participants could perform to some level of mastery. Although perturbations were presented in a random temporal fashion, they were of constant magnitude. Correlation results suggested that in addition to the τ-variables used in the undisturbed version (control condition), participants employed visual information that was identical to the characteristics of the perturbation ($\dot{\theta}$), to adjust their movements. Participants could not master any of the other angular velocity perturbations

as seen in the average balance time results. Interestingly however, it appeared that participants used the same the τ-variable information to keep the pole upright as long as they did.

Following the control condition, the next easiest poles to balance consisted of a group of three: the vertically flipped pole, the action-mapped pole, and the occluded pole. In the vertically flipped pole, a transformation to the balance angle changed the visual image to the extent that it described a completely different, stable system. However, as soon as the pole was in motion, it became apparent that it was not a normal pendulum with a stable equilibrium point, but rather behaved as an inverted pendulum upside down (i.e. with the intrinsic dynamics of a repellor). Consistent with previous results, participants were able to deduce the appropriate balance angle of the pole once they had manipulated it (Foo et al., 2000), and were observed to use τ_{bal} and τ_{fall} information in these conditions. If anything, participants relied even more on τ-variables in the inverted versus control conditions.

Participants appeared to be able to infer the intrinsic "fall time" of the pendulum during the parametrically altered pole condition. In this condition the visible pole length remained constant while the effective pole length, which determined the pendulum frequency, was varied. Participants in other experiments have been demonstrated to be sensitive to the inertial tensor of wielded objects even without vision (see Turvey et al., 1992). They have also shown their ability to stabilize physical poles of similar intrinsic frequency to the virtual ones presented here (Treffner & Kelso, 1995; 1997; 1999). Since the relationships between pole mechanics and pole behavior remain lawful, sufficient

visual information, again in the form of time-to-balance variables proved sufficient to support the stabilization process.

In a similar manner, participants were able to adapt to the change in mapping between hand actions and pole motions. Recall that in this condition while the mechanics of the pole remained the same, the hand was required to move in the *opposite* direction to that specified by pole angle. Again, results clearly showed that τ_{bal} and τ_{fall} information was used to stabilize the pole, even though the execution of that specified motion was made more difficult. The perturbed version of this task exhibited the worst performance of all the experimental manipulations. Under the perturbation regime, not only were subjects forced to react to unexpected changes in the angular velocity, they were also required to implement a symmetric transform on their actions before any success was possible. Thus failure could be brought on by either of both of these difficulties, and indeed more failure was evident.

The occluded pole was intended to test the hypothesis that τ_{bal} is a key quantity in successfully avoiding catastrophes. With the cart and pole information removed (and thus the visible angle) participants were still able to balance successfully the pole. Participants revealed on exit interviews that even though they could not see the pole, they surmised the geometry of the invisible pole (possibly an order effect of balancing visible versions in the other conditions), and attempted to use proprioceptive (and peripheral visual) information of their hand position to estimate the angle of the pole, or at least to which side of vertical the pole was leaning (the sign of pole angle). In this condition, it was confirmed that hand motions were significantly correlated with angle (θ) an inferred

quantity as well as the directly available τ-variable thereby providing some evidence of this self-reported strategy. Another more direct possibility is that participants were simply attending to the position of the visible circle (at the top of the occluded pole) and its motion. The relative (to the position of the cart) horizontal component of the circle's motion reveals the sign of the angle of the pole, and the vertical component can indicate the magnitude of pole angle.

In this experiment, it has been shown that participants are sensitive to both classes of τ-variables, the time-to-balance (τ_{bal}) and the time-to-fall (τ_{fall}), and their derivatives. Both classes of τ-variables have previously been implicated in functional stabilization (Foo et al., 2000; Treffner & Kelso, 1995), and these two measures differ only in that time to balance is calculated from the angle of the pole with respect to vertical, and the time to fall uses the angle with respect to horizontal. In terms of modeling functional stabilization, it can be shown that the pair $(\tau_{fall}, \tau_{bal})$ can be derived from $(\theta, \dot{\theta})$ and vice versa. Thus, from a mathematical point of view no information is lost between the two classes of τ-variables. Each is just represented and perceived differently. Importantly, it has been shown that participants use the same type of visual information to balance the virtual poles in critical situations as they used when balancing the physical object itself.

In fact, the results of the present experiment demonstrate that participants used τ-variable information not only when they were successfully avoiding a catastrophic fall of the pole via a due to an uncontrolled overshoot of the balance point (see Foo et al., 2000), but also during other pole motions that followed a crossover of the vertical. It is possible that the constraints of the virtual apparatus were responsible for these differences. Here

the displacement of the digitizing pen was scaled so that participants would not reach the limits of the linear track. This had the desired result of constraining cart motion to a range of approximately 20 cm (compare to the 180 cm physical track in Foo et al., 2000).

Upon exit interviews, all participants mentioned this constraint, and their comments suggested that they attempted to keep the balancing pole closer to its balance point and minimize its angular velocity lest they run out of track to correct the fall of the pole (by either reversing or arresting the fall of the pole). Distributions of the types of failures revealed that a substantial number (21.2 %) of pole failures were due to this type of error. Using the routes-to-failure analysis developed in Foo et al. (2000), one may say that participants are using time-to-balance and time-to-fall information to avoid a catastrophic fall of the cart due to a spatial boundary constraint, instead of avoiding a "failure-to-reverse" as in Path 2 (see Figure 3.4). Thus the basic model of functional stabilization remains.

Finally, the virtual pendulum paradigm should allow one to investigate the nature of long-range correlations that have been seen in earlier in functional stabilization (see Treffner and Kelso 1995; 1999). Hurst time-series analysis suggested that for shorter balancing poles, at time scales of 2 seconds or less, the angle of the pole (with respect to vertical) demonstrated *persistence* ($H>0.5$), where the previous direction of movement was preserved, whereas *antipersistence* (direction of previous movements reversed; $H < 0.5$) was seen at time scales greater than 2 seconds. In the longer pole conditions, the angle of the pole switched from persistence to antipersistence at about 3 seconds. The switch from persistent to antipersistant behavior has been postulated to be a signature of

an open and closed-loop control of posture (Collins & De Luca, 1994; 1995), a hypothesis that has more recently been challenged (see e.g. Liebovitch & Yang, 1997; Newell, Slobounov, Slobounova, & Molenaar, 1997). It has been asserted that the antipersistent regime is a result of the bounded nature of the system (i.e. one cannot move the body's center of mass beyond its base of support, or move the cart-pole system beyond the ends of the linear track). Although not analyzed in detail here, the parametric variation of length condition from the present experiment, coupled with an ordered variation in the scaling of x-axis movements of the digitizing pen should lead to further understanding of this phenomenon.

3.5 Conclusion

To thrive in an ever-changing environment, biological systems must often stablize inherently unstable situations. We have studied the prototypical task of inverted pendulum balancing as a window into the mechanisms of these stabilization processes. The results of this experiment confirm and extend earlier research in the physical pendulum that show that participants utilize visually available time-to-balance and time-to-fall information to successfully avoid a catastrophic fall of the pole. This visually geared localized correction was observed in a virtual simulation of pendulum balancing across several, quite drastic experimental manipulations and perturbations, providing evidence for the generalizability of this control strategy. Along with previous evidence, our results show that humans use visually specified time-to-balance and time-to-fall information to gear corrective motions that are needed to avoid a catastrophic fall of the pole.

4.0 Intermanual and Interpersonal

Stabilization of Unstable Fixed Points

4.1 Experiment 3: Introduction

In the contemporary study of human behavior, a research paradigm that has come to be termed coordination dynamics has shown that biological coordination may be governed by the generic process of self-organization (see Kelso, 1995, for an extensive review). In its elementary form, a tripartite scheme that examines three levels of description (task level, collective variable level, and individual component level, see Kelso, 1995, pp. 66-67) has successfully captured and predicted stable patterns of coordination in terms of the dynamical behavior of stable fixed points or attractors of a nonlinear dynamical system (see the experiments of Kelso, 1981, 1984; and Haken et al., 1985; Schöner et al., 1986 for the modeling of these phenomena). Quantitative predictions of coordination dynamics have been tested in numerous experimental systems (Haken, 1996; Kelso, 1995 for reviews). This approach has also captured coordination when effectors are asymmetric (see Treffner & Turvey, 1996), between persons (Amazeen et al., 1995; Schmidt et al., 1998; Schmidt et al., 1990), and even the interactive coupling between participants and the environment (Kelso et al., 1990; Kelso et al., 1998; Wimmers et al., 1992). More recently, factors that stabilize coordination patterns during unstable situations have been enumerated, including learning (see Zanone

& Kelso, 1992, 1997), the recruitment of additional degrees of freedom (Buchanan, & Kelso, 1999; Fink et al., 2000), and the use of specific information in the environment (Fink et al., 2000; Jirsa et al., 2000). Finally, the coordination dynamics of the brain (Kelso, 1992) has been a major target of investigation in the last decade, due not only to concepts, but also advances in functional neuroimaging (Fuchs et al., 1992; Fuchs et al., 2000; Wallenstein et al., 1995; Fuchs et al., 2000; Kelso et al., 1991; 1992; Mayville et al., 1999).

In coordination dynamics, the organism and the environment are considered to be a coupled dynamical system (Kelso et al., 1990; Schöner & Kelso, 1988a; 1988b). In a related approach (Warren, 1998), the dynamics of the environment are assumed to exist within the domain of classical mechanics and are a function of the initial state and any external forces applied by the organism. These dynamics determine the successful solutions that must be discovered and exploited by the organism, although it should be noted that co-evolved intrinsic properties of the organism allow it to detect only limited types of information about the environment. In the first experiment we employed a specialized apparatus that required collaboration between effectors of an individual before any successful coordination with the environment was possible. In the second experiment we increased the complexity of the system even more by asking pairs of participants to perform the same task. Here the between-effectors collaboration was made more difficult by the social nature of the coupling. In the second experiment each participant must develop coupling with the environment *and* coupling with another person for success.

One task that may serve as a window into this type of *emerging* coordination is the stabilization of an inherently unstable system, such as balancing a broomstick on the end of one's finger (see Foo et al., 2000; Treffner & Kelso, 1995). In contrast to other tasks used in the study of coordination that exhibit the dynamics of an attractor, or a stable fixed point, here an inverted pendulum shows the characteristics of an *unstable* fixed point or a repellor (e.g. Strogatz, 1994). The intrinsic dynamics of this repellor system dictate that after any infinitesimal deviation from its balance point, the system will deviate and asymptotically move to failure and a fall of the pendulum. Thus, in pole balancing participants are presented with a system that is *always* tending toward destabilization and failure. Because of these intrinsic failure-seeking dynamics, if participants simply react to the pole's motion, they will react (within the range of typical reaction times) too late and the pole will fall (see Foo et al., 2000). Furthermore, at every point in time, the participant is actually perturbing (both positively and possibly negatively) the very system he or she is trying to stabilize, indicative of the bi-directional couplings between actor and environment (i.e. task/environment affects the participant and vice versa, see Lee et al., 1998; Sternad, Duarte, Katsumata, & Schall, in review; Warren, 1998). The task of balancing an inverted pendulum presents participants with a singularly difficult coordination challenge: a mechanical system that tends toward destabilization in which the human controller must anticipate the motions of the pole, and where his or her own motions may provide a destabilizing influence.

Early works on hemispheric specialization included the use of unimanual dowel balancing as an interference task, although no attempt was made to analyze the movement

91

kinematics (for a review, see Kinsbourne & Hicks, 1978). Other experiments have shown that inverted pendulum balancing demonstrates long-memory properties (Treffner & Kelso, 1995; 1999) similar to that seen during standing posture (Collins & De Luca, 1994; 1995), unpaced walking dynamics (Hausdorff et al. 1996), or paced tapping (Chen, Ding, & Kelso, 1997). Studies of posture have shown that coupling to an entraining oscillating perceptual stimulus can help stabilize the postural system (Jeka et al., 1997; Lee & Aronson, 1974; Thelen, 1990). In contrast, when no externally available entraining stimulus is available, a similar action-perception coupling was documented during successful balancing (Foo et al., 2000; Treffner & Kelso, 1995; 1999). Foo et al. also demonstrated that during critical situations in inverted pendulum balancing, participants use an environmentally available, visually specified 'time to balance' (τ_{bal}) to prevent catastrophic falls of the pole, a phenomenon that was reproduced in model simulations (Foo et al., 2000; Treffner & Kelso, 1995) and virtual reality (Foo, Kelso, & de Guzman, in preparation). Foo et al. developed a classification system that quantified the distributions of pole motions that participants demonstrate after sufficient practice, including "jiggling" oscillations similar to "bang-bang" control in engineered systems and "running", when the base and the top of the pole travel in the same direction.

The literature on control theory has much to contribute regarding possible successful solutions to the problem of balancing of an inverted pendulum. This task has often been used to illustrate basic control concepts and validate design techniques (see Geva & Sitte, 1993 for a review). Linear control, in which the force used to balance the

pole F is linear with respect to the pole angle θ (i.e. $F = k\theta$, k constant), has been widely used to balance an inverted pendulum successfully when the angle of the pole remains within a small range near vertical (Kwakernaak & Sivan, 1972). Systems have also been designed that successfully balance the pendulum by monitoring only the direction of the angle (sans magnitude) the so called bang-bang control (Schaefer, 1965). Artificial neural networks that employ movement data (such as cart position and pole angle) or images of the cart-pole system in action as a learning template, have successfully balanced the inverted pendulum (Guez & Selinsky, 1988; Tolat and Widrow, 1988), and have often been claimed to provide possible insights into how biological systems may accomplish this task. Typically these engineered systems develop a uniform oscillation of the pole around its balance point, with ever decreasing oscillation magnitudes. This behavior may be termed asymptotic balancing, and represents a successful solution to the inverted pendulum task. However, such behavior is not what is typically observed when humans perform this task (Foo et al., 2000), suggesting some limitations to control-theoretic views, at least with respect to the issue of functional stabilization in biological systems. Also of note, typically the goal of engineering approaches is to determine the control force F that is necessary to maintain upright balance of the pendulum without regard to *how* these forces are generated. In contrast, in the present investigation we are interested in exactly the opposite, namely how participants successfully coordinate the necessary control forces that balance the pole.

In the present experiment the goal was to discover how actions are coordinated by two potentially independent effectors to produce the appropriate forces necessary to

stabilize an unstable cart-pole system. To this end we designed the experimental apparatus so that both effectors must *collaborate* to produce the appropriate forces *necessary before any successful coordination with the pole is possible*. Two pull cords were affixed to each side of the cart such that each allowed only unidirectional control, and were instrumented so that the forces exerted on the base of the cart could be measured directly and independently from the motions of the cart. Each effector was able to move the base of the pole only unidirectionally, by *pulling* on each cord, thereby forcing the two effectors to cooperate in order to produce the bi-directional movements necessary for successful balancing.

In the present experiments we introduce new conditions into the functional stabilization paradigm: an intermanual and an interpersonal balancing requirement. In the intermanual condition (Experiments 3 and 4) participants controlled *two independent* hands to balance the pole, a coordination task that is markedly more difficult than previous experiments where the only goal was to produce a required pattern (e.g. the bimanual drawing task of Preilowski, 1972; and the aforementioned coordination experiments mentioned above). This task is also more difficult than previous instantiations of inverted pendulum balancing (Foo et al., 2000; Treffner & Kelso, 1995, 1999) where the participant unimanually grasped the cart directly for control. There the participant could move the cart in both directions with a single effector. In Experiment 4 we required participants to balance the pendulum as pairs (interpersonal balancing) in addition to intermanually. Recall that the design of the apparatus ensures that the potentially independent effectors *must work together* to complete the task, a criticism of

prior interpersonal work (Ingham et al., 1974; Schmidt et al., 1990).

What differences may one expect to see between interpersonal and intermanual balancing? It has already been demonstrated that the visual coupling in successful interpersonal coordination is weaker than when the effectors to be coupled reside in the same subject (e.g. Schmidt et al., 1998). Thus we predict that the participants performing intermanual balancing will outperform their counterparts in the interpersonal conditions on the general performance measures of number of trials to reach the performance criterion and amount of balance time. However, the kinematics of successful balancing should be similar in either case, since these successful solutions are governed, in part by the physics of an identical task. What is not predictable here is exactly *how* this successful balancing will be produced. To summarize, we present a self-perturbing task where participants (or hands) are forced to collaborate before any successful coordination with the pole is possible and where the participants themselves must develop coordination patterns to successfully perform this inherently unstable functional stabilization task. This paradigm thus allows one to examine how parts of the body cooperate to achieve a functional goal, and/or how parts of a social system must cooperate to do the same.

4.2 Method

4.2.1 Participants

Eight healthy adults (7 men, 1 woman) aged 21-36 years participated in this experiment. All participants were students at Florida Atlantic University, and signed informed consent waivers in accordance with the ethical standards of the American

Psychological Association (APA).

4.2.2 Apparatus

The inverted pendulum apparatus was the same one used in previous experiments (see Foo et al., 2000; Treffner & Kelso, 1995, 1999) with important modifications (see schematic, Figure 4.1). An aluminum balancing pole (108 cm, 208 g) was attached to a cart (338 g) that slid along a linear track (180 cm) at approximately waist-height for the participants (92 cm). Two IREDs, placed at the pivot at the base and approximately half way (60 cm distal) up the pole were used to reconstruct pole position and angle. In order to ensure the collaboration of the effectors in this task, two pull cords (33 cm) were attached to strain gauges (Advanced Custom Sensors, Inc. Model 6000) on each side of the cart (see Figure 4.1).

4.2.3 Conditions and Procedure

The task was to balance the inverted pendulum continuously for 30 s without allowing it to fall. Participants were required to demonstrate consistency by performing 3 out of 5 successful consecutive trials to complete the testing session, the same performance criteria used previously (Foo et al., 2000). In contrast to earlier studies where participants were asked to merely "keep the pole upright," in the present experiment, participants were instructed to balance the pole as close to vertical as possible (the balance point for the straight pole). Participants began each trial by grasping a pull cord in each hand. Upon receiving the appropriate signal from the experimenter, the participant balanced the pole by pulling on the two cords at the base of the pole until failure or the criterion time was reached. Importantly, while participants received visual feedback as to their success or
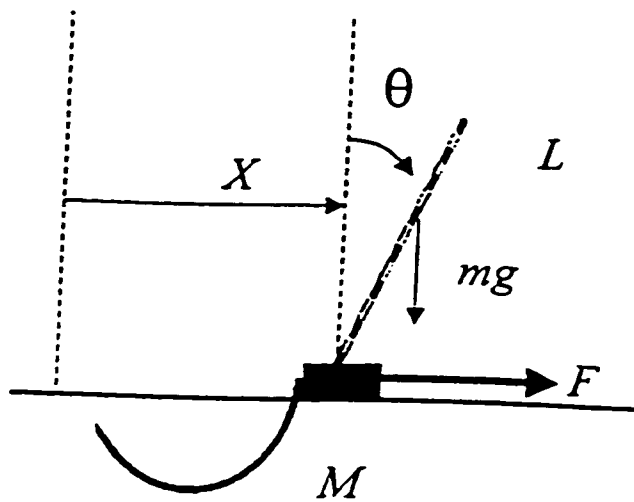
Figure 4.1. The experimental setup consisting of an inverted pendulum pivoting on a cart with two pull cords affixed to a horizontal linear track. The convention used is: θ is positive (negative) when the pole is right (left) of the vertical; M = mass of the cart, L = pole length, m = pole mass, F = force applied by pulling the (right hand) cord at the base; g = acceleration due to gravity. Strain gauges recorded the horizontal components of each force applied with the pull cords. Note the apparatus was designed so the hands must collaborate to produce the bi-directional motions required for successful completion of the task.

failure to balance the pole, no feedback was given to the participants regarding to how to balance the pole.

4.2.4 Design

Participants were asked to balance the pole using their two hands until the performance and consistency criteria were reached. Since the goal of this experiment was to characterize coordination patterns that support successful stabilization of this unstable system, only balancing trials that met the 30 s performance criterion were included in the final data analysis. Thus the present data set included 24 successful trials.

4.2.5 Data Analysis

An OPTOTRAK 3010 system was used to record pole kinematics and forces at 256 Hz. The sign convention used was that forces on both the right and left cord were always positive as subjects pulled them in their respective directions. However during analysis of the net forces, the positive sign denoted net forces to the right of the cart, and a negative net force pointed to the left. These data were smoothed and low pass Butterworth filtered (set at 7 Hz) for further analysis. During the course of testing, kinematic data for the cart velocity ($\dot{x}$) and pole angular velocity ($\dot{\theta}$) were obtained by numerically differentiating the time series data for the cart position (x) and the pole angle (θ), respectively. Continuous relative phase (ϕ) was calculated between the forces generated by the left (f_L) and right (f_R) hands on the cart. The observable kinematics and kinetics and their Pearson product-moment correlations were examined using inferential statistics.

4.3 Results

In this experiment participants were asked to coordinate their two hands to perform a functional task. First we report how participants met the trials to criterion and balance time requirements successfully; second we examine the kinematics and kinetics to understand how the pole's motions were produced by the net forces on the cart; third we examine exactly how those net forces were generated.

4.3.1 Trials to Criterion

All eight participants were able to reach the performance criterion of 3 successful (30 s long) trials in 5 consecutive trials. The average number of trials required was 26, the range extending from 74 trials needed for participant three and 3 trials needed for participant seven.

4.3.2 Distributions of Pole Motions

In the present experiment participants performed the jiggling strategy, or a continued oscillation of the pole about its balance point on average 45.0 % of the time during successful balancing (see Path 1 of Figure 2.9). Participants produced the running strategy 24.1 % of the time (here the sum of cycles in Paths 4 and 6 in Figure 2.9), and the mixed strategy accounted for the remaining 31.0 % of pole motions (Paths 2,3 and 5 combined) during the 2,342 recorded balancing cycles.

4.3.3 Kinematic Analysis of Balancing

Three representative time series for one balancing trial are presented in Figure 4.2a-c. Figure 4.2a shows representative time series of the hand position (x: solid line) and pole angle (θ: dashed line) for one participant balancing the pole. Here the participant
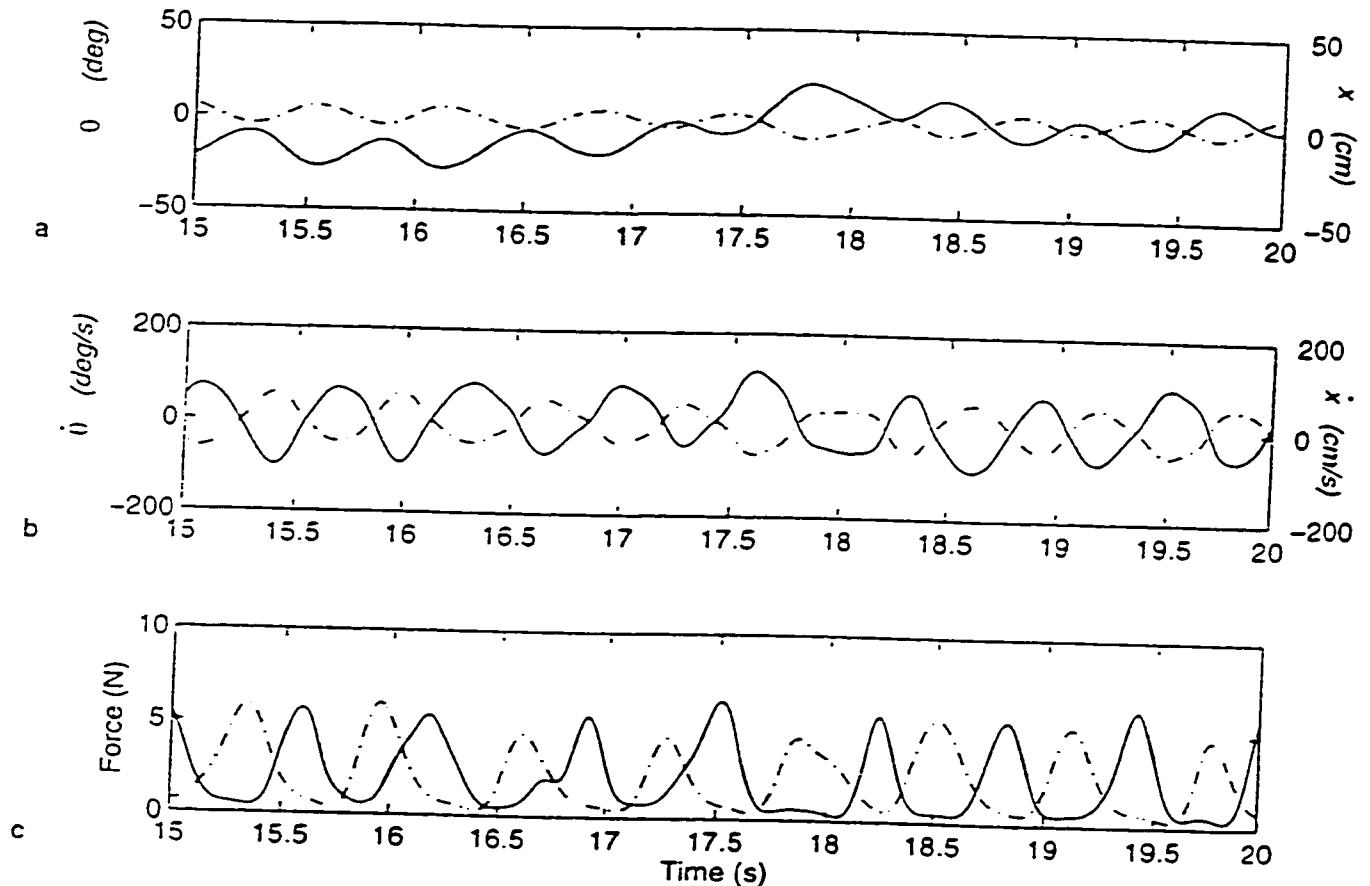
Figure 4.2a-c. (a) Representative time series of cart position (x: solid line) and the pole angle (θ: dashed line) during successful intermanual balancing. (b) Time series plots of the cart velocity (ẋ: solid line) and pole angular velocity (θ̇: dashed line) showing tight antiphase coupling during successful balancing. (c) Plots of the force exerted by the right (solid line) and left (dashed line) hands showing the hands alternating their pulling on the cart so as to produce the resulting pole oscillations. These kinematic data are essentially identical to data from the interpersonal (Experiment 4) conditions, and previous unimanual balancing (compare with Figures 2.2 and 2.4), thus only intermanual behavior is shown here.

is balancing the pole by oscillating it around its balance point, demonstrating the jiggling strategy that can be seen as the cart moves in opposition to the pole angle. In Figure 4.2b (see also Figure 4 in Foo et al., 2000), notice that the peaks (valleys) of the cart velocity ($\dot{x}$: solid line) coincide with valleys (peaks) of the pole angular velocity ($\dot{\theta}$: dashed line), indicating an antiphase coordination pattern suggestive of strong action-perception coupling that was quantified previously (Foo et al., 2000). Finally, in figure 4.2c one can see the time series of the forces generated by the right (solid line) and left (dashed line) pull cords. Here the participant is alternating use of the hands to produce the oscillations that balance the pole.

What kinds of quantitative variation in pole kinematics were seen during successful balancing? The time series for the successful balancing trials were examined, and the angular displacement and angular velocity averaged to determine if the participants succeeded at balancing the pole at vertical with minimal angular velocity (i.e. $\theta = 0$, $\dot{\theta} = 0$, see Table 4.1). The participants in this experiment produced an average angular displacement of -0.4 deg across these successful trials, with an angular deviation (AD) of 3.4 deg. The average angular velocity was -0.1 deg/s with a corresponding angular deviation of 19.5 deg/s. These values are consistent with those seen in previous results (e.g. Foo et al., 2000), and suggest that participants can balance the pole whether they held the cart directly with their hand or, as here, did not.

Table 4.1 Experiment 3: Magnitudes of Pole Kinematics and Pole Kinetics in Successful

Balancing

	θ (deg)	$\dot{\theta}$ (deg/s)	f_{net} (N)	f_L (N)	f_R (N)
Participant 1	-0.4 (4.5)	-0.2 (33.2)	1.3 (3.1)	3.0 (1.2)	4.4 (2.5)
Participant 2	-0.6 (2.8)	0.0 (17.9)	0.4 (2.1)	2.5 (1.8)	3.0 (1.7)
Participant 3	-0.6 (4.7)	-0.2 (17.8)	0.0 (1.8)	3.5 (1.5)	3.5 (1.4)
Participant 4	-0.4 (3.0)	0.0 (21.7)	0.4 (3.9)	4.8 (1.9)	5.2 (2.8)
Participant 5	-0.4 (4.1)	-0.2 (16.9)	-0.4 (4.7)	3.9 (2.9)	3.5 (2.3)
Participant 6	-0.4 (1.9)	-0.1 (12.3)	0.1 (3.3)	3.1 (1.7)	3.2 (1.9)
Participant 7	-0.3 (1.0)	0.0 (5.6)	0.8 (1.4)	1.2 (0.6)	2.0 (1.0)
Participant 8	-0.1 (3.4)	0.0 (21.5)	-0.1 (2.6)	3.3 (1.8)	3.2 (1.9)
Average	-0.4 (3.4)	-0.1 (19.5)	0.3 (3.1)	3.5 (2.2)	3.2 (2.0)

Note. The values represent mean (and within-trial angular or standard deviation) for each participant successfully performing intermanual coordination. Here θ is the pole angle, $\dot{\theta}$ is the angular velocity, and f_{net} is the difference of the forces produced by the left (f_L) and right (f_R) hands.

How are the forces that are produced by the effectors related to the variation in pole kinematics? A correlation analysis was performed between the time series of the net forces (f_{net}) produced by the hands on the cart and the kinematic variables of pole angle (θ) and angular velocity ($\dot{\theta}$). These correlation values are reported in Table 4.2 for all eight participants and are all statistically significant ($p < .001$) due to the large sample

size (n = 23,040 per participant). A significantly stronger correlation was found between the net force (on the cart) and angular velocity of the pole (r = -.62) than between the net force and the angle of the pole (r = .29), as shown in Table 4.2 (t (7) = 5.75, p < .001). This significant relationship suggests that the forces produced by the hands on the cart were used to control the angular velocity, and not the angle of the pole during successful balancing. Furthermore, this relationship between the average net force and the angular velocity of the pole (r = -.62) was significantly stronger than either the relationship between left hand force and angular velocity (r = .46; t (7) = -2.38, p < .05) or right hand force and angular velocity (r = - .45; t (7) = 3.49, p < .01), which were not significantly different from each other, t (7) = 1.72, p > .05 (see Table 4.3).

How were the net forces on the cart produced? Did one hand or the other contribute unequally to the production of net forces on the cart? A t-test was used to compare the relationships between the net force (f_{net}) and the forces produced by the right (f_R) and left (f_L) hands across all participants (see Table 4.2, columns 3-4). No significant differences were found (t (7) = 1.13, p > .05), suggesting that both hands contributed equally to the net forces acting on the cart (f_R: r = -.75; f_L: r = .70). Were there differences in the average magnitudes of forces produced by either hand? A closer inspection of the average forces produced by the left (f_L mean = 3.5 N, SD = 2.2 N) and right (f_R mean = 3.2 N, SD = 2.0 N) hands did not reveal any significant difference between the magnitudes of the two, t (7) = - 0.67, p > .05 (see Table 4.1, columns 4-5). Finally, there was no relationship between the forces produced by the right and left hands (r = -.08). These results suggest that variations in net forces on the cart (that connected the hands to

the pole's motions) were not produced by an asymmetry between each hand's contribution to net force, nor from a difference in the magnitudes of the forces of each hand. Moreover, the forces generated by each hand were uncorrelated: the magnitudes of one was relatively independent of the other. Next we examined the possibility that a difference in the relative timing between these approximately symmetric effectors produced the variation in net forces on the cart.

Table 4.2 Experiment 3: Correlation Between f_{net} (N) and Individual Hand Forces (f_L, f_R) and Pole Kinematics

	θ (deg)	$\dot{\theta}$ (deg/s)	f_L (N)	f_R (N)
Participant 1	.48	-.72	.62	-.92
Participant 2	.37	-.69	.63	-.60
Participant 3	.57	-.59	.62	-.59
Participant 4	.32	-.81	.75	-.89
Participant 5	.15	-.63	.92	-.87
Participant 6	.17	-.68	.90	-.92
Participant 7	.18	-.58	.72	-.92
Participant 8	.36	-.66	.68	-.73
Average	.29	-.62	.70	-.75

Table 4.3 Experiment 3: Correlation Between Forces Generated by the Left (f_L) and Right (f_R) Hands and Pole Kinematic Variables (θ, $\dot{\theta}$)

| | f_L | | | f_R | |
	θ (deg)	$\dot{\theta}$ (deg/s)		θ (deg)	$\dot{\theta}$ (deg/s)
Participant 1	-.39	.55		.39	-.60
Participant 2	-.02	.58		.46	-.27
Participant 3	-.20	.45		.49	-.26
Participant 4	-.04	.69		.41	-.66
Participant 5	-.07	.62		.20	-.50
Participant 6	-.01	.69		.27	-.55
Participant 7	-.07	.46		.20	-.50
Participant 8	-.04	.54		.52	-.40
Average	-.08	.46		.33	-.45

4.4.4 Characterization of Collaboration: Continuous Relative Phase

Here we employed a continuous relative phase measure between the force-time profiles of the right and left hands to capture the collaboration between effectors that produced the forces necessary to balance the pole. The continuous relative phase (Φ) between the force trajectories of the two hands was calculated as the difference between the right and left phase angles, which were defined as the arctangent of the ratio of each hand force and its derivative (Kelso, Scholz, & Schöner, 1986). The mean and within

participants angular deviation of continuous relative phase for each trial was calculated using circular statistics (Batschelet, 1981).

Table 4.4 Experiment 3: Relative Phase Between Forces Generated by the Left (f_L) and Right (f_R) Hand

	ϕ (deg)
Participant 1	172.5 (5.5)
Participant 2	-111.0 (16.6)
Participant 3	-129.6 (4.8)
Participant 4	-151.1 (4.4)
Participant 5	-158.7 (3.4)
Participant 6	-145.3 (0.9)
Participant 7	-166.9 (6.1)
Participant 8	-132.9 (14.5)
Average	-147.8 (23.5)

Note. Mean (and between trial angular deviation) of continuous relative phase between the force-time profiles of the two hands during intermanual balancing. The negative sign indicates the right hand leads the left. Participant 1 was the sole left-handed participant and shows a left-hand lead during antiphase coordination.

Results from the continuous relative phase analysis are summarized in Table 4.4. The mean continuous relative phase for the eight participants (-147.8 deg) denotes, on average, an antiphase coordination pattern with the right hand leading the left (~180 deg) for all participants across all successful trials. The sole exception was participant 1, the
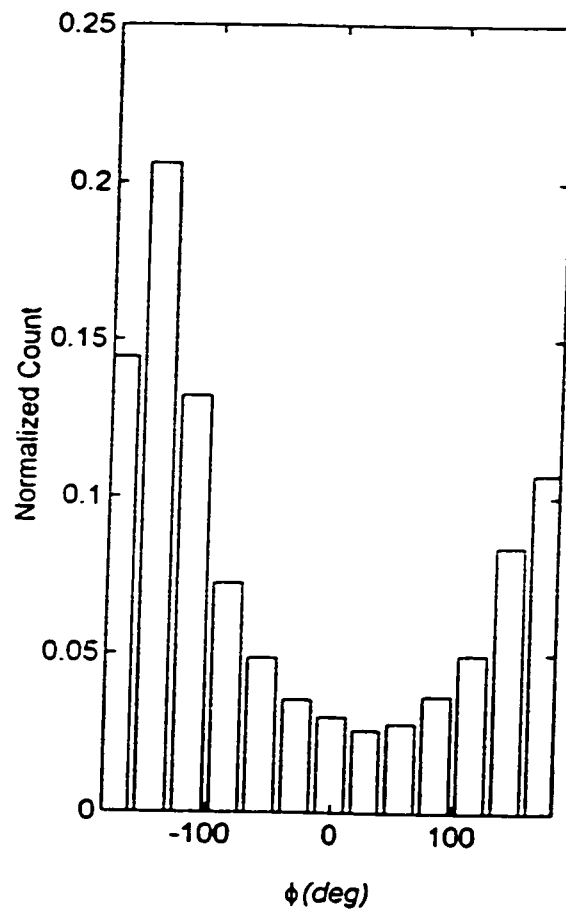
Figure 4.3 Distribution of continuous relative phase Φ values during successful intermanual balancing. The mean continuous relative phase for the eight participants (-147.8 deg) denotes on average, an antiphase coordination pattern with the right hand leading the left (~180 deg, see also Table 4.4).

only left-handed participant, who demonstrated an antiphase coordination pattern with the left hand leading the right. Across trials, the variability (average angular deviation of 23.5 deg, with a minimum value of 0.9 deg for subject 6) suggested that these coordination patterns were quite stable within the timescale (30 s) examined here. In Figure 4.3 the distribution of continuous relative phase values for these successful intermanual balancing trials clearly shows the stable unimodal behavior of this coordination strategy.

4.4 Discussion: Experiment 3

In the present experiment we explore the kinds of coordination strategies two independent effectors develop (in the absence of a prescribed pattern) when required to perform a functional stabilization task. Here participants balanced an inverted pendulum until a minimum balance time and consistency criterion was reached. The apparatus was designed so as to ensure collaboration between the two effectors (intermanual coordination) before any successful coordination with the pole was possible, thus providing a window into how emerging coordination develops to produce the forces necessary to complete the task.

How did the forces produced by the hands on the cart affect the pole's motions? A significant linear relationship was found in the present experiment between the net forces produced by the hands on the cart (f_{net}) and the angular velocity ($\dot{\theta}$). No such relationship was observed between net force and angle (θ) of the pole (see also Figure 4.2). This result is consistent with earlier findings in which a significant relationship was observed between the angular velocity of the pole and the velocity of the cart ($\dot{x}$) and reflects the tight action-perception coupling that supports functional stabilization (see

Figure 3, Foo et al., 2000), regardless if one performs it with two (independent) effectors or one.

Do the two hands contribute equally to balance the pole? In order to produce the bi-directional oscillations required to successfully stabilize the pole, participants needed to produce oscillatory net forces on the cart. Since the two hands were responsible for creating the resulting net force, an analysis was performed on the forces produced by each hand to determine how each contributed to the net forces. It was demonstrated that both the right and left hands were equally related to the net force (but not directly to the angular velocity of the pole, see Table 4.3), and that the magnitudes of the forces generated by each effector were not significantly different (see Tables 4.1 and 4.2). The hands were also not significantly linearly related to each other, but a specific relative timing strategy between forces produced by the hands was revealed as an antiphase coordination pattern (Table 4.4 and Figure 4.3).

In the left hand column of Figure 4.4 we show an example time series of the forces exerted by the hands (Figure 4.4a) and the corresponding continuous relative phase (Figure 4.4c) during intermanual balancing in Experiment 3. In the left-hand figures (the same data shown in the Figure 4.2), one can see the behaviors that characterize antiphase coordination equivalent to an alternation balancing strategy. In figure 4.4a the participant is oscillating the pole by pulling alternately on the cart with both the right (solid line) and left (dashed line) pull cords. The corresponding continuous relative phase values exhibit some within trial variability, but are clearly centered at a 180 deg or antiphase coordination.
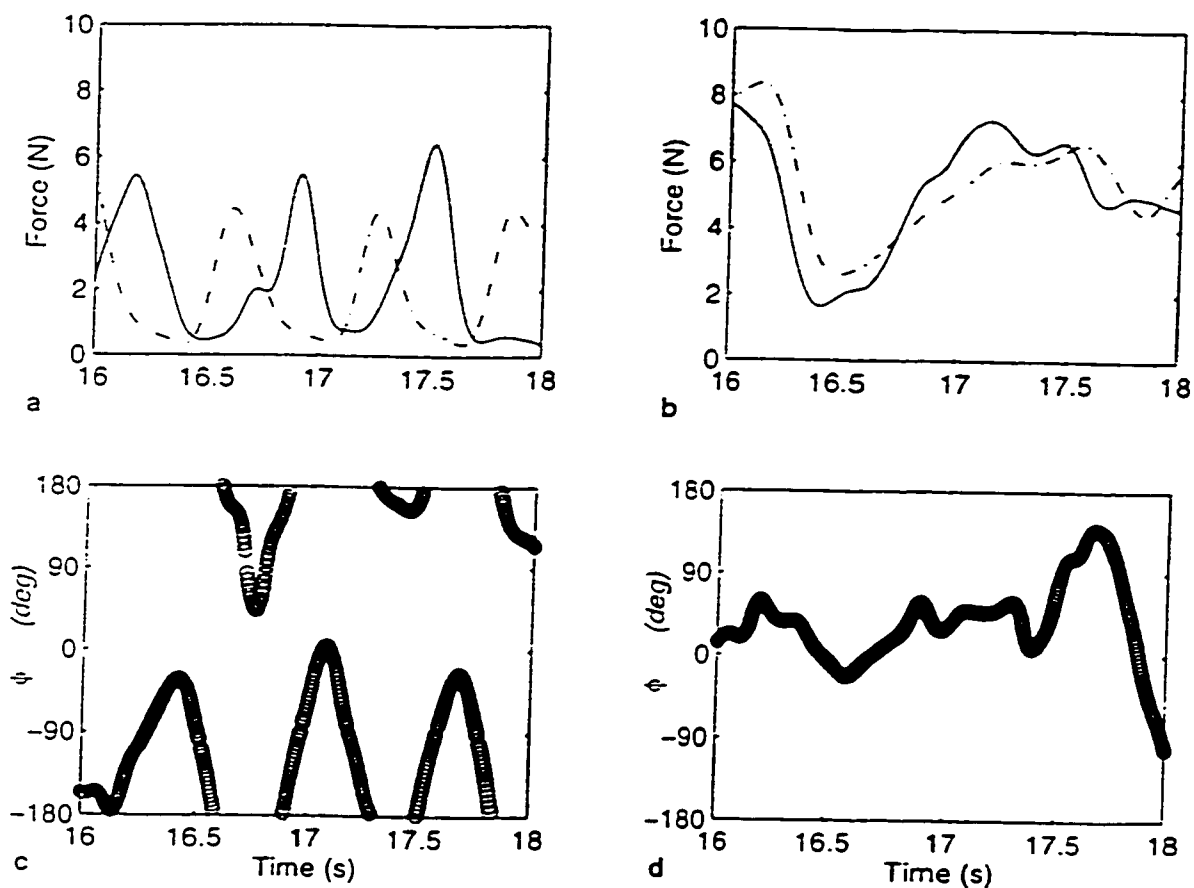
Figure 4.4a-d. Representative time series of the alternation (left column, figures a, c) and co-contraction (right column, figures b, d) balancing strategies and their corresponding continuous relative phase values. The topmost figures (a, b) plot the time series of the forces exerted by the right (solid line) and left (dashed line) hands on the cart, while the bottommost figures (c, d) show the commensurate continuous relative phase values. Note that during alternation, relative phase Φ values are centered around 180 deg (c), whilst in co-contraction the coordination pattern shows a relative phase Φ centered around 0 deg (d).
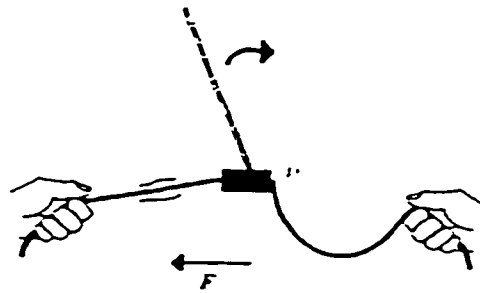
a
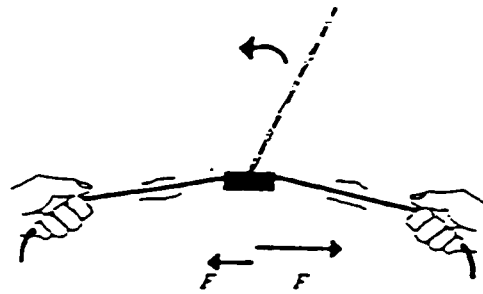
b

Figure 4.5a-b. a). Demonstration of the alternation strategy used to balance and control the pole. Here the hand on the left is pulling and the right hand is not. The net effect on the cart is to move it to the left. This corresponds to an antiphase coordination pattern (180 deg) between the forces from the hands, and was observed for the intermanual conditions in Experiments 3 and 4 (see also Tables 4.4 and 4.8). b). Schematic of two hands using the co-contraction strategy to balance the pole. Both hands exert simultaneous tension on the pull cords, although here the right hand is pulling harder, and the net effect moves the cart to the right. This balancing strategy was seen during interpersonal balancing (Experiment 4), and corresponds to an inphase (0 deg) coordination pattern between the forces from the hands (see also Table 4.12).

Exactly what does this antiphase coordination strategy mean in terms of the task of balancing the pole? In Figure 4.5a one can see a the alternation strategy used by participants in this experiment to balance and control the pole. Here the hand on the left is pulling whereas the right hand is not. The net effect on the cart is to move it to the left. This corresponds to an antiphase coordination pattern between the forces of the hands, and represents one possible organization of the effectors during performance of this task. In the present experiment, participants utilized an antiphase coordination strategy to produce the oscillating net forces on the cart, which was coupled to the angular velocity of the pole and resulted in functional stabilization. The antiphase, or alternating coordination strategy is one possible pattern that participants use to oscillate and balance the pole. These results may at first glance appear to be consistent with those of Prielowski (1972) who found that the most accurate performance on a bimanual drawing task occurred in those conditions where only one hand was required to move at a time. However, the task goal in the Prielowski "etch-a-sketch" task was for participants to merely produce different phasing relationships between the two hands, without any external coordination constraint. This is clearly not the case in the present experiment where the participants' most important task goal is to stabilize an inherently unstable system that has been shown to require an anticipatory action-perception coupling for success (see Foo et al., 2000). These results also suggest that participants use their two separate hands in an asymmetric (antiphase) bimanual fashion (Guiard, 1987). Guiard's Kinematic Chain Model postulates that this kind of collaborative behavior is based on a serial organization, where the output of one hand serves as the input for the other hand.

But this task lies somewhere in the middle of the serial/parallel dichotomy, because while the hands do alternate, neither hand appears to be completely inactive.

4.5 Experiment 4: Introduction

In Experiment 3 it was shown that participants utilize a relative timing strategy of the forces from the hands (antiphase coordination) and not differences in the magnitudes of forces, nor differences in the individual relationships between each effector and the net force, nor individual relationships between each effector and the pole's motion directly, to stabilize an unstable mechanical device successfully. In Experiment 4 we extend the paradigm to examine how two individuals (two nervous systems) cooperate with each other to perform the same task. This question addresses the informational nature of the coordination between two people in the service of a common goal. Here we use a repeated measures design across balancing modalities (across intermanual and interpersonal conditions) in order to: 1) replicate the findings of Experiment 3; 2) observe whether the *same* individuals will employ similar or different cooperation strategies as seen in that experiment; 3) observe any transfer of balancing skill between conditions.

4.6 Method

4.6.1 Participants

Eight adult participants (6 men, 2 women; grouped randomly into 4 pairs), aged 22-30 years participated in the second experiment. All participants were right-handed graduate or undergraduate students at Florida Atlantic University. All participants were naïve to the purpose of the experiment, and signed informed consent waivers in accordance with the ethical principles of the APA prior to data collection. Two people

(participants 1 and 2) had also participated in Experiment 3.

4.6.2 Apparatus

The inverted pendulum apparatus from Experiment 3 was used again here. However, instead of one participant using two hands to balance the pole, here each member of the pair grasped a pull cord with their right hand. Note again that participants could move the base of the pole in one direction only, forcing the participants to cooperate in order to successfully balance the pole.

4.6.3 Conditions and Procedure

The eight participants in this experiment were required to balance the inverted pendulum continuously for 30 s, both individually (as in Experiment 3) and as pairs (interpersonal). Participants completed a test and retest session for both the intermanual and interpersonal conditions. The instructions to participants performing intermanual balancing were identical to those used in Experiment 3. In the interpersonal balancing conditions participant pairs were required to balance the pole by having each individual use a single pull cord. No instruction about how to balance the pole was given to participants. Participants were given 5 min of rest after the first 50 trials.

4.6.4 Design

As in Experiment 3, four of the eight participants were initially tested intermanually until they achieved the performance criterion of three successive successful balance trials, after which they were tested as pairs in the interpersonal condition. After successfully mastering the interpersonal task, these participants were retested on both tasks. The other four participants were tested in reverse order. The three successful trials

from each testing session were included in the final data analysis, unless the participants did not meet the balance time and consistency criteria, whereupon the final three trials were included. Thus a total of 144 trials (8 participants x 4 sessions x 3 trials + 4 pairs x 4 sessions x 3 trials) comprised the data set for this experiment.

<u>4.6.5 Data Analysis</u>

Kinematic data of the cart position (x) and pole angle (θ) were collected, using the three dimensional position of two IREDs recorded at 256 Hz using an OPTOTRAK 3010 system. Forces on the two pull cords were also sampled at 256 Hz, and the same sign/direction convention from Experiment 3 was used. Kinematic data of the pole and cart were smoothed and low pass Butterworth filtered at 7 Hz. Cart velocity ($\dot{x}$) and pole angular velocity ($\dot{\theta}$) were calculated by numerically differentiating the cart position and pole angle time series, respectively. The continuous relative phase (ϕ) was calculated between the forces pulling to the left (f_L) and right (f_R) of the cart (intermanually these were generated by the left and right hands of the same person, but interpersonally they were from individuals standing to the left and right of the cart). As in Experiment 3, the observable kinematics and kinetics and their Pearson product-moment correlations were examined using inferential statistics.

4.7 Results

In this experiment participants were asked to coordinate either intermanually (with their own two hands) or interpersonally (as a pair) to perform a functional task. As in the previous experiment we first report how participants met the trials to criterion and balance time requirements, followed by an examination of the kinematics and kinetics to

understand how the pole's motions were produced by the net forces on the cart. Finally we examine exactly how those net forces were generated by each participant and the timing strategy used to balance the pole.

4.7.1 Trials to Criterion

Those participants that were initially tested intermanually required more trials (mean = 56, maximum = 100, minimum = 21) to reach the balance time criterion than participants in Experiment 3 (mean = 22, maximum = 48, minimum = 3). One of these participants was unable to reach the performance criterion even after 100 trials. The participants that were initially tested as a pair also demonstrated this diminished performance in initial intermanual balancing (mean = 46, maximum = 98, minimum = 21). However, after an intervening session of interpersonal balancing (consisting of both successful and unsuccessful trials) all eight participants improved their intermanual performance (mean = 7, maximum = 26, minimum = 3 for all retest trials). Thus practice on a related task, even if performed unsuccessfully, helped performance, consistent with the positive transfer effects previously seen in unimanual balancing (Foo et al., 2000).

In general, participants performed better in the intermanual conditions as compared with the interpersonal conditions across the testing and retesting sessions. Participants required on average, fewer trials to meet the consistency and balance time criteria in the intermanual case (mean = 29, maximum = 98, minimum = 3) versus balancing the pole as a pair (mean = 85, maximum = 100, minimum = 29). In the interpersonal balancing conditions, the four participants that were initially tested as a pair could not meet the performance criterion either during the test or retest. On the other

hand, two of the participants initially tested intermanually were able to balance the pole as a pair only during the retest.

These results indicate that interpersonal balancing was more difficult than intermanual balancing. Furthermore improvements in performance were observed between the test and retest conditions. Specifically, with the exception of those participants who never mastered the task, interpersonal performance improved (or at least remained equal) after an intervening practice session on a similar (intermanual) task, even when those practice trials were unsuccessful.

4.7.3 Balance Time

All eight subjects were able to balance the pole intermanually for 30 s during the retest sessions. However, only one of the four pairs of participants successfully met this criterion during the initial testing sessions of the interpersonal condition, and by the retest still only two of the four pairs were successful. When collapsed across testing sessions, the trend is clear, with the average balance time for interpersonal balancing (mean = 13.7 s, maximum = 30.0s, minimum = 1.8 s) falling far short of the times of the intermanual conditions (mean = 29.7 s, maximum = 30.0 s, minimum = 7.0 s).

4.7.4 Distributions of Pole Motions

What kinds of pole motions did participants produce when balancing the pole? Participants produced the jiggling strategy during 48.6 % of the 12,765 successful intermanual balancing cycles in this experiment. The remaining intermanual behavior was comprised of 22.6 % running cycles, where the top and bottom of the pole travel in the same direction, followed by 28.8% of mixed cycles. The distribution of these

behaviors was not significantly different in the interpersonal conditions where participants produced 45.8 % jiggling, 26.5 % running, and 27.7 % mixed of 7,785 balancing cycles, χ^2 (5, N = 200) = 2.48, p > .05. In addition, these distributions were not significantly different from those of Experiment 3 (p > .05).

4.7.4 Kinematic Analysis of Balancing: Intermanual Balancing

Here we examine the kinematics of intermanual balancing followed by a similar treatment of interpersonal balancing. First we investigate how participants' hand motions were connected to the motions of the pole. The participants in the intermanual conditions produced an average angular displacement of −0.5 deg (angular deviation of 4.0 deg) during successful trials, with a mean angular velocity of −0.1 deg/s (AD = 17.5 deg/s, see Table 4.5).

A correlation analysis was performed between the time series of the net forces (f_{net}) produced on the cart by the hands, and pole angle (θ) and angular velocity ($\dot{\theta}$). Results revealed a significantly stronger correlation between the net force and angular velocity of the pole (r = -.53) than between net force and pole angle (r = .34, see Table 4.6, t (7) = -4.00, p < .01). The correlation values reported in Table 4.6 were statistically significant (p < .001) due to the large sample size (n = 46,080 per participant). This significant relationship observed between net force and angular velocity was consistent with the results of Experiment 3 and suggests that the forces were used to control the angular velocity, and not the angle of the pole during successful balancing. This relationship between net force and angular velocity of the pole was significantly stronger

118

than the relationship between right hand force and angular velocity ($r = -.32$; t (7) = -3.33, $p < .02$), but not between left hand force and angular velocity ($r = .46$; t (7) = -1.15, $p < .01$, see Table 4.7). However, the latter two correlations were not significantly different from each other, t (7) = 2.03, $p > .05$.

Table 4.5 Experiment 4: Intermanual. Magnitudes of Pole Kinematics and Pole Kinetics in Successful Balancing

	θ (deg)	$\dot{\theta}$ (deg/s)	f_{net} (N)	f_L (N)	f_R (N)
Participant 1	-0.6 (4.1)	-0.1 (16.3)	-0.1 (1.8)	3.2 (1.4)	3.1 (1.4)
Participant 2	-0.5 (2.4)	-0.0 (17.0)	0.1 (3.4)	4.4 (1.8)	4.6 (2.5)
Participant 3	-0.5 (5.9)	-0.4 (20.1)	-0.6 (2.8)	3.1 (1.6)	2.5 (1.8)
Participant 4	-0.2 (2.9)	-0.1 (16.2)	-0.5 (2.2)	3.3 (1.5)	2.7 (1.5)
Participant 5	-0.5 (5.1)	-0.1 (23.7)	0.9 (3.7)	3.7 (1.8)	4.6 (2.7)
Participant 6	-0.5 (3.7)	-0.0 (14.6)	0.5 (2.0)	2.2 (0.9)	2.7 (1.5)
Participant 7	-0.4 (4.1)	-0.0 (17.1)	-0.5 (2.9)	2.9 (2.0)	2.5 (1.4)
Participant 8	-0.6 (2.9)	-0.1 (12.5)	0.3 (2.0)	3.7 (1.7)	4.0 (1.8)
Average	-0.5 (4.0)	-0.1 (17.5)	0.0 (2.7)	3.3 (1.7)	3.4 (2.1)

Note. The values represent mean (and within-trial angular or standard deviation) for each participant successfully performing intermanual coordination. θ is the pole angle, $\dot{\theta}$ is the angular velocity, and f_{net} is the difference of the forces produced by the left (f_L) and right (f_R) hands.

Table 4.6 Experiment 4: Intermanual. Correlation Between f_{net} (N) and Individual Hand Forces (f_L, f_R) and Pole Kinematics

	θ (deg)	$\dot{\theta}$ (deg/s)	f_L (N)	f_R (N)
Participant 1	.52	-.56	.64	-.65
Participant 2	.28	-.75	.87	-.71
Participant 3	.36	-.33	.86	-.82
Participant 4	.32	-.57	.72	-.72
Participant 5	.36	-.62	.88	-.74
Participant 6	.42	-.51	.90	-.65
Participant 7	.32	-.66	.76	-.89
Participant 8	.39	-.59	.60	-.51
Average	.34	-.53	.77	-.65

How were the net forces on the cart produced during intermanual balancing? A comparison between the forces produced by the right (f_R: $r = -65$) and left (f_L: $r = .77$) hands revealed that both hands were equally correlated with net forces acting on the cart (t (7) = -1.16, $p > .05$), and that there were no significant differences (t (7) = - 0.06, $p > .05$, see Tables 6 and 7) between the magnitudes of these forces (f_L mean = 3.3 N, SD = 1.7 N vs. f_R mean = 3.4 N, SD = 2.1 N). In addition forces produced by the hands were not correlated with each other ($r = -.02$).

Table 4.7 Experiment 4: Intermanual. Correlation Between Forces Generated by the Left
(f_L) and Right (f_R) Hand and Pole Kinematic Variables (θ, $\dot\theta$)

	f_L		f_R	
	θ (deg)	$\dot\theta$ (deg/s)	θ (deg)	$\dot\theta$ (deg/s)
Participant 1	-.17	.48	.50	-.23
Participant 2	-.03	.62	.36	-.60
Participant 3	-.20	.31	.39	-.24
Participant 4	.01	.48	.47	-.34
Participant 5	-.37	.68	.25	-.40
Participant 6	-.24	.44	.40	-.40
Participant 7	-.17	.63	.40	-.45
Participant 8	-.07	.36	.34	-.31
Average	-.16	.46	.31	-.32

As in the previous experiment, the relative timing of the forces produced by each

hand was examined to account for the variation in the net forces on the cart. The results

of the mean continuous relative phase analysis are reported in Table 4.8. When collapsed

across the intermanual test and retest conditions, participants produced, on average mean

relative phase of −151.9 deg with an across trials angular deviation of 17.4 deg (for an

example time series see Figure 4.4a and c). This mean continuous relative phase describes

an antiphase coordination pattern with a right (dominant) hand lead for all participants, consistent with the results from Experiment 3. The overall distribution of continuous relative phase during the intermanual trials can be seen in Figure 4.6a, and shows a unimodal peak near −180 deg.

Table 4.8 Experiment 4: Intermanual. Relative Phase Between Forces Generated by the Left (f_L) and Right (f_R) Hand

	ϕ (deg)
Participant 1	-133.4 (5.3)
Participant 2	-151.6 (3.8)
Participant 3	-159.9 (8.3)
Participant 4	-126.5 (14.3)
Participant 5	-176.7 (4.3)
Participant 6	-167.4 (8.5)
Participant 7	-154.2 (3.6)
Participant 8	-144.4 (6.2)
Average	-.151.9 (17.4)

Note. Mean (and between trial angular deviation) of continuous relative phase between the force-time profiles of the two hands during intermanual balancing. The overall mean continuous relative phase value shows an antiphase coordination pattern (~180 deg).
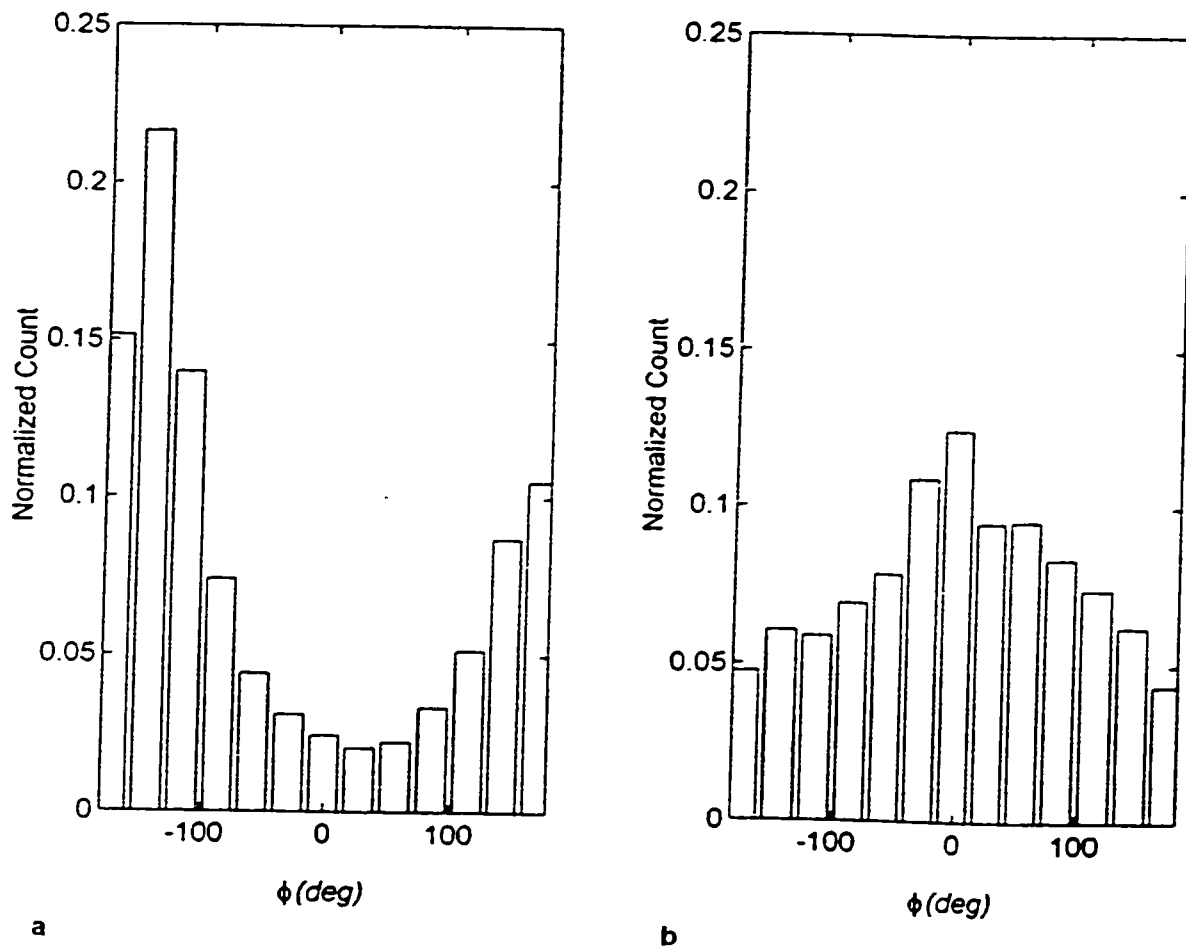
Figure 4.6a-b. (a) Distribution of continuous relative phase Φ values during successful intermanual balancing. The mean continuous relative phase denotes on average, an antiphase coordination pattern with the right hand leading the left (~180 deg, see also Table 4.8). (b) Distribution of continuous relative phase Φ values during successful interpersonal balancing. Here the mean continuous relative phase describes an inphase coordination pattern (~0 deg, see also Table 4.12).

4.7.5 Kinematic Analysis of Balancing: Interpersonal Balancing

How did the kinematics of the pole vary during interpersonal balancing? In Table 4.9 the average angular displacement (-0.5 deg, AD = 7.0 deg) and angular velocity (-0.3 deg/s, AD = 18.0 deg/s) values are reported. These results suggest that participants performing interpersonal balancing were able to balance the pole close to vertical and with similar variation in both pole angle and angular velocity as in the intermanual conditions (compare to Tables 4.1 and 4.5).

Table 4.9 Experiment 4: Interpersonal. Magnitudes of Pole Kinematics and Pole Kinetics in Successful Balancing

	θ (deg)	$\dot{\theta}$ (deg/s)	f_{net} (N)	f_L (N)	f_R (N)
Pair 1	-0.7 (2.6)	-0.2 (11.5)	0.1 (1.4)	2.0 (1.3)	2.1 (1.7)
Pair 2	-0.1 (6.6)	-0.1 (18.4)	-0.7 (2.2)	2.6 (1.6)	1.9 (1.4)
Pair 3	1.0 (14.3)	-3.3 (33.5)	-0.2 (3.3)	2.3 (2.7)	2.0 (2.0)
Pair 4	-4.0 (16.1)	3.0 (29.5)	-0.5 (3.2)	2.6 (2.7)	2.2 (1.6)
Average	-0.5 (7.0)	-0.3 (18.0)	-0.2 (2.1)	2.3 (1.7)	2.0 (1.6)

Note. The values represent mean (and within-trial angular or standard deviation) for each pair successfully performing interpersonal coordination. θ is the pole angle, $\dot{\theta}$ is the angular velocity, and f_{net} is the difference of the forces produced by the persons on the left (f_L) and right (f_R) of the cart.

How were the net forces on the cart related to the variation in pole kinematics during interpersonal balancing? Correlations were performed between the time series of the net forces (f_{net}) produced by the subjects on the cart, and the kinematic variables of pole angle (θ) and angular velocity ($\dot{\theta}$), and are reported in Table 4.10. In contrast to the intermanual cases no significant differences were found between the correlations of net force (on the cart) and angular velocity of the pole ($r = -.19$) versus between net force and the angle of the pole ($r = .33$), $t(3) = -1.42$, $p > .05$. In addition, this relationship between the net force and the angular velocity of the pole ($r = -.19$) was not significantly stronger than either the relationship between left subject's force and angular velocity ($r = .13$; $t(3)$ $= -1.04$, $p > .05$) or right person's force and angular velocity ($r = -.11$; $t(3) = 1.10$, $p >$ $.05$).

Table 4.10 Experiment 4: Interpersonal. Correlation Between f_{net} (N) and Individual Forces Generated by the Persons on the Right and Left of the Cart (f_L. f_R) and Pole Kinematics

	θ (deg)	$\dot{\theta}$ (deg/s)	f_L (N)	f_R (N)
Pair 1	.53	-.46	.67	-.23
Pair 2	.31	-.27	.72	-.77
Pair 3	.35	-.08	.55	-.79
Pair 4	.34	-.18	.53	-.86
Average	.33	-.19	.62	-.64

Furthermore as in the intermanual conditions (both Experiment 3 and here) the two subjects' forces were not different from each other, t (3) = -0.14, p > .05 (see Table 4.11). Finally, there were no significant differences in the correlations of these individual's effectors with pole angle as compared to with angular velocity (t (3) = -2.78, p > .05 for the left person, and t (3) = -1.38, p > .05, for the right, see Table 4.11).

Table 4.11 Experiment 4: Interpersonal. Correlation Between Forces Generated by the Participants to the Left (f_L) and Right (f_R) of the Cart and Pole Kinematic Variables ($\theta, \dot{\theta}$)

| | f_L | | f_R | |
	θ (deg)	$\dot{\theta}$ (deg/s)	θ (deg)	$\dot{\theta}$ (deg/s)
Pair 1	.25	.17	.64	-.26
Pair 2	-.26	.25	.20	-.14
Pair 3	-.30	.07	.14	-.06
Pair 4	-.25	.13	.27	-.13
Average	-.17	.13	.23	-.11

How were the net forces on the cart produced when two individuals collaborated to perform this task? A t-test revealed that relationships of equivalent strength were seen between the net force (f_{net}) and the forces produced by the right (f_R: r = -.64) and left (f_L =

.62) subjects across all participant pairs (t (3) = 0.29, p > .05, see Table 4.10). There were also no significant differences (t (3) = 2.06, p > .05, see Table 4.9) between the magnitudes of the average forces produced by either person (f_L mean = 2.3 N, SD = 1.7 N, f_R mean = 2.0 N, SD = 1.6 N). Finally, there was no linear relationship between the forces produced by the right and left participants (r = .18) again consistent with intermanual conditions. Note however, that the correlation between the right and left subjects was stronger for the only pair of participants to successfully complete the interpersonal task on both testing sessions (Pair 1, r = .56).

Were the variations in net forces on the cart produced by relative timing differences between the forces produced by each person? We have seen that participants produce an antiphase coordination pattern when balancing the pole intermanually. In contrast, when these *same* participants were tested in the interpersonal conditions, they exhibited a mean continuous relative phase of 7.6 deg, or an approximately inphase (~0 deg with some lead/lag asymmetry, see Table 4.12) coordination pattern, albeit with greater variability across trials (on average 59.1 deg AD). While the majority of these interpersonal trials were unsuccessful short trials (i.e. see the section on balance time above) and demonstrate some variability, the overall distributions of these patterns clearly suggest a unimodal distribution centered at 0 deg (with a right hand lead, see Figure 4.6b).

Table 4.12 Experiment 4: Interpersonal. Relative Phase Between Forces Generated by the Persons on the Left (f_L) and Right (f_R) of the Cart

ϕ (deg)

Pair 1	-2.6 (11.7)
Pair 2	116.8 (59.4)
Pair 3	-11.7 (54.0)
Pair 4	-11.8 (47.7)
Average	7.6 (59.1)

Note. Mean (and between trial angular deviation) of continuous relative phase between the force-time profiles of the persons on the left and right (f_L, f_R) of the cart. The overall mean continuous relative phase value shows an inphase coordination pattern (~0 deg).

4.8 Discussion: Experiment 4

In this second experiment we compare what coordination strategies participants develop when required to perform a functional stabilization task in either an intermanual (one individual using two hands, as in Experiment 3) or interpersonal condition (two persons, one hand each). Participants performed better in the intermanual trials (re: balance time and consistency criteria), and with the exception of those participants who never mastered the task, improvements in performance were observed in both conditions.

A previously developed classification system was used to quantify the gross balancing behaviors in this experiment (Foo et al., 2000). Participants in both the intermanual and interpersonal conditions demonstrated similar distributions of pole motions as in Experiment 3, and in previous unimanual balancing (Foo et al., 2000). These results suggested that mixture of observed balancing behavior depended on the mechanics of the apparatus and not how the participants held the cart.

How were the pole motions connected to the net forces produced by the two persons during interpersonal versus intermanual balancing? During intermanual balancing net force (f_{net}) was strongly coupled to pole angular velocity ($\dot{\theta}$) to support successful stabilization (agreeing with the correlation between angular velocity and cart velocity shown in Foo et al., 2000). The net force was more strongly related to pole angular velocity than either hand's force with angular velocity. These results were consistent with the results of Experiment 3, although participants appeared to control the pole differently during interpersonal balancing. In interpersonal balancing net force was strongly correlated to the pole's angle (θ) along with its angular velocity. However, as in the intermanual case, the net force was more related to this variable than either person's correlation with pole angle. This result was tempered by the fact that participants did not balance the pole as successfully in the interpersonal as in the intermanual conditions. It is possible that with more successful interpersonal balancing, similar correlations between net force and angular velocity may have developed. Note the importance of (angular) velocity as a quantity which has been observed to support action perception coupling in

behavior as well as coordination between behavior and the brain (Kelso et al., 1998; Jeka, et al., 1997).

Across the different balancing conditions, participants tended to create the net force on the cart in similar ways. The variations in net force required for successful balancing were not a result of differences in magnitudes of forces produced by the hands, nor of differences in how each hand was correlated to net force. Variations in net force were primarily created via relative timing differences between the hands. Two distinct relative timing patterns emerged between intermanual and interpersonal coordination. Specifically, when balancing the pole interpersonally, subjects produced predominantly inphase instead of antiphase patterns of coordination. In addition, significant positive inter-hand correlations were observed when performing successful interpersonal balancing that were not evident in intermanual behavior.

In Figure 4.4b,d we show a representative time series of hand forces and relative phase values for a pair of participants performing this inphase coordination pattern. Here the participants are oscillating the pole by pulling simultaneously on each cord at the base of the cart. The continuous relative phase values of the respective force-time profiles are hence centered about 0 deg, and characterize a coordination pattern that may be termed a co-contraction balancing strategy. Figure 4.6b shows a schematic of two hands using the co-contraction strategy to balance the pole. Both hands exert simultaneous tension on the pull cords, although here the right hand is pulling harder, and the net effect moves the cart to the right. Finally, the lead/lag relationships seen in interpersonal balancing mirrored the results of Experiment 3. During interpersonal balancing the more skilled performer

(on intermanual sessions) invariably led the other participant like the dominant hand led its counterpart in Experiment 3. Theoretically, this co-contraction strategy is organized in a parallel fashion, where the participants perform symmetric bimanual motions that are easier to coordinate with the environment (Guiard, 1987;see Kelso, Putnam, & Goodman, 1983; Kelso, Southard, & Goodman, 1979; Marteniuk & Mackenzie, 1980). These results are also consistent with studies of split-brain patients, where it was found that under conditions of impoverished coupling, patients tended to produce symmetric, inphase movements (Tuller & Kelso, 1989; Prielowski, 1972).

These results, when taken together, suggest the following account. During successful intermanual balancing, the net force (f_{net}) or action component is strongly coupled to the perceptual component of angular velocity of the pole ($\dot{\theta}$). When one person performs this task with an antiphase coordination between the hands, strong visual afferent, reafferent proprioceptive and cutaneous, and neuromuscular efferent connections are available to subserve the required precise timing relationships between effectors.

During interpersonal balancing, f_{net} is also correlated to $\dot{\theta}$, but in a weaker manner. When collaborating with another person, unless a co-contraction inphase coordination pattern is utilized, no afferent (from the motions of the other person) haptic information is available, nor are efferent connections to the other person (as opposed to the other hemisphere) since the pull cord is slack. In addition, the slack pull cord introduces a delay in the application of forces that makes successful performance of this anticipatory task even more difficult. Although afferent visual information remains, the coupling between

persons is weaker, and performance is depressed (see also Schmidt et al., 1998).

In contrast, when a pair of subjects employs a co-contraction strategy (observed as inphase coordination) and maintains simultaneous tension on both pull cords, participants establish efferent connections to the cart and other person, reduce the delay in force application, and augment with afferent haptic connections the information available to support interpersonal coupling. While this strategy may require more visual attention (i.e. participants seem to pay attention to θ as well as $\dot{\theta}$), successful completion of the task is now possible.

4.9 General Discussion

The goal of these experiments was to examine what patterns of coordination develop when humans are asked to perform a functional stabilization task and how these patterns are generated. This type of emerging coordination represents a new direction, since much of the previous work on coordination has focused on examining the coordination dynamics of systems in which the coordination pattern to be produced is the only goal for the participant. Here we have employed a functional stabilization task to serve as a window into the emerging coordination where the effectors were forced to work together and where the collaboration between the individual effectors could be directly measured.

The interpersonal conditions of Experiment 4 allow one to quantify some of the basic elements of social coordination. The ability to quantify dynamically the behavioral kinematics of this social situation makes this approach qualitatively different from previous approaches that employ self-report questionnaires (either after the fact, or

continuously during a testing session) to measure social phenomena (Nowak & Vallacher, 1998). The present situation ensures that both participants depend on each other to perform successfully the bi-directional motions necessary to complete this task, forcing the participants to cooperate. The alternation and co-contraction strategies seen in intermanual and interpersonal balancing constitute two different methods of *cooperating* together to perform this task successfully. The present experiments may be extended to test other concepts in social coordination such as competition by utilizing some form of deception (e.g. the use of a confederate who is trying to destabilize the pole), or a specialized reward schedule.

It should be noted that systematic asymmetries that may be attributed to decision-making processes were observed during all interpersonal sessions where the more skilled (re: intermanual performance) performer set the initial conditions of the pole, and whose hand motions consistently led the more novice performer. In one striking set of trials, the less skilled participant closed his eyes and merely exerted a (constant) tension on his pull cord as the second, more skilled participant made all the decisions to balance the pole successfully. Clearly, this paradigm would support many further investigations of decision-making (e.g. across dimensions of skill level, leadership styles, gender, group cohesion, motivation, etc.).

In the present experiments, a more complex task was presented to the subjects than previous instantiations of inverted pendulum balancing (e.g. Foo et al., 2000). In addition to the added difficulty presented by the pull cords, participants were asked to minimize the angle and angular velocity of the pole. These more difficult criteria go

beyond merely balancing the pole to fulfill a balance time and consistency criteria (compare to the "just keep it upright" criterion used previously in Foo et al., 2000) and allowed one to see participants demonstrating a higher level of control over the pole (e.g. Participant 7, see Table 4.1). In pilot data it was shown that subjects with this level of skill could perform the task for extended periods of time (at least 10 min) and "played" with the pole, as if they had discovered and stabilized the necessary control law for successful balancing and were now exploring its parameter space (see Warren, 1998). It was also observed in pilot data that individuals could intermanually perform both the alternation and co-contraction balancing strategies at will, opening up the possibility of determining the functional significance or differential stability of these two patterns in future experiments.

The present data may have important implications for the modeling of the visual control of this task. The previous observation of participant's use of visually specified time-to-balance variables during critical balancing situations (Foo et al., 2000) was not tested here due to a paucity of data in these types of critical situations.

Finally, the existence of relatively stable coordination patterns opens the possibility of observing some of the behaviors that are normally associated with inherently stable systems like bistability, spontaneous or intentional phase transitions, enhancement of fluctuations, hysteresis, critical slowing down and other measures of stability, and even learning dynamics (see e.g. Kelso, 1984; Kelso et al., 1988; Zanone & Kelso, 1992). Three points must be reiterated here. Foremost is the fact that the inherent dynamics of the inverted pendulum system are unstable, and that only through the

subject's skill and performance is any kind of stable coordination pattern observed. Secondly, these coordination patterns are being observed as a result of performing a functional task, and not as the only goal for the participant. Finally, these coordination patterns represent two different cooperation strategies, both across and within individuals, and represent an entry into examining more complex concepts in social psychology and perhaps other fields.

5.0 General Discussion

5.1 Functional Stabilization of Inherently Unstable Systems

The work presented in this dissertation represents one of two lines of research that examines processes of stabilization in coordination. In a related research, we have investigated how self-organized coordination patterns may be stabilized during situations that would normally render them unstable. In the present thesis we examine how biological systems functionally stabilize *inherently unstable* systems. In this general discussion we begin with an illustration of the many similar features between these two stabilization processes.

5.2 Use of Specific Local Information that has Global Stabilization Effects

In bimanual coordination, it has been shown that specific local environmental information can provide both spatial and temporal stabilization on coordination (Byblow, Carson, & Goodman, 1994). This so called 'anchoring' effect was first observed by Byblow et al. (1994), but no theoretical modeling was performed. We have replicated these experimental results and embedded them firmly in a theoretical framework (Fink et al., 2000; Jirsa et al., 2000). Experimentally, we demonstrated that a local source of specific environmental information (the metronome beat) served to stabilize the local spatial and temporal behavior of the system as observed from an analysis of movement trajectories (although recently it has been observed that such environmental information can also *destabilize* a typically stable pattern, see Kelso, Fink, & DeLaplain, under

review). This local stabilization had global effects on the coordination patterns. The less stable antiphase coordination pattern remained viable past critical movement frequencies where it would normally become unstable. Furthermore, the variability of inphase coordination was also reduced. From a theoretical modeling standpoint, adding a single parametric driving term to the HKB model successfully captures the observed phenomena.

By developing a classification scheme that focuses on local pole events during successful balancing and just prior to failures we have shown similar effects in functional stabilization (compare to previous experiments which focused on global behavior, e. g. Treffner & Kelso, 1995; 1997; 1999). In pole balancing (Experiments 1 and 2), specific environmental information (here the visual quantity time-to-balance, τ_{bal}) appears to gear the corrective motions of the hand during critical local pole motions. The result of these local events is to keep the pole upright for at least *one more cycle*. Note that when examined on a longer timescale (across the whole balancing trial) the correlations between hand velocity and τ_{bal} were not observed. Globally, the serial repetition of successfully avoiding a fall of the pole results in functional stabilization.

5.3 Recruitment aids Stabilization

Studies of unimanual and bimanual coordination have documented a phenomenon whereby active degrees of freedom (*df*) may be annihilated, and previously quiescent *df* spontaneously recruited to achieve stability when fulfilling an environmental task (Buchanan, Kelso, de Guzman, & Ding, 1997; Kelso, Buchanan, de Guzman, & Ding, 1993). A similar phenomenon has also been shown to occur within the swinging

pendulum paradigm (Buchanan, & Kelso, 1999; Fink et al., 2000) where it accounts for earlier, seemingly contradictory evidence (see Kugler & Turvey, 1987; Mitra et al., 1997; Schmidt et al., 1998). These results are captured theoretically by an amplitude-mediated transition process whereby organisms may stabilize less-stable coordination patterns by recruiting biomechanical *df*. In Experiments 3 and 4 we have observed similar recruitment effects.

During interpersonal coordination organisms may develop coordination patterns to recruit previously unavailable afferent and efferent connections that support the performance of a task. When stabilizing a pole interpersonally, if the strategy used during successful intermanual balancing is employed (alternation), afferent haptic information and efferent connections to the other person (as opposed to the other hemisphere in the intermanual conditions) are no longer available and performance is depressed. We have observed the *same subjects* (now comprising a social dyad) developing a *different* coordination pattern (co-contraction) that recruits those previously unavailable efferent and afferent connections helping to support interpersonal coupling and successful functional stabilization.

5.4 Learning as a Stabilization Process.

Studies of bimanual coordination have demonstrated that the process of learning (and other intentional processes) can stabilize previously unstable, to-be-learned patterns of coordination (Kelso et al., 1988; Scholz & Kelso, 1990; Zanone & Kelso, 1992, 1997). There the participant was given specific feedback about his/her performance (the relative timing of the effectors compared to the target timing) over several sessions of physical

practice. Upon retention testing, it was found that not only were the target patterns stabilized, but evidence for the stabilization of symmetrical patterns was also observed to have spontaneously developed. In the present experiments one can find evidence for similar learning and transfer effects.

Participants were able to acquire the skill of functional stabilization in almost all conditions (i.e. unimanually, intermanually, and interpersonally) over repeated practice trials, without the benefit of instruction or directed feedback. In addition to showing significant transfer effects, some participants demonstrated the ability to control the pole, minimizing the angle and angular velocity and moving it at will to different parts of the track, as opposed to merely keeping it upright. Our results suggest that what is learned and what is transferred across conditions is the effective use of time-to-balance information.

5.5 Visual Control of Functional Stabilization

We have shown in both virtual and real physical systems and even across very drastic manipulations, that the *same* visual information, time-to-balance, τ_{bal}, was significantly related to hand motions used to stabilize unstable systems. Time-of-closure variables have been implicated as sources of guidance across different sensory modalities (e.g. vision, audition, echolocation, electrolocation, etc., see Lee, 1998) and are postulated to guide the actions of organisms. Under a generalized τ theory, the time to closure for each physical gap and its current closure rate is sensed and constantly controlled and multiple τ variables are linearly coupled to produce the organism's desired interception path. In the absence of external stimuli, an intrinsically produced τ is coupled

to perform the task (Lee, 1998; Lee et al., 1999). While our observation that participants can anticipate a time to contact with an invisible or transposed balance angle would seem to support the use of internally generated τ variables (see the occluded pole in Experiment 2), other evidence presented here strongly suggests that τ information is used only intermittently in each balancing cycle (i.e. at the onset of hand deceleration). Moreover we have shown that participants use τ variable information only during specific potentially disastrous motions of the pole, and possibly in conjunction with other quantities. For example, participants were attuned to angular velocity ($\dot{\theta}$) when the pole's motion was disrupted (along with τ-variables, see perturbed control condition of Experiment 2). The linear coupling of τ information postulated by Lee (1998) would have to be modified to account for switching between these informational quantities (e.g. $\dot{\theta}$ and τ_{bal}).

5.6 Modeling Functional Stabilization

Our empirical results should aid further modeling of functional stabilization. We have presented a control strategy that uses constraints on a perceptual variable (τ_{bal}, a temporal measure) to adjust a parameter of a linear controller (Experiment 1). This controller uses the perceptual variables τ_{bal} and $\dot{\tau}_{bal}$ to monitor and sometimes adjust the weightings of this linear control function, on a cycle-by-cycle basis, during critical actions where it must actively intervene in order to prevent a failure. This model may be expanded to encompass the results of the second experiment, were participants were observed be sensitive to other variables (e.g. θ and $\dot{\theta}$) during critical situations.

Furthermore, in Experiments 3 and 4 participants did not display the critical situations normally observed in the first two experiments, and a full account of functional stabilization must include how humans balance the pole when they are controlling the pole with such an increased skill level.

6.0 Conclusion

Under the aegis of a theoretical framework known in the literature as coordination dynamics, coordination has been demonstrated to be self-organized. Patterns of coordination that emerge can be derived in terms of nonlinear interactions among intrinsically nonlinear components. These nonlinear couplings give rise to functional synergies that possess dynamical properties (e.g. multistability, bifurcations, hysteresis, etc.). Near instabilities, the high dimensional dynamics of the system may be captured by a few low dimensional order parameters that encompass the relevant degrees of freedom of the system. By manipulating external control parameters, one may push the system to change and transition between coordination modes. The dynamical mechanism for these effects is instability, as revealed in measures of variability, intentional switching, or local relaxation times (critical slowing down). These generic mechanisms can be found in other areas of nature as well as across experimental levels of description. In recent years the strategy of coordination dynamics has been extended all the way down to excitatory/inhibitory connections between local regions of the cortex (Jirsa, Fuchs, & Kelso, 1998; Kelso, Fuchs, & Jirsa, 1998).

A relatively recent extension of coordination dynamics deals with biological self-stabilization processes. In parametric stabilization, specific environmental information is used to stabilize spatial and temporal coordination on a local level with commensurate effects on global coordination dynamics. Organisms may also use recruitment processes

(e.g. of redundant biomechanical *df*) to achieve the stability needed to complete a task. Furthermore, the learning process stabilizes unstable systems since it is through learning that the organism discovers and retains what information is important to the successful completion of the task

As a result of this thesis, we extend previous work on coordination dynamics to include the functional stabilization of inherently unstable systems. These systems are ubiquitous in nature, and represent constant challenges to biological organisms. We have used pole balancing as a window into these stabilization processes. Across these experiments, one may observe that the same visual time-to-balance information is discovered and employed for successful stabilization across even drastic manipulations to a mechanical (or virtual) unstable system. We have shown how specific sensory (i.e. τ_{bal}) information can both locally and, in time globally (functionally) stabilize coordination. Furthermore, we have demonstrated how potentially independent forces combine to produce successful stabilization. These results suggest some similarities between the current line of research and the self-stabilization processes mentioned previously. Finally, in this paradigm coordination patterns emerge as participants perform a functional task (vs. previous work where the coordination pattern *was* the main task). This type of emerging coordination represents a new direction, and reflects our belief that the task goal in voluntary movements provides meaning to existing information sources in the environment as well as the coordination strategies that support the performance of that task.

7.0 References

Amazeen, P. G., Schmidt, R. C., Turvey, M. T. (1995). Frequency detuning of the phase entrainment dynamics of visually coupled rhythmic movements. *Biological Cybernetics, 72*, 511-518.

Anderson, C. W. (1989). Learning to control an inverted pendulum using neural networks. *IEEE Control Systems Magazine, 4*, 31-36.

Aston, S. J., DeSylvia, D. A., Mancil, G. C., Boerner, R., & Doyle, J.J. (1990). *Optometric gerontology: a resource manual.* Rockville, MD: Association of Schools and College of Optometry.

Bachman, J. C. (1961). Specificity vs. generality in learning and performing two large muscle motor tasks. *Research Quarterly, 32*, 3-11.

Barto, A. G., Sutton, R. S., & Anderson, C. W. (1983). Neuron-like adaptive elements that can solve difficult learning control problems. *IEEE Transactions on Systems, Man, and Cybernetics, 5*, 834-846.

Batschelet, E. (1981). *Circular Statistics in Biology.* London: Academic.

Bertenthal, B. I., & Bai, D. L. (1989). Infants' sensitivity to optical flow for controlling posture. *Developmental Psychology, 25*, 936-945.

Bertenthal, B. I., Rose, J. L., & Bai, D. L. (1997). Perception-action coupling in the development of visual control of posture. *Journal of Experimental Psychology: Human Perception and Performance, 23, 6*, 1631-1643.

Bootsma, R. J., & Oudejans, R.R.D. (1993). Visual information about time to collision between two objects. *Journal of Experimental Psychology: Human Perception and Performance, 19,* 1041-1052.

Bootsma, R. J., Fayt, V., Zaal, F. T. J. M. & Laurent, M. (1997). On the information-based regulation of movement: what Wann (1996) may want to consider. *Human Movement Science, 13,* 1282-1289.

Buchanan, J. J., & Kelso, J. A. S. (1999). To switch or not to switch: recruitment of degrees of freedom stabilizes biological coordination. *Journal of Motor Behavior, 31,2,* 126-144.

Buchanan, J. J., Kelso, J. A. S., de Guzman, G. C., & Ding, M. (1997). The spontaneous recruitment and suppression of degrees of freedom in rhythmic hand movements. *Human Movement Science, 16,* 1-32.

Byblow, W. D., Carson, R. G., & Goodman, D. (1994). Expressions of asymetries and anchoring in bimanual coordination. *Human Movement Science, 13,* 3-28.

Castro, A.C., Postigo, J. F., & Manzano, J. (April, 2000). Integration of a force feedback joystick with a virtual reality system. *Latin American Applied Research, 30,2,* 171-178.

Chen, Y., Ding, M., & Kelso, J. A. S. (1997). Long memory processes ($1/f^{\alpha}$) in human coordination. *Physical Review Letters, 79, 22,* 4501-4504.

Collins, J. J. & De Luca, C. J. (1994). Random walking during quiet standing. *Physical Review Letters, 73(5),* 764-767.

Collins, J. J. & De Luca, C. J. (1995). The effects of visual input on open-loop and

    closed-loop postural control mechanisms. *Experimental Brain Research, 103,*

    151-163.

Dutta, D. (July, 1999). Simulation in military training: Recent developments. *Defense*

    Science Journal, 49, 3, 275-285.

Elgerd, O. I. (1967). *Control Systems Theory.* New York: Mcgraw-Hill Book Co.

Fink, P. W., Kelso, J. A. S., Jirsa, V. K., & de Guzman, G. C. (2000). Recuitment of

    degrees of freedom stabilizes coordination. *Journal of Experimental Psychology:*

    Human Perception and Performance, 26, 2, 671–692.

Fink, P.W., Foo, P., Jirsa, V.K., & Kelso, J.A.S. (in press). Local and global stabilization

    of coordination by sensory information. *Experimental Brain Research.*

Foo, P., & Kelso, J. A. S. (in press). Goal directed meaning connects perception and

    specification. Invited commentary to Stoffregen, T. A., & Bardy, B. G. (2001) On

    specification and the senses. *Behavioral and Brain Sciences, 24,* xxx-xxx.

Foo, P., de Guzman, G. C., & Kelso, J. A. S., (in preparation). Intermanual and

    interpersonal stabilization of unstable fixed points.

Foo, P., Kelso, J. A. S., & de Guzman, G. C. (2000). Functional stabilization of unstable

    fixed points: human pole balancing using "time to balance" information. *Journal*

    of Experimental Psychology: Human Perception and Performance, 4, 1281-1297.

Fuchs, A., Deecke, L., Kelso, J. A. S. (2000). Phase transitions in the human brain revealed by large SquID arrays: Response to Daffertshofer, Peper and Beek. *Physics Letters A, 266(4-6),* 303-308.

Fuchs, A., Kelso, J. A. S., Haken, H. (1992). Phase transitions in the human brain: spatial mode dynamics. *International Journal of Bifurcation and Chaos, 2,* 917-939.

Fuchs, A., Mayville, J., Cheyne, D., Weinberg, H., Deecke, L., & Kelso, J. A. S. (2000). Spatiotemporal analysis of neuromagnetic events underlying the emergence of coordinative instabilities. *Neuroimage, 12,* 71-84.

Geva, S., & Sitte, J. (1993, October). A cartpole experiment benchmark for trainable controllers. *IEEE Control Systems,* 13,5, 40-51.

Guez, A., & Selinski, J. (1988). A trainable neuromorphic controller. *Journal of Robotic Systems, 5,* 363-388.

Guiard, Y. (1987). Asymmetric division of labor in human skilled bimanual action: The kinematic chain as a model. *Journal of Motor Behavior, 19,* 486-517.

Haken, H. (1996). *Principles of Brain Functioning: A Synergetic Approach to Brain Activity, Behavior and Cognition.* Berlin: Springer-Verlag.

Haken, H., Kelso, J. A. S., & Bunz, H. (1986). A theoretical model of phase transitions in human hand movements. *Biological Cybernetics, 51,* 347-356.

Hansson, A. (March, 2000). Space tourism (Virtual reality, computers). *Architectural Design, 144,* 26-29.

Hausdorff, J. M., Purdon, P. L., Peng, C.-K., Ladin, Z., Wei, J. Y., & Goldberger, A. L. (1996). Fractal dynamics of human gait: stability of long-range correlations in stride interval fluctuations. *Journal of Applied Physiology, 80(5),* 1448-1457.

Houde, J. F., Jordan, M. I. (1998). Sensorimotor adaptation in speech production. *Science, 279, 5354,* 1213-1216.

Ingham, A. G., Levinger, G., Graves, J., & Peckham, V. (1974). The Ringelmann effect: studies of group size and group performance. *Journal of Experimental Social Psychology, 10,* 371-384.

Jeka, J. J., & Lackner, J. R. (1994). Fingertip contact influences human postural control. *Experimental Brain Research, 100,* 495-502.

Jeka, J. J., & Lackner, J. R. (1995). The role of haptic cues from rough and slippery surfaces in human postural control. *Experimental Brain Research, 103,* 267-276.

Jeka, J. J., Schöner, G., Dijkstra, T., Ribeiro, P., & Lackner, J. R. (1997). Coupling of fingertip somatosensory information to head and body sway. *Experimental Brain Research, 113,* 475-483.

Jirsa, V.K., Fink, P.W., Foo, P., & Kelso, J.A.S. (2000). Parametric stabilization of biological coordination: a theoretical model. *Journal of Biological Physics, 26,* 85-112.

Jirsa, V. K., Fuchs, A., & Kelso, J. A. S. (1998). Connecting cortical and behavioral dynamics: Bimanual coordination. *Neural Computation, 10,* 2019-2045.

Kelso, J. A. S. (1981). Contrasting perspectives on order and regulation in movement. In Long, J., & Baddeley, A. (Eds.), *Attention and Performance IX* (pp. 437-457). Hillsdale, NJ: Lawrence Erlbaum Associates.

Kelso, J. A. S. (1984). Phase transitions and critical behavior in human bimanual coordination. *American Journal of Physiology: Regulatory, Integrative and Comparative Physiology, 15*, R1000-R10004.

Kelso, J. A. S. (1992). Theoretical concepts and strategies for understanding perceptual-motor skill: from information capacity in closed systems to self-organization in open, non-equilibrium systems. *Journal of Experimental Psychology: General, 121,3*, 260-261.

Kelso, J.A.S. (1995). *Dynamic Patterns: The Self-Organization of Brain and Behavior*. Cambridge, MA: The MIT Press.

Kelso, J. A. S., Bressler, S. L., Buchanan, S., de Guzman, G. C., Ding, M., Fuchs, A., & Holroyd, T. (1991). Cooperative and critical phenomena in the human brain revealed by multiple SquIDs. In D. Duke, & W. Pritchard (Eds.), *Measuring Chaos in the Human Brain* (pp. 97-112). Teaneck, NJ: World Scientific.

Kelso, J. A. S., Bressler, S. L., Buchanan, S., de Guzman, G. C., Ding, M., Fuchs, A., & Holroyd, T. (1992): A phase transition in human brain and behavior. *Physics Letters A, 169*, 134-144.

Kelso, J. A. S., Buchanan, J. J., de Guzman, G. C., & Ding, M. (1993). Spontaneous recruitment and annihilation of degrees of freedom in biological coordination. *Physics Letters A, 179*, 364-371.

Kelso, J. A. S., Fink, P. W., & DeLaplain, C. R. (under review). Haptic information

stabilizes and destabilizes coordinated movement: a reply to Carson et al. (1999).

Proceedings of the Royal Society of London

Kelso, J. A. S., Fuchs, A., & Jirsa, V. K. (1998). Traversing scales of brain and

behavioral organization I: concepts and experiments. In C. Uhl (Ed.), *Analysis of*

Neurophysiological Brain Functioning. Berlin: Springer.

Kelso, J. A. S., Fuchs, A., Lancaster, R., Holroyd, T., Cheyne, D., & Weinberg, H.

(1998). Dynamic cortical activity in the human brain reveals motor equivalence.

Nature, 392, 814-818.

Kelso, J. A. S., Putnam, C. A., & Goodman, D. (1983). On the space-time structure of

human interlimb coordination. *Quarterly Journal of Experimental Psychology,*

35A, 347-376.

Kelso, J. A. S., Scholz, J. P., & Schöner, G. (1986). Nonequilibrium phase transitions in

coordinated biological motion: Critical fluctuations. *Physics Letters A, 118,*

279-284.

Kelso, J. A. S., Scholz, J. P., & Schöner, G. (1988). Dynamics governs switching among

patterns of coordination in biological movement. *Physics Letters A, 134, 1,* 8-

12.

Kelso, J. A. S., Southard, D. L., & Goodman, D. (1979). On the nature of human

interlimb coordination. *Science, 203,* 1029-1031.

Kelso, J.A.S., Delcolle, J.D., & Schöner, G. (1990). Action-perception as a pattern formation process. In: Jeannerod, M. (Ed.), *Attention and performance XIII* (pp. 139-169). Hillsdale, NJ: Erlbaum.

Kinsbourne, M., & Hicks, J. (1978). Functional cerebral space: a model for overflow, transfer, and interference effects in human performance: a tutorial review. In Requin, J. (Ed.), *Attention and Performance VII* (pp. 345-362). Hillsdale, N. J.: Erlbaum.

Kugler, P. N., & Turvey, M. T. (1987). *Information, Natural Law, and the Self-Assembly of Rhythmic Movement.* Hillsdale, NJ: Erlbaum.

Kwakernaak, H., & Sivan, R. (1972). *Linear Optimal Control Systems.* John Wiley & Sons, Inc., New York.

Lee, D. N. (1976). A theory of visual control of braking based on information about time-to-collision. *Perception, 5,* 437-459.

Lee, D. N. (1998). Guiding movement by coupling taus. *Ecological Psychology, 10,* 221-250.

Lee, D. N., & Aronson, E. (1974). Visual proprioceptive control of standing in human infants. *Perception and Psychophysics, 15,* 529-532.

Lee, D. N., & Reddish, P. E. (1981). Plummeting gannets: a paradigm of ecological optics. *Nature, 293,* 293-294.

Lee, D. N., Craig, C. M., & Grealy, M. A. (1999). Sensory and intrinsic coordination of movement. *Proceedings of the Royal Society of London, B266,* 2029-2035.

Lee, D. N., Young, D. S. & Rewt, D. (1992). How do somersaulters land on their feet? *Journal of Experimental Psychology: Human Perception and Performance, 18, 4,* 1195-1202.

Liebovitch, L. S. & Yang, W. (1997). Transition from persistent to antipersistent correlation in biological systems. *Physical Review E, 56:4557-4566.*

Marteniuk, R. G., & Mackenzie, C. L. (1980). A preliminary theory of two-handed movement control. In G. E. Stelmach, & J. Requin (Eds.) *Tutorials in Motor Behavior.* Amsterdam: North Holland.

Mayville, J.M., Bressler, S.L., Fuchs, A., & Kelso, J. A. S. (1999). Spatiotemporal reorganization of electrical activity in the human brain associated with a timing transition in rhythmic auditory-motor coordination. *Experimental Brain Research 127,* 371-381.

McGonigle, B., & Flook, J. (1978). Long-term retention of single and multistate prismatic adaption by humans. *Nature, 272, 5651,* 364-366.

Mehta, B., Schaal, S. (1999). Visuomotor control of an unstable dynamical task. *Society for Neuroscience Abstracts, 25,* 1302.

Mitra, S., Amazeen, P.G., & Turvey, M.T. (1997). Dynamics of bimanual rhythmic coordination in the coronal plane. *Motor Control, 1,* 44-71.

Morizono, T., & Kawamura, S. (1998). Toward virtual sports with high speed motion. *Experimental Robotics V, 232,* 116-127.

Newell. K. M., Slobounov, S. M., Slobounova, E. S., & Molenaar, P. C. M. (1997). Stochastic processes in postural center-of-pressure profiles. *Experimental Brain Research, 113,* 158-164.

Nowak. A., & Vallacher, R. R. (1998). *Dynamic Social Psychology.* New York: Guilford Press.

Ogata, K. (1978). *System Dynamics.* New Jersey: Prentice-Hall, Inc. pp. 531-536.

Pagano, C. C., & Turvey, M. T. (1992). Eigenvectors of the interia tensor and perceiving the orientation of a hand-held object by dynamic touch. *Perception and Psychophysics, 52,* 617-624.

Playter. R., & Raibert, M. (1997). A virtual surgery simulator using advanced haptic feedback. *Minimally Invasive Therapy & Allied Technologies. 6, 2,* 117-121.

Preilowski, B. F. B. (1972). Possible contribution of the anterior forebrain commissures to bilateral motor coordination. *Neuropsychologia, 10,* 267-277.

Redding. G. M., & Wallace, B. (2000). Prism exposure aftereffects and direct effect for different movement and feedback times. *Journal of Motor Behavior, 32,* 83-99.

Savelsbergh, G. J. P. (1995). Catching "Grasping tau." Comments on J. R. Tresilian (1994). *Human Movement Science, 14,* 125-127.

Savelsbergh, G. J. P., Whiting, H. T. A. & Bootsma, R. J. (1991). Grasping Tau. *Journal of Experimental Psychology: Human Perception and Performance, 17, 2,* 315-322.

Savelsbergh, G. J. P., Whiting, H. T. A. & Pepers, J. R. (1992). The control of catching. In Summers, J.J. (Eds.), *Approaches to the Study of Motor Control and Learning.* Amsterdam, North-Holland: Elsevier Science Publishers.

Schaefer, J. F. (1965). *On the bounded control of some unstable mechanical systems.* Unpublished doctoral dissertation. Stanford University.

Schiff, W. (1965). Perception of impending collision: A study of visually directed avoidance behavior. *Psychological Monographs: General and Applied, 79,* (11, Whole No. 604)

Schiff, W., Caviness, J.A., & Gibson, J.J. (1962). Persistent fear responses in Rhesus monkeys to the optical stimulus of 'looming'. *Science, 136,* 982-983

Schmidt, R. C., Bienvenu, M., Fitzpatrick, P. A., & Amazeen, P. G. (1998). A comparison of intra- and interpersonal interlimb coordination: Coordination breakdowns and coupling strength. *Journal of Experimental Psychology: Human Perception and Performance,* 24, 3, 884-900.

Schmidt, R. C., Carello, C. C., & Turvey, M. T. (1990). Phase transitions and critical fluctuations in the visual coordination of rhythmic movements between people. *Journal of Experimental Psychology: Human Perception and Performance,* 16, 227-247.

Scholz, J. P. & Kelso, J. A. S. (1990). Intentional switching between patterns of bimanual coordination depends on the intrinsic dynamics of the patterns. *Journal of Motor Behavior, 22, 1,* 98-124.

Scholz, J. P., Kelso, J. A. S., & Schöner, G. (1987). Nonequilibrium phase transitions in coordinated biological motion: critical slowing down and switching time. *Physics Letters A, 123, 8,* 390-394.

Schöner, G. & Kelso, J. A. S. (1988a). A synergetic theory of environmentally-specified and leaned patterns of movement coordination. I Relative phase dynamics. *Biological Cybernetics, 58,* 71-80.

Schöner, G. & Kelso, J. A. S. (1988b). A synergetic theory of environmentally-specified and leaned patterns of movement coordination. II Component oscillator dynamics. *Biological Cybernetics, 58,* 81-89.

Schöner, G., Haken, H., & Kelso, J. A. S. (1986). A stochastic theory of phase transitions in human hand movement. *Biological Cybernetics, 53,* 247-257.

Seuss, Dr. (1957). *The Cat in the Hat.* New York: Random House, Inc.

Shaw, B. K., McGowan, R. S. & Turvey, M. T. (1991). An acoustic variable specifying time-to-contact. *Ecological Psychology, 3, 3,* 253-261.

Sternad, D., Duarte, M., Katsumata, H., & Schall, S. (under review). Bouncing a ball: Tuning into dynamic stability. *Journal of Experimental Psychology: Human Perception and Performance.*

Strogatz, S. H. (1994). *Nonlinear Dyanmics and Chaos: with Applications to Physics, Biology, Chemistry, & Engineering* (pp. 26-36). Reading, MA: Addison-Wesley Publishing.

Thelen, E. (1990). Coupling perception and action in the development of skill: A dynamic approach. In Bloch, H. & Bertenthal, B. I. (Eds.), *Sensory-motor Organization and Development in Infancy and Early Childhood* (pp.39-56). Dordrecht, the Netherlands: Kluwer.

Tolat, V.V., & Widrow, B. (July, 1988). An adaptive 'broom balancer' with visual inputs, in *Proceedings of the International Conference on Neural Networks, San Diego, CA*, II-641-II-647.

Treffner, P. J., & Kelso, J. A. S. (1995). Functional stabilization of unstable fixed points. In B. Bardy, R. Bootsma, & Y. Guiard, Y. (Eds.). *Studies in Perception and Action: III* (pp. 83-86). Hillsdale, NJ: Erlbaum.

Treffner, P. J., & Kelso, J. A. S. (1997). Scale-invariant memory during functional stabilization. In M. A. Schmuckler, & J. M. Kennedy (Eds.), *Studies in Perception and Action: IV* (pp. 275-279). Hillsdale, NJ: Erlbaum.

Treffner, P. J., & Kelso, J. A. S. (1999). Dynamical encounters: Long-memory during functional stabilization. *Ecological Psychology, 11, 2,* 103-137.

Treffner, P. J., & Turvey, M. T. (1996). Symmetry, broken symmetry, and handedness in bimanual coordination dynamics. *Experimental Brain Research, 107,* 463-478.

Tresilian, J. R. (1994). Perceptual and motor processes in interceptive timing. *Human Movement Science, 13,* 335-373.

Tresilian, J. R. (1995). Visual modulation of interceptive action. A reply to Savelsbergh. *Human Movement Science, 14,* 129-132.

Tuller, B. & Kelso, J. A. S. (1989). Environmentally-specified patterns of movement

    coordination in normal and split-brain subjects. *Experimental Brain Research*,

    75, 306-316.

Turvey, M. T., Burton, G., Pagano, C.C., Solomon, H. Y., & Runeson, S. (1992). Role of

    the inertia tensor in perceiving object orientation by dynamic touch. *Journal of*

    Experimental Psychology: Human Perception and Performance, 18, 714-727.

Wagner, H. (1982). Flow-field variables trigger landing in flies. *Nature, 297,* 147-148.

Wallenstein, G. V., Kelso, J. A. S., & Bressler, S. L. (1995). Phase transitions in

    spatiotemporal patterns of brain activity and behavior. *Physica D, 84,* 626-634.

Wann, J. P. (1996). Anticipating arrival: is the tau-margin a specious theory? *Journal*

    of Experimental Psychology: Human Perception and Performance, 22, 4, 1031-

    1048.

Warren, W. H. Jr. (1988). The visual guidance of action. In Meijer, O. G. & Roth, K.

    (Eds.), *Complex Movement Behavior.* Amsterdam, North-Holland: Elsevier

    Science Publishers.

Warren, W. H. Jr. (1998). Visually controlled locomotion: 40 years later. *Ecological*

    Psychology, 10(3-4), 177-219.

Warren, W. H., & Kelso, J. A. S. (1985). Work group on perception and action. In W. H.

    Warren & R. E. Shaw (Eds.), *Persistence and Change: Proceedings of the 1ˢᵗ*

    International Conference on Event Perception, (pp. 269-281). Mahwah, NJ:

    Erlbaum.

Widrow, B., & Smith, F. W. (1964). Pattern recognizing control systems. *Computer and Information Sciences (COINS) Proceedings, Washington, D.C.,* 288-317.

Wimmers, R., H., Beek, P., J., & van Wieringen, P. C. W. (1992) Phase transitions in rhythmic tracking movements: a case of unilateral coupling. *Human Movement Science, 11,* 217-226.

Zanone, P. G., & Kelso, J. A. S. (1992). The evolution of behavioral attractors with learning: Nonequilibrium phase transitions. *Journal of Experimental Psychology: Human Perception and Performance, 18, 2,* 402-421.

Zanone, P. G., & Kelso, J. A. S. (1997). The coordination dynamics of learning and transfer: Collective and component levels. *Journal of Experimental Psychology: Human Perception and Performance, 23, 5,* 1-27.

8.0 Appendices

8.1 Appendix A: Physical Equations of Motion for the Cart-Pole System

The configuration of the pole balancing apparatus is shown in Figure 2.1b. The horizontal position of the cart is given by X and the pole angle measured from the vertical reference line is θ. The equations for X and θ for this straight pole are given by

$$\tfrac{4}{3}(m + M)L\ddot{\theta} + (m + M)\ddot{X}\cos\theta = (m + M)g\sin\theta \tag{A1}$$

$$(m + M)\ddot{X} - mL\dot{\theta}^2 \sin\theta + mL\cos\theta\ddot{\theta} = F \tag{A2}$$

To reduce the number of parameters, we normalize the variables and parameters as follows: $\mu = m \cdot (m + M)^{-1}$, $\omega^2 = gL^{-1}$, $x = L^{-1}X$, $f = (m + M)^{-1}L^{-1}F$. The relevant physical parameters are therefore the frequency ω, the reduced mass μ, and those needed to specify force f. The parameter ω is a measure of how fast the pole will fall when started with an infinitesimal velocity from an upright position if the cart is fixed at the bottom. Using these transformations, we express Equations (A1) and (A2) in a standard format,

$$(\tfrac{4}{3} - \mu\cos^2\theta)\ddot{\theta} = \omega^2\sin\theta - \mu\dot{\theta}^2\sin\theta\cos\theta - f\cos\theta \tag{A3}$$

$$(\tfrac{4}{3} - \mu\cos^2\theta)\ddot{x} = -\mu\omega^2\cos\theta\sin\theta + \tfrac{4}{3}\mu\dot{\theta}^2\sin\theta + \tfrac{4}{3}f \tag{A4}$$

Motion around balanced condition

Near balanced condition, $\sin\theta \approx \theta$, $\cos\theta \approx 1$, and $\dot\theta \approx 0$ and the previous equations reduce to

(A5)

$$(\tfrac{4}{3} - \mu)\ddot\theta = \omega^2\theta - f$$

$$(\tfrac{4}{3} - \mu)\ddot{x} = -\mu\omega^2\theta + \tfrac{4}{3} f \qquad\text{(A6)}$$

Since $\mu < 1$, we divide both sides by $4/3-\mu$ and rewrite (A5) and (A6) in the form

$$\ddot\theta = -k_1\theta \ , \quad \ddot{x} = k_2\theta \qquad\text{(A7)}$$

where k_1 and k_2 are given by

$$k_1 \equiv \left(\frac{4}{3} - \mu\right)^{-1}\left(\frac{f}{\theta} - \omega^2\right) \qquad\text{(A8)}$$

$$k_2 \equiv \left(\frac{4}{3} - \mu\right)^{-1}\left(\frac{4}{3}\frac{f}{\theta} - \mu\omega^2\right) \qquad\text{(A9)}$$

8.2 Appendix B: Source Code for Virtual Balancing Simulation

```
//---------------------------------------------------------------
// File: DDEx1.CPP
//
//          Desc: Pole Balancing program - Uses cart position and acceleration
//          from mouse and accelerometer. respectively, and computes future
//          pole angle and velocity. Graphics on DirectDraw routines.
//
//          Hardware:   Data Translation A/D board. Program checks board type
//          and capabilities.
//
//          Based on DDex1 DirectX 6.1 and SVADC sample programs
//---------------------------------------------------------------


#ifndef WIN32_LEAN_AND_MEAN
#define WIN32_LEAN_AND_MEAN
#endif


//---------------------------------------------------------------
// Include files
//---------------------------------------------------------------
#include <windows.h>
#include <ddraw.h>
#include <stdio.h>
#include <stdarg.h>
#include "resource.h"
#include <math.h>
#include <stdlib.h>
#include <ddutil.h>
#include <time.h>
#include <stddef.h>
//---------------------------------------------------------------


// **** Data Translation include files and definitions ******************
#include <olmem.h>
#include <olerrors.h>
#include <oldaapi.h>
//******************************************************************************
**

#define STRLEN 200      /* string size for general text manipulation   */
char str[STRLEN];       /* global string for general text manipulation */
```

```
#define KKK_MAX                   300
#define MAXPOINTS                 5000
#define RADIAN_TO_DEGREE          57.2957795I3
#define PI                        3.1415926536
#define TWOPI                     6.2831853072
#define PIOVERTWO                 1.5707963263
#define THETA_CRIT                1.58


// Based on 1280 x 1024 sized window
#define TRACK_XLOW                -20     //20
#define TRACK_XHI                 1300  //1260
#define TRACK_YLOW                800
#define TRACK_YHI                 TRACK_YLOW-20
#define CART_PIVOTY               TRACK_YLOW-40
#define CART_LENGTH               20
#define VISIBLE_POLE_LENGTH 500
#define TRACK_YLOW_INV            300
#define TRACK_YHI_INV             TRACK_YLOW_INV-20
#define CART_PIVOTY_INV           TRACK_YLOW_INV+20


HBRUSH hBrushClient;
HBRUSH hBrushCart;
HBRUSH hBrushPole;
HBRUSH hBrushTrack;
HPEN   hPenPole;

POINT g_cartNow;                  // Current cart/cursor pixel coordinates
DOUBLE g_theta;                   // Current pole position in radians
DOUBLE g_omega=1.0;               //Current pole frequency
LONG g_fmark;                     //current pole fail marker
LONG gu_iCount=0;
FLOAT gf_volts;
DOUBLE x_theta,x_thetaDot;
FLOAT g_offsetvolts = 0.0;
DOUBLE gravity = 9.8;
FLOAT offsetvolts[KKK_MAX];
FILE *fp;                         // this is for saving the data to file
typedef struct TDATA              // data structure so you can save the data
{
        LONG ccNow;               //g_cartNow
        LONG tthet;               //g_theta array
        LONG tthetdot;            //thetadot array
        LONG aax;                 // x acceleration array
```

162

```c
        LONG fmark;                  // fail marker
} Data;
static Data TrialData[MAXPOINTS];
static LONG deltatime=0;
static LONG maxdeltatime=0;
static LONG mindeltatime=100;
DOUBLE XSCALE_FACTOR = -550.0;  // Volts to accel conversion factor
/* Error handling macros for Data Translation commands */
#define                                          SHOW_ERROR(ecode)
MessageBox(HWND_DESKTOP,olDaGetErrorString(ecode,\
            str,STRLEN),"A/D Error", MB_ICONEXCLAMATION | MB_OK);
#define CHECKERROR(ecode) if ((board.status = (ecode)) != OLNOERROR)\
            {\
            SHOW_ERROR(board.status);\
            olDaReleaseDASS(board.hdass);\
            olDaTerminate(board.hdrvr);\
            return ((UINT)NULL);}
#define CLOSEONERROR(ecode) if ((board.status = (ecode)) != OLNOERROR)\
            {\
            SHOW_ERROR(board.status);\
            olDaReleaseDASS(board.hdass);\
            olDaTerminate(board.hdrvr);\
            return (TRUE);}
/* simple structure used with board */
typedef struct tag_board {
    HDRVR hdrvr;      /* driver handle          */
    HDASS hdass;      /* sub system handle      */
    ECODE status;     /* board error status     */
    HBUF  hbuf;       /* sub system buffer handle */
    WORD FAR* lpbuf;  /* buffer pointer         */
    char name[STRLEN]; /* string for board name   */
    char entry[STRLEN]; /* string for board name  */
} BOARD;

typedef BOARD FAR* LPBOARD;
static BOARD board;

/* Global A/D related variables for this particular application */
    DBL gdMin,gdMax,gdRange;
    UINT guEncoding,guResolution;
    UINT guChannel = 0;
    DBL gdGain = 1.0;

static BOOLEAN bVisibleTopOnly=FALSE;
```
163

```
//-------------------------------------------------------------
// Local definitions
//-------------------------------------------------------------
#define NAME              "DDExample1"
#define TITLE             "Direct Draw Example 1"


//-------------------------------------------------------------
// Global data
//-------------------------------------------------------------
LPDIRECTDRAW4            g_pDD = NULL;       // DirectDraw object
LPDIRECTDRAWSURFACE4 g_pDDSPrimary = NULL;// DirectDraw primary surface
LPDIRECTDRAWSURFACE4 g_pDDSBack = NULL;  // DirectDraw back surface
BOOL                    g_bActive = FALSE;   // Is application active?
LPDIRECTDRAWPALETTE     g_pDDPal = NULL;    // The primary surface palette
//-------------------------------------------------------------
// Local data
//-------------------------------------------------------------
static char         szMsg[] = "Page Flipping Test: Press F12 to exit";
static char         szFrontMsg[] = "(F12 to quit) Buffer front";
static char         szBackMsg[] = "(F12 to quit) Buffer back";
static char         szBackground[] = "BACK";
static int          xhop = -1;              //flips the pole
static double       LPOLE=5.0;              //make it a global variable
// Pole variable computations; new values replace old values
void computeAngle(double *theta, double *thetaDot, double ax, double dt)
{
//double LPOLE;
double OMEGA2;
double MU;
double thetaNew, thetaDotNew,thetaDotDotCurrent;
double stheta,ctheta,ctheta2;
double coeffRest = 0.0;
double coeff_friction = 0.05;
double friction;
double sgn;
// modified may 2000
// LPOLE = 5.0;
//OMEGA2= 20;
MU = 0.3;
// old one OMEGA2=gravity/LPOLE;
OMEGA2=g_omega*g_omega;
// try friction
friction = -coeff_friction*(*thetaDot);
thetaNew = *theta+ *thetaDot*dt;
```

```
        if (abs(thetaNew) < THETA_CRIT ) {
                stheta=sin(*theta);
                ctheta=cos(*theta);
                ctheta2=ctheta*ctheta;
//              thetaDotDotCurrent=-0.75*ax*ctheta/LPOLE+0.75*OMEGA2*stheta;
                thetaDotDotCurrent=friction-
0.75*ax*ctheta/LPOLE+0.75*stheta*gravity/LPOLE;
                thetaDotNew=  *thetaDot +thetaDotDotCurrent*dt;
        } else {
                sgn = (*theta > 0?1.0:-1.0);
                thetaNew = (1+coeffRest)*THETA_CRIT*sgn-coeffRest*thetaNew;
                thetaDotNew = -coeffRest*(*thetaDot);
        }

        *theta = thetaNew;
        *thetaDot = thetaDotNew;
        // this is the fail marker
        g_fmark=10;              //default: good trial
        if (abs(*theta)>PI/2)
        {
                g_fmark=0;       //failmarker
        }

        if (*theta >= +PI) *theta -= TWOPI; // wrap
        if (*theta <= -PI) *theta += TWOPI;
}
/*****************************************************************
This is a callback function of olDaEnumBoards, it gets the strings
of the Open Layers board and attempts to initialize the board.
If successful, enumeration is halted.
*****************************************************************/
BOOL __export FAR PASCAL GetDriver(LPSTR lpszName, LPSTR lpszEntry,
LPARAM lParam)
//  lpszName =    board name
//  lpszEntry =   system.ini entry
//  lParam   =    optional user data
{
  LPBOARD lpboard = (LPBOARD)(LPVOID)lParam;

  /* fill in board strings */
  lstrcpyn(lpboard->name,lpszName,STRLEN);
  lstrcpyn(lpboard->entry,lpszEntry,STRLEN);

  /* try to open board */
```

```c
    lpboard->status = olDaInitialize(lpszName,&lpboard->hdrvr);
    if  (lpboard->hdrvr != NULL)
       return FALSE;        /* false to stop enumerating */
    else
       return TRUE;         /* true to continue       */
}
//-------------------------------------------------------------------
// Name: ReleaseAllObjects()
// Desc: Finished with all objects we use: release them
//-------------------------------------------------------------------
static void
ReleaseAllObjects(void)
{
   if (g_pDD != NULL)
   {
      if (g_pDDSPrimary != NULL)
      {
         g_pDDSPrimary->Release();
         g_pDDSPrimary = NULL;
      }
      g_pDD->Release();
      g_pDD = NULL;
   }
}




//-------------------------------------------------------------------
// Name: InitFail()
// Desc: This function is called if an initialization function fails
//-------------------------------------------------------------------
HRESULT
InitFail(HWND hWnd, HRESULT hRet, LPCTSTR szError,...)
{
   char              szBuff[128];
   va_list           vl;
   va_start(vl, szError);
   vsprintf(szBuff, szError, vl);
   ReleaseAllObjects();
   MessageBox(hWnd, szBuff, TITLE. MB_OK);
   DestroyWindow(hWnd);
   va_end(vl);
   return hRet;
}
```

```
// See A/D in Use message
//-------------------------------------------------------------------
// Name: UpdateFrame()
// Desc: Displays the proper text for the page
//-------------------------------------------------------------------
static int ptop = -1;
static int lhop = -1;
static void
UpdateFrame(HWND hWnd, BOOLEAN bMonitorData)
{
    HDC             hdc;
    DDBLTFX         ddbltfx;
    RECT            rc;
        POINT           poleTop;
        static BOOLEAN bkFlag=TRUE;

    // Use the blter to do a color fill to clear the back buffer

//      if (bkFlag) {
    ZeroMemory(&ddbltfx, sizeof(ddbltfx));
    ddbltfx.dwSize = sizeof(ddbltfx);
    ddbltfx.dwFillColor = 0;
    g_pDDSBack->Blt(NULL, NULL, NULL, DDBLT_COLORFILL | DDBLT_WAIT,
&ddbltfx);
//      bkFlag=FALSE;
//      }

                if (g_pDDSBack->GetDC(&hdc)  == DD_OK) // Get handle to device
context
                {
                        SetBkColor(hdc, RGB(100, 0, 255));
                        SetTextColor(hdc, RGB(255, 255, 0));
                        GetClientRect(hWnd, &rc);
                        /* Draw track */
        SelectObject(hdc,hBrushTrack);
                        SetBkColor(hdc,TRANSPARENT);
                    if (ptop==1) // normal
                        {
                        //go beyond the track
                        g_cartNow.x=(g_cartNow.x * 2)-500;
                        Rectangle(hdc,TRACK_XLOW,TRACK_YHI
,TRACK_XHI,TRACK_YLOW);
                        DeleteObject(SelectObject(hdc,hBrushTrack));
/*
```

```
                // for no cart movement
                poleTop.x= (int) (505+500*sin(g_theta));
                poleTop.y= (int) (530+500*cos(g_theta));
*/

                // for normal
                poleTop.x=                                              (int)
(g_cartNow.x+VISIBLE_POLE_LENGTH*sin(g_theta));
                poleTop.y=              (int)          (CART_PIVOTY-
VISIBLE_POLE_LENGTH*ptop*cos(g_theta));
                // this draws a y axis crosshair
                /*      SelectObject(hdc,hPenPole);
                        MoveToEx (hdc, g_cartNow.x, 0, NULL) ;
                        LineTo(hdc,g_cartNow.x,760);
                        DeleteObject(SelectObject(hdc,hPenPole));
*/

                if (!bVisibleTopOnly){      /* Draw Cart & Pole */
                SelectObject(hdc,hBrushCart);

                //for normal
                Rectangle(hdc,g_cartNow.x-CART_LENGTH,CART_PIVOTY
,g_cartNow.x+CART_LENGTH,TRACK_YHI);
                //for no x base cart movement
//              Rectangle(hdc,500,530 ,510,550);
                DeleteObject(SelectObject(hdc,hBrushCart));
                SelectObject(hdc,hPenPole);
                // for no x
//              MoveToEx (hdc, 505, 530, NULL) ;

                //for normal
                MoveToEx (hdc, g_cartNow.x, CART_PIVOTY, NULL) :
                // for reversal
//              MoveToEx (hdc, g_cartNow.x, 550, NULL) ;
                LineTo(hdc,poleTop.x,poleTop.y);
                DeleteObject(SelectObject(hdc,hPenPole));
                } else{ /* Draw Top & Bottom circles only-here only top */
                SelectObject(hdc,hBrushCart);
                MoveToEx (hdc, g_cartNow.x, CART_PIVOTY, NULL) :
                //Ellipse(hdc,g_cartNow.x-7,530-7,g_cartNow.x+7,530+7):
                //above draws the cart dot (need to change both of these)
                Ellipse(hdc,poleTop.x-7,poleTop.y-7,poleTop.x+7,poleTop.y+7);
                DeleteObject(SelectObject(hdc,hBrushCart));
                }
                }
                else  // inverted and horizontally flipped
```

```
{
//go beyond the track
g_cartNow.x=(g_cartNow.x * 2)-500;
Rectangle(hdc.TRACK_XLOW.TRACK_YHI_INV
,TRACK_XHI,TRACK_YLOW_INV);
          DeleteObject(SelectObject(hdc,hBrushTrack));


// for normal
poleTop.x=                                              (int)
(g_cartNow.x+VISIBLE_POLE_LENGTH*sin(g_theta));
          poleTop.y=          (int)          (CART_PIVOTY_INV-
VISIBLE_POLE_LENGTH*ptop*cos(g_theta));
          // this draws a y axis crosshair
/*        SelectObject(hdc,hPenPole);
          MoveToEx (hdc, g_cartNow.x, 0, NULL) ;
          LineTo(hdc,g_cartNow.x,760);
          DeleteObject(SelectObject(hdc,hPenPole));
*/

          if (!bVisibleTopOnly){        /* Draw Cart & Pole */
          SelectObject(hdc,hBrushCart);
          //for normal
          Rectangle(hdc,g_cartNow.x-
CART_LENGTH.TRACK_YLOW_INV
.g_cartNow.x+CART_LENGTH,CART_PIVOTY_INV);
          //for no x base cart movement
//        Rectangle(hdc.500.530 .510.550);
          DeleteObject(SelectObject(hdc,hBrushCart));
          SelectObject(hdc,hPenPole);
          // for no x
//        MoveToEx (hdc, 505, 530, NULL) ;
          //for normal
          MoveToEx (hdc, g_cartNow.x, CART_PIVOTY_INV, NULL) ;
          // for reversal
//        MoveToEx (hdc, g_cartNow.x, 550, NULL) ;
          LineTo(hdc,poleTop.x,poleTop.y);
          DeleteObject(SelectObject(hdc,hPenPole));
          } else{ /* Draw Top & Bottom circles only-here only top */
          SelectObject(hdc,hBrushCart);
          MoveToEx (hdc. g_cartNow.x, CART_PIVOTY_INV, NULL) ;
          //Ellipse(hdc,g_cartNow.x-7,530-7,g_cartNow.x+7,530+7);
          //the above does the cart dot
          Ellipse(hdc.poleTop.x-7,poleTop.y-7.poleTop.x+7,poleTop.y+7);
          DeleteObject(SelectObject(hdc,hBrushCart));
          }
```

169

```
                              }
                              if (bMonitorData) { // Press 'm' or 'M' to (in)activate this
//                            TextOut(hdc,20,20,str,wsprintf(str,"CartPosition:
%ld",g_cartNow.x));
//                            TextOut(hdc,20,40,str,sprintf(str,"PoleAngle:
%.0f",g_theta*RADIAN_TO_DEGREE));
                              TextOut(hdc,20, 60,str,wsprintf(str,"Sample: %ld",gu_iCount));
                              TextOut(hdc,20,80,str,wsprintf(str,"MaxSamples:
%ld",MAXPOINTS));
//                            TextOut(hdc,20,100,str,wsprintf(str,"DeltaTime: %ld",deltatime));
//                            TextOut(hdc,20,120,str,wsprintf(str,"MinDeltaTime:
%ld",mindeltatime));
//                            TextOut(hdc,20,140,str,wsprintf(str,"MaxDeltaTime:
%ld",maxdeltatime));
                              //TextOut(hdc,20,160,str,sprintf(str,"PoleVelocity:
%.0f",thetaDot*RADIAN_TO_DEGREE));
                              TextOut(hdc,20,180,str,sprintf(str,"Reading(gf_volts) @ Channel
0: %.4f",gf_volts));
//                            TextOut(hdc,20,200,str,sprintf(str,"InitialPoleAngle:
%.0f",x_theta*RADIAN_TO_DEGREE));
                              //TextOut(hdc,20,220,str,sprintf(str,"InitialPoleVelocity:
%.0f",x_thetaDot*RADIAN_TO_DEGREE));

   // declaration of g-omega2, omega2 and the case q/w
//                            TextOut(hdc,20,280,str,sprintf(str,"g_fmarker: %ld",g_fmark));

//                            TextOut(hdc,20,260,str,sprintf(str," pole length: %.4f",LPOLE));
                              TextOut(hdc,20,220,str,sprintf(str,"g_offset                volts:
%.4f",g_offsetvolts));
//                            TextOut(hdc,20,240,str,sprintf(str,"Gain ( Accel units / Volt ):
%.0f",XSCALE_FACTOR));
//                            TextOut(hdc,20,700,str,wsprintf(str,"C:Counter    R:Random   IC
U:Upright IC F:Freeze I/D:Inc/Dec Gain  V:Pole/Dots M:Monitor  S:Save P/O:perturb
up/down Q/W:Pole len flip/down ESC or F12: Quit",0));
//         TextOut(hdc,20,740,str,wsprintf(str,"X: flippit  A/Z: Manual offset up/down
G:resample offset  H: horizontal flip ",0));
                              }
                              g_pDDSBack->ReleaseDC(hdc);    // Release handle to device
context
                  }
}
//-----------------------------------------------------------------------
// Name: WindowProc()
// Desc: The Main Window Procedure
```

170

```
//-----------------------------------------------------------------------
long FAR PASCAL
WindowProc(HWND hWnd, UINT message. WPARAM wParam, LPARAM lParam)
{
    HRESULT              hRet;

    /* A/D and drawing declarations */
    long value;
    ULNG samples;
//      TDATA TrialData;
        static BOOLEAN bFreeze = FALSE;
    static long iCount = 0;
    static long iCountOld = 0;
    static float volts;
        static float newvolts;
        static float sumvolts;
    static POINT cartNow, cart[MAXPOINTS];
    static DOUBLE theta = 0.0;
    static DOUBLE thetaDot = 0.0;
    static DOUBLE ax;
    DOUBLE DELTA_T = 1.0/50.0;
        DOUBLE volts_temp;
        static BOOLEAN bStartAD=TRUE;
        LONG size=5;
        static long kkk=0;
    static LONG oldmtime;
        LONG newmtime;
        //static LONG deltatime;

        static BOOLEAN bMonitorData = TRUE;
        static BOOLEAN bResetCount = FALSE;
    static BOOLEAN take_offset = TRUE;
        static BOOLEAN enoughpoints = FALSE;
    switch (message)
    {
      case WM_ACTIVATEAPP:
        // Pause if minimized or not the top window
        g_bActive = (wParam == WA_ACTIVE) || (wParam == WA_CLICKACTIVE);
        return 0L;
      case WM_DESTROY:
        // Clean up and close the app
        ReleaseAllObjects();
        PostQuitMessage(0);
        return 0L;
```

171

```c
       case OLDA_WM_BUFFER_REUSED:   /* message: buffer reused */
                        break;
       case OLDA_WM_BUFFER_DONE:    /* message: buffer done */
                        CHECKERROR (olDaGetBuffer(board.hdass, &board.hbuf));   /*
get buffer off done list */
              if (board.hbuf != NULL){                           /* if there is a buffer */
                        newmtime = GetMessageTime();
          deltatime=newmtime-oldmtime;
                        oldmtime=newmtime;
                        if (iCount>2) {
                        maxdeltatime=max(maxdeltatime,deltatime);
                        mindeltatime=min(mindeltatime,deltatime);
                        }
              CLOSEONERROR (olDmGetMaxSamples(board.hbuf,&samples));   /* get max
samples in input buffer */
              value = board.lpbuf[samples-1];                   /* get last sample in buffer */
              CHECKERROR (olDaPutBuffer(board.hdass, board.hbuf));   /* put buffer back to
ready list */


              /* convert value to volts */
              if (guEncoding != OL_ENC_BINARY) {
                value ^= 1L << (guResolution-1)  ;  /* convert to offset binary by inverting sign
bit */

                value &= (1 L << guResolution) - 1;  /* zero upper bits */
              }
              volts = ((float)gdRange)/(1L<<guResolution) * value + (float)gdMin;
//                        volts -= g_offsetvolts;
                        if (take_offset==TRUE)
                        {
                                g_offsetvolts = 0.0;
                                sumvolts += volts;
                   if (++kkk == KKK_MAX-1)
                        {
                                g_offsetvolts = sumvolts/KKK_MAX;
                                take_offset = FALSE;
                                kkk = 0;
                        }
                        }
                        volts -= g_offsetvolts;
                volts_temp = 100.0*volts;
                if (volts_temp <0) newvolts = ceil(volts_temp);
                if (volts_temp >0) newvolts = floor(volts_temp);
                newvolts = 0.01*newvolts;
                // note the new volts
```

```
                    ax = XSCALE_FACTOR*newvolts;  // acceleration
                    gf_volts=newvolts;
                    if (bResetCount==TRUE)    // see if Counter is to be reset
                            {
                            bResetCount=FALSE;
                            iCount=1;
                            maxdeltatime=0;
                            mindeltatime=100;


                    }
// perturbation

                    if ((iCount) == perturb(I)) {
                            if (g_theta>=0.0)// make this <= in hflip
                                    {
                                    x_thetaDot=thetaDot = .30;
                                    //g_fmark=5;
//marker

                                    }
                                    else
                                    {
                                    x_thetaDot=thetaDot = -.30;
                                    //g_fmark=5;
//marker

                                    }
                    }

/*                  if ((iCount % 200) == 0) {  // change the pole length
                            lhop*=-1;                //switches pole length
                            if (lhop>=0.0)           // make this <= in hflip
                                    {
                                            LPOLE=2.5;         //decreases pole len
                            // g_fmark=8;
//marker

                                    }
                                    else
                                    {
                                            LPOLE=5.0;         //original pole length
                                            //g_fmark=10;
//marker

                                    }
                    }
*/
```

173

```
                        if (++iCount>MAXPOINTS) iCount=1;        /* increment sample
count    */
            GetCursorPos(&cartNow);                    /* get screen mouse position */
            cart[iCount]=cartNow;                      /* save for later file write */
        if (!bFreeze) computeAngle(&theta,&thetaDot,ax,DELTA_T);  /* compute pole
variables    */
                        g_cartNow=cartNow;  // save the ff. in global variables
                        g_theta=theta;
                        gu_iCount=iCount;
                        if (xhop==1)
                        {
                        ///horizontal flip
                        g_cartNow.x=1280-g_cartNow.x;
                            g_theta=-g_theta;
                            ax=-ax;
                        }
                        //we assign these variables to the structure
                        TrialData[iCount].ccNow=(long(g_cartNow.x));
                        TrialData[iCount].tthet=(long(g_theta*1000));
                        TrialData[iCount].tthetdot=(long(thetaDot*1000));
                        TrialData[iCount].aax=(long(ax*1000));
                        TrialData[iCount].fmark=g_fmark;
        /*testbed

                        TrialData[iCount].ccNow=(long)1;
                        TrialData[iCount].tthet=(long)2.0;
                        TrialData[iCount].tthetdot=(long)3.0;
                        TrialData[iCount].aax=(long)4.0;
                        TrialData[iCount].fmark=(long)0;

*/

        if (g_bActive)                               // Direct Draw flip
            {
            UpdateFrame(hWnd,bMonitorData);
            while (TRUE)
            {
              hRet = g_pDDSPrimary->Flip(NULL, 0);
              if (hRet == DD_OK)
                 break;
              if (hRet == DDERR_SURFACELOST)
              {
                hRet = g_pDDSPrimary->Restore();
                if (hRet != DD_OK)
                   break;
              }
            }
```

```
            if (hRet != DDERR_WASSTILLDRAWING)
                break;
        }// End Direct Draw flip
    }
    break;


    }
    return (TRUE);


        case WM_RBUTTONDOWN:
                /* start conversion - must use this; there is error, though!!!!! */

                if (bStartAD) {
                CLOSEONERROR (olDaStart(board.hdass));
                bStartAD=!bStartAD;
                }
        break;
case WM_KEYDOWN:
    // Handle any non-accelerated key commands
    switch (wParam)  // Keyboard options
    {
                case 'x':
                case 'X':                // flips the pole!
                        ptop*=-1;
                        break;


                case 'h':
                case 'H':                // flips the pole!
                        xhop*=-1;
                        break;
                case 'p':
                case 'P':
                        // add the perturbation here
                        // make it directional dependent
                        if (g_theta>=0.0)
                        {
                        x_thetaDot=thetaDot = -.50;
                        //g_fmark=6;
//marker

                        }
                        else
                        {
                        x_thetaDot=thetaDot = .50;
```

```
                                  //g_fmark=6;
//marker

                                  }
                                  break;
                        case 'o':
                        case 'O':
                                  // add the perturbation here
                                  // make it directional dependent
                                  if (g_theta>=0.0)
                                  {
                                  x_thetaDot=thetaDot = .50;
                                  //g_fmark=7;
//marker

                                  }
                                  else
                                  {
                                  x_thetaDot=thetaDot = -.50;
                                  //g_fmark=7;
//marker

                                  }
                                  break;

                        case 'g':
                        case 'G':
                                  take_offset = TRUE;
                                  kkk=0.0;
g_offsetvolts=0.0;
                                  sumvolts = 0.0;
                                  break;
                        case 'a':   // give a little offset
                                  g_offsetvolts+=0.0001;
                                  break;
                        case 'A':   //  give a bigger offset
                                  g_offsetvolts+=0.001;
                                  break;
                        case 'z':   //  give a little offset
                                  g_offsetvolts-=0.0001;
                                  break;
                        case 'Z':   //  give a bigger offset
                                  g_offsetvolts-=0.001;
                                  break;

                        case 'i':
                        case 'I':
```

176

```
                              XSCALE_FACTOR +=50;    // Increase software
gain of input voltage

                        break;
                case 'd':
                case 'D':
                              XSCALE_FACTOR -=50;    // Decrease software
gain of input voltage

                        break;
                case 'q':
                case 'Q':
                        lhop*=-1;              //switches pole length
                        break;
                case 'w':
                case 'W':
                        LPOLE-=0.1;            //decreases pole length
                        break;


                case 'r':
                case 'R':             // Random initial angle only
                        x_theta=g_theta=theta=((double)(RAND_MAX/2-
rand()))/((double)RAND_MAX);
                        x_thetaDot=thetaDot= 0;    // Note: Initial pole
velocity always zero

                        // make this a non-zero velocity
                        if (g_theta>=0.0)
                        {
                        x_thetaDot=thetaDot = .10;
                        g_fmark=0;
//marker

                        }
                        else
                        {
                        x_thetaDot=thetaDot = -.10;
                        g_fmark=0;
//marker

                        }
                        bFreeze=TRUE;
                        g_fmark=0;
//marker

                        break;

                case 'u':
                case 'U':
                        x_theta=g_theta=theta =0.0; // Vertical initial angle


                                177
```

```cpp
                                    x_thetaDot=thetaDot = 0.0;
                                    g_fmark=0;
            //marker
                                    bFreeze=TRUE;
                                    break;
                        case 'v':
                        case 'V':
                                    bVisibleTopOnly=!bVisibleTopOnly;        //
                                    break;

                        case 'm':
                        case 'M':
                                    bMonitorData = !bMonitorData; // Display numeric
data
                                    break;
                        case 'c':
                        case 'C':
                                    bResetCount = !bResetCount;  // Reset counters
                                    break;

                        case 'f':
                        case 'F':
                                    {
                                    bFreeze=!bFreeze; // Freeze pole angle but not cart
position
                                    g_fmark=0;
            //marker
                                    }
                                    break;
            case VK_ESCAPE:
            case VK_F12:
                PostMessage(hWnd, WM_CLOSE, 0, 0);  // Quit the application
                return 0L;
            }
            break;
        case WM_SETCURSOR:
            // Turn off the cursor since this is a full-screen app
            SetCursor(NULL);
            return TRUE;

    }
    return DefWindowProc(hWnd, message, wParam, lParam)
}
//------------------------------------------------------------------------
```

```
// Name: InitApp()
// Desc: Do work required for every instance of the application:
//       Create the window, initialize data
//-----------------------------------------------------------------
static HRESULT
InitApp(HINSTANCE hInstance, int nCmdShow)
{
    HWND                hWnd;
    WNDCLASS            wc;
    DDSURFACEDESC2          ddsd;
    DDSCAPS2            ddscaps;
    HRESULT            hRet;
    LPDIRECTDRAW           pDD;
        /* A/D related variables */
    DBL  freq;
    UINT size,dma,gainsup;
    int i;
/*****************************************************************/
/*  Generate (global) brushes for fill and pen for drawing lines */
/*****************************************************************/
    hBrushCart = CreateSolidBrush(RGB(0,0,255));
    hBrushPole = CreateSolidBrush(RGB(0,255,200));
    hBrushTrack = CreateHatchBrush (HS_BDIAGONAL,RGB(255,0,0) );
        hPenPole = CreatePen(PS_INSIDEFRAME,3,RGB(255,0,0));
/*****************************************************************/
        srand( (unsigned)time( NULL ) ); // seed randomizer
    // Set up and register window class
    wc.style = CS_HREDRAW | CS_VREDRAW;
    wc.lpfnWndProc = WindowProc;
    wc.cbClsExtra = 0;
    wc.cbWndExtra = 0;
    wc.hInstance = hInstance;
    wc.hIcon = LoadIcon(hInstance, MAKEINTRESOURCE(IDI_MAIN_ICON));
    wc.hCursor = LoadCursor(NULL, IDC_ARROW);
    wc.hbrBackground = (HBRUSH )GetStockObject(BLACK_BRUSH);
    wc.lpszMenuName = NAME;
    wc.lpszClassName = NAME;
    RegisterClass(&wc);
    // Create a window
    hWnd = CreateWindowEx(WS_EX_TOPMOST,
                NAME,
                TITLE,
                WS_POPUP,
                0,
```

```
                    0,
                    GetSystemMetrics(SM_CXSCREEN),
                    GetSystemMetrics(SM_CYSCREEN),
                    NULL,
                    NULL,
                    hInstance,
                    NULL);
        if (!hWnd)
            return FALSE;
        ShowWindow(hWnd, nCmdShow);
        UpdateWindow(hWnd);
        SetFocus(hWnd);
        /* Get first available Open Layers board */
        /* Note the forced typecasting of GetDriver */
        board.hdrvr = NULL;
        CHECKERROR                 (olDaEnumBoards((int              (__stdcall
    *)(void))GetDriver,(LPARAM)(LPBOARD)&board));
        /* check for error within callback function */
        CHECKERROR (board.status);
        /* check for NULL driver handle - means no boards */
        if (board.hdrvr == NULL){
            MessageBox(HWND_DESKTOP, " No Open Layer boards!!!", "Error",
                MB_ICONEXCLAMATION | MB_OK);
            return ((UINT)NULL);
        }


        /* get handle to A/D sub system */
        CHECKERROR (olDaGetDASS(board.hdrvr,OLSS_AD,0,&board.hdass)):
        /* set up the ADC - multiple wrap so we can get buffer reused window messagess */
        CHECKERROR
    (olDaGetSSCapsEx(board.hdass,OLSSCE_MAXTHROUGHPUT,&freq));
        CHECKERROR (olDaGetSSCaps(board.hdass,OLSSC_NUMDMACHANS,&dma));
        CHECKERROR
    (olDaGetSSCaps(board.hdass,OLSSC_SUP_PROGRAMGAIN,&gainsup));
        dma  = min (1, dma);          /* try for one dma channel  */
        freq = min (1000.0, freq);     /* try for 1000hz throughput */
        CHECKERROR (olDaSetDataFlow(board.hdass,OL_DF_CONTINUOUS));
        CHECKERROR (olDaSetWrapMode(board.hdass,OL_WRP_MULTIPLE));
        CHECKERROR (olDaSetClockFrequency(board.hdass,freq));
        CHECKERROR (olDaSetDmaUsage(board.hdass,dma));
        CHECKERROR (olDaSetChannelListEntry(board.hdass,0,guChannel));
        /* only set the gain if the board supports it!!! */
        if (gainsup)
            CHECKERROR (olDaSetGainListEntry(board.hdass,0,gdGain));
```

```
CHECKERROR (olDaSetChannelListSize(board.hdass,1));
CHECKERROR (olDaConfig(board.hdass));
/* get sub system information for code/volts conversion */
CHECKERROR (olDaGetRange(board.hdass,&gdMax,&gdMin)):
CHECKERROR (olDaGetEncoding(board.hdass,&guEncoding));
CHECKERROR (olDaGetResolution(board.hdass,&guResolution)):
gdRange = gdMax - gdMin;
/* set window that will receive messages */
CLOSEONERROR (olDaSetWndHandle(board.hdass, hWnd,(UINT)NULL));
CLOSEONERROR (olDaConfig(board.hdass)):
size = (UINT)freq/100;    /* tenth second buffer */
/* Allocate 3 input buffers. Put the buffer to the ADC */
for (i=0;i<2;i++){
   CHECKERROR (olDmCallocBuffer(0,0,(ULNG) size,2,&board.hbuf)):
   CHECKERROR (olDmGetBufferPtr(board.hbuf,(LPVOID FAR*)&board.lpbuf));
   CHECKERROR (olDaPutBuffer(board.hdass, board.hbuf));
}
/* start conversion - must use this; there is error!!!!! */
//  CLOSEONERROR (olDaStart(board.hdass));
//////////////////////////////////////////////////////////////////////
// Create the main DirectDraw object
//////////////////////////////////////////////////////////////////////
hRet = DirectDrawCreate(NULL, &pDD, NULL);
if (hRet != DD_OK)
    return InitFail(hWnd, hRet, "DirectDrawCreate FAILED");
// Fetch DirectDraw4 interface
hRet = pDD->QueryInterface(IID_IDirectDraw4, (LPVOID *) & g_pDD);
if (hRet != DD_OK)
    return InitFail(hWnd, hRet, "QueryInterface FAILED");
// Get exclusive mode
hRet    =     g_pDD->SetCooperativeLevel(hWnd,     DDSCL_EXCLUSIVE    |
DDSCL_FULLSCREEN);
if (hRet != DD_OK)
    return InitFail(hWnd, hRet, "SetCooperativeLevel FAILED"):
// Set the video mode to 800x600x16
//  hRet = g_pDD->SetDisplayMode(1600, 1200, 8, 0, 0);
hRet = g_pDD->SetDisplayMode(1280, 1024, 8, 0, 0);
if (hRet != DD_OK)
    return InitFail(hWnd, hRet, "SetDisplayMode FAILED");
// Create the primary surface with 1 back buffer
ZeroMemory(&ddsd, sizeof(ddsd));
ddsd.dwSize = sizeof(ddsd);
ddsd.dwFlags = DDSD_CAPS | DDSD_BACKBUFFERCOUNT:
```

```
        ddsd.ddsCaps.dwCaps = DDSCAPS_PRIMARYSURFACE |
            DDSCAPS_FLIP |
            DDSCAPS_COMPLEX;
        ddsd.dwBackBufferCount = 1;
        hRet = g_pDD->CreateSurface(&ddsd, &g_pDDSPrimary, NULL);
        if (hRet != DD_OK)
            return InitFail(hWnd, hRet, "CreateSurface FAILED");
        // Get a pointer to the back buffer
        ddscaps.dwCaps = DDSCAPS_BACKBUFFER;
        hRet = g_pDDSPrimary->GetAttachedSurface(&ddscaps, &g_pDDSBack);
        if (hRet != DD_OK)
            return InitFail(hWnd, hRet, "GetAttachedSurface FAILED");
        // Create and set the palette
            /*
        g_pDDPal = DDLoadPalette(g_pDD, szBackground);
        if (g_pDDPal == NULL)
            return InitFail(hWnd, hRet, "DDLoadPalette FAILED");
        hRet = g_pDDSPrimary->SetPalette(g_pDDPal);
        if (hRet != DD_OK)
            return InitFail(hWnd, hRet, "SetPalette FAILED");
        // Load a bitmap into the back buffer.
        hRet = DDReLoadBitmap(g_pDDSBack, szBackground);
        if (hRet != DD_OK)
            return InitFail(hWnd, hRet, "DDReLoadBitmap FAILED");
            */
        return DD_OK;
}
//-----------------------------------------------------------------------
// Name: WinMain()
// Desc: Initialization, message loop
//-----------------------------------------------------------------------
int PASCAL
WinMain(HINSTANCE hInstance,
        HINSTANCE hPrevInstance,
        LPSTR lpCmdLine,
        int nCmdShow)
{
    MSG                 msg;
    if (InitApp(hInstance, nCmdShow) != DD_OK)
        return FALSE;
    while (GetMessage(&msg, NULL, 0, 0))
    {
        TranslateMessage(&msg);
        DispatchMessage(&msg);
```

182

```
    }
// now we do a quit and save here
                        fp = fopen("f:\\subvp10.dat","wb+");
                        fwrite(&TrialData,sizeof(TDATA),MAXPOINTS,fp);
                        fclose(fp);


        // to end. release the subsystem and the board
    CHECKERROR (olDaReleaseDASS(board.hdass));
    CHECKERROR (olDaTerminate(board.hdrvr));
    return msg.wParam;
}
```

8.3 Appendix C: MatlabAnalysis Code

```matlab
function [corres] = tuchk8(tau,time,omega,vel,tdot,theta,tauf,tfdot)
%% This program will perform the correlations between the perceptual variables and the
%% period length of x dot
%%%%%%%%%%%%%%%%%%%%%%%%%%%%%%%%
corres=ones(1,14);              % 12 colums for delta,omega,vel,tau,taudot,theta etc
% corres=corres*99;             % put in dummy variable of 99
%%%%%%%%%%%%%%%%%%%%%%%%%%%%%%%%%%%%%pick   the   comega   zero   crossings
[aa]=zeroc(omega,1);            % zero crossing the point before the croxx
[bb]=zeroc(omega,-1);          % zero crossing the point after the cross
%%%%%%%%%%%%%%%%%%%%%%%%%%%%
for i = 1:length(aa)-1
        %plot(tau(aa(i):bb(i+1)));
        somega=(omega(aa(i):bb(i+1)));     % cut to 1 piece of comega
        svel=(vel(aa(i):bb(i+1)));          % cut to 1 piece of cvel
        stime=(time(aa(i):bb(i+1)));        % cut to 1 piece of ctime
        stau=(tau(aa(i):bb(i+1)));          % cut to 1 piece of ctau
        stdot=(tdot(aa(i):bb(i+1)));        % cut to 1 piece of cttdot
        stheta=(theta(aa(i):bb(i+1)));      % cut to 1 piece of ctheta
        stauf=(tauf(aa(i):bb(i+1)));        % cut to 1 piece of ctauf
        stfdot=(tfdot(aa(i):bb(i+1)));      % cut to 1 piece of ctfdotf
spo1=find(somega==max(somega)); spo1=spo1(1);% find max of timeseries of somega
if (spo1==1 | spo1==length(aa(i):bb(i+1)))        % if this max is at either end
        spo1=find(somega==min(somega)); spo1=spo1(1);  % use the min of somega and
    svo1=find(svel==max(svel));    svo1=svo1(1);% max of svel
else
        svo1=find(svel==min(svel));svo1=svo1(1);  % else use max of somega and min
end                                                  % of svel
        %%%%%%%%%%%%%%%%%%%
        %              this is where we find the period half-lengths from aa(i) to somega
        %              and then from somega to bb(i+1)
leader=svo1;
tailer=length(svel)-svo1;
%%%%%%%%%%%%%%%%%%%%%
    sexcor=xcorr(somega,svel);                % compute the cross correlation
    medpt=(length(sexcor)-1)/2;               % find the zero lag point
    sexmm=find(sexcor==min(sexcor));          % find the min of the xcor
curve
        sexmm=sexmm(1);                        % we are antiphase here..
else

                                               % this would be the max pt
    sexmm2=find(sexcor==max(sexcor));          % this is in case it's not
antiphase
```

```
        sexmm2=sexmm2(1);
        delp(i)=sexmm-medpt;                        % delta offset

        if (sexmm==1|sexmm==length(sexcor))         % if the curves aren't antiphase
                                                    % and the peak is not in the middle
                                                    % of the sexcor but at the ends
                                                    % then use the max of sexcor as
sexmm2
            delp(i)=sexmm2-medpt;
        end
                    omept=spo1;         % time of max or min of omega
                    velpt=svo1;         % time of max or min vel
                    ompt(i)=somega(spo1);     % amplitude of somega at its extrema pt (1)
                    vlpt(i)=svel(svo1);   % amplitude of svel at the extrema pt       (2)
                    tupt(i)=stau(svo1);   % amplitude of stau at the hand extrema pt  (3)
                    tdpt(i)=stdot(svo1);  % amplitude of stdot at the hand extrema pt (4)
                    thpt(i)=stheta(svo1); % amplitude of stheta at the hand extrema pt(5)
                    ompt2(i)=somega(svo1);   % amp of somega at the cvel extrema pt (6)
                                          % delta via xcorr                           (7)
                    tfpt(i)=stauf(svo1);  % amp of stauf at hand extrema pt           (8)
                    ftdpt(i)=stfdot(svo1); % amp of stfdot at hand extrema pt         (9)
% now place values in the array
                    corres(i,1)=ompt(i);
                    corres(i.2)=vlpt(i);
                    corres(i,3)=tupt(i);
                    corres(i.4)=tdpt(i);
                    corres(i.5)=thpt(i);
                    corres(i,6)=ompt2(i);
                    corres(i,7)=delp(i);    % delta via xcorr
                    corres(i,8)=tfpt(i);
                    corres(i,9)=ftdpt(i);
                    corres(i,13)=leader;
                    corres(i,14)=tailer;
%                                           #10 R/A/O    timing information
%                                           #11          tau type
%                                           #12 will be the cuplet type
%                                           # 13 will be (leader) the time from the zero crossing
to the comega point
%                                           # 14 will be (tailer) the time from the comega point
to the next zero cross

                    corres(i,12)=0;         % this is the default (not the last cuplet) to fill the
last
                    corres(i,13)=10;        % this is default cuplet type (to fill the last
```

185

```
%%%%%%%%%%% classification  of timing (r/a/o) %%%%%
%        all work and no play makes pat a dull boy        %%
%%%%%%%%%%%%%%%%%%%%%%%%%%%%%%%%%%%%%%%
if (delp(i)<0)
        corres(i,10)=1;                    %anticipation  = 1
else if (delp(i)>0)
                corres(i,10)=2;            %reaction    = 2
        else
                corres(i,10)=3;            %right on     = 3
        end
end


%%%%%%%%%%%%   classification of tau type

if tau(aa(i))*tau(bb(i+1))<0
        corres(i,11)=1;                    %sigmoid, tau cross
else
    if tau(aa(i))<0
        corres(i,11)=2;                    %inverted u succ brake
    else
        corres(i,11)=3;                    %u unsucc cross
    end
end
end
%%%%%%%%%%%%%%%%%%%%%%%%%%%%%


% Intro for the tau type. gcycs(i,11)
% legend sigmoid, tau cross = 1
% old legend inverted u =2
% vlegend u =3
% enter the reaction, anticipation  gcycs(i,10)
% joint anticipation = 1
% under reaction = 2
% synchro = 3
% t tests of the values
% indicate the significance of
% null results
% entered previously
babbl=length(corres(:,1))-1;
for i = 1 : babbl

if i==babbl
```

186

```
        corres(i,12)=1;      % this means it's the last cuplet
end

    if ((corres(i,11)==1)&(corres(i+1,11)==1))          % (1) if we get a sig + sig
            corres(i,12)=1;         % cuplet tautype 1
    elseif ((corres(i,11)==1)&(corres(i+1,11)==2))      % (2) if we get a sig + inv U
            corres(i,12)=2;         % cuplet tautype 2
    elseif ((corres(i,11)==1)&(corres(i+1,11)==3))      % (3) if we get a sig +u
            corres(i,12)=3;         % cuplet tautype 3
    elseif ((corres(i,11)==2)&(corres(i+1,11)==1))      % (4) if we get a inv U + sig
            corres(i,12)=4;         % cuplet tautype 4
    elseif ((corres(i,11)==2)&(corres(i+1,11)==2))      % (5) if we get a inv U + inv
U
            corres(i,12)=5;         % cuplet tautype 5
    elseif ((corres(i,11)==2)&(corres(i+1,11)==3))      % (6) if we get a inv U + U
            corres(i,12)=6;         % cuplet tautype 6
    elseif ((corres(i,11)==3)&(corres(i+1,11)==1))      % (7) if we get a  U + sig
            corres(i,12)=7;         % cuplet tautype 7
    elseif ((corres(i,11)==3)&(corres(i+1,11)==2))      % (8) if we get a  U + inv U
            corres(i,12)=8;         % cuplet tautype 8
    elseif ((corres(i,11)==3)&(corres(i+1,11)==3))      % (9)if we get a  U + U
            corres(i,12)=9;         % cuplet tautype 9
    end
end
```

8.4 Curriculum Vitae

Patrick S. Foo
Center for Complex Systems and Brain Sciences
Florida Atlantic University
Boca Raton, FL 33431
telephone: 561-297-2230
E-mail: foo@walt.ccs.fau.edu

Educational Background:

Florida Atlantic University (Boca Raton, FL)   1995-2000

Ph.D. September 2000

Complex Systems and Brain Sciences,
Dr. J. A. S. Kelso, committee chair
Dr. Gonzalo de Guzman, Dr. Betty Tuller, & Dr. Armin Fuchs, committee
members

University of Colorado (Boulder, CO)   1992-1995

M.S. Kinesiology,
Dr. Stephen Wallace, advisor

University of California (Berkeley, CA)   1984-1989

B.A. Physical Education

Research Interests:

The elaboration and application of nonlinear dynamical systems theory to
understanding human behavior and its neural correlates. Current research addresses
functional stabilization of unstable systems, including its perceptual basis and the
coupling between action and perception. I am studying this both within and between
people, as well as in virtual experiments in which physical and informational variables
can be decomposed.

Research Experience:

Graduate Research Assistant, Human Brain and Behavior Laboratory,   1995-present
Dr. J. A. S. Kelso. Center for Complex Systems and Brain Sciences,
Florida Atlantic University, FL.

Research Skills:

Extensive experience in testing human subjects in laboratory and computer-controlled conditions, in particular the collection and analysis of kinematic and neuromuscular data using the WATSMART and OPTOTRAK infrared and A/D real-time motion analysis. Construction of custom apparatii to measure applied forces during stabilization, and of human/computer interfaces. Computer skills include experience in the C programming language and FORTAN. Experience using MATLAB, SAS, SPSS, EXCEL, Statview, as well as Microsoft Word and Powerpoint presentation packages. Familiar with graded exercise testing, max VO2 assessment, electromyographic (EMG), and electrocardiographic (EKG) analysis of humans.

Teaching Experience:

Instructor, University of Colorado, Boulder, CO   1995
Introductory Statistics and Research Methods, spring semester.

Graduate Teaching Assistant, University of Colorado, Boulder, CO   1992-1994
Introductory Statistics and Research Methods. Attended lectures,
conducted weekly review and discussion sections, wrote test questions and
graded exams.

Graduate Teaching Assistant, Florida Atlantic University,   1996
Boca Raton, FL
Proseminar in Complex Systems. Reviewed and summarized critiques
of weekly lectures by Professor Kelso. Assisted in preparation of
individual student presentations.

Informal Teaching Activities:
Tutored High School Chemistry, Algebra, and Biology. I have also tutored Statistics,

Research Design, and Exercise Physiology at the University level.

Awards and Fellowships:

Predoctoral Training Fellowship, National Institutes of Mental Health   1995-1997

Newell Doctoral Fellowship   1999-2000

Program in Complex Systems and Brain Sciences   1998
Departmental Achievement Award

Professional Memberships:

American Psychological Association
North American Society for Psychology of Sport and Physical Activity
Society for Neuroscience

Publications:

Foo, P., de Guzman, G. C., & Kelso, J. A. S. (in preparation). Intermanual and interpersonal stabilization of unstable fixed points.

Foo, P., Kelso, J. A. S., & de Guzman, G. C. (in preparation). Functional stabilization of virtual systems using time to balance information.

Foo, P., Kelso, J. A. S., & DeGuzman, G. C. (2000). Functional stabilization of unstable fixed points: human pole balancing using "time to balance" information. *Journal of Experimental Psychology: Human Perception and Performance. 4*, 1281-1297.

Fink, P.W., Foo, P., Jirsa, V.K., & Kelso, J.A.S. (in press). Local and global stabilization of coordination by sensory information. *Experimental Brain Research.*

Jirsa, V.K., Fink, P.W., Foo, P., & Kelso, J.A.S. (2000). Parametric stabilization of biological coordination: a theoretical model. *Journal of Biological Physics. 26*, 85-112.

Wallace, S.A., Weeks, D. L., & Foo, P. (2000). A dynamical systems approach to understanding reaching movements with a prosthetic arm. *Nonlinear Dynamics, Psychology, and Life Sciences. 4, 4*, 311-338.

Selected Abstracts (national and international meetings):

Foo, P., & Kelso, J. A. S. The Nature of Social Coordination in Stabilizing Unstable Systems: Two rains Versus One. (2000). *North American Society for the Psychology of Sport and Physical Activity Abstracts, 22*, S39.

Foo, P., Kelso, J. A. S., & de Guzman. G. C. (1999). Social coordination in functional stabilization of unstable fixed points. *Dynamical Neuroscience VII Abstracts, 7*, 41.

Fink, P. W., Kelso, J. A. S., Foo, P. & Jirsa, V. K. (1999). Parametric stabilization of rhythmic movements. *Dynamical Neuroscience VII Abstracts, 7*, 40.

Foo, P., & Kelso, J. A. S. Stabilizing unstable systems: kinematics of success and failure in an inverted pendulum task. (1999). *North American Society for the Psychology of Sport and Physical Activity Abstracts, 21*, S44.

de Guzman, G. C., Kelso, J. A. S., & Foo, P. (1999). Balance control of inherently unstable mechanical systems using visual information. *Society for Neuroscience Abstracts, 25,* 1294.

Foo, P. & Kelso, J. A. S. (1998). Learning how to stabilize unstable systems. *North American Society for the Psychology of Sport and Physical Activity Abstracts, 20,* S34.

Fink, P. W., Kelso, J. A. S., Jirsa, V., & Foo, P. (1998). Informational stabilization of bimanual finger coordination. *North American Society for the Psychology of Sport and Physical Activity Abstracts, 20,* S33.

Foo, P. & Kelso, J. A. S. (1997). Learning how to stabilize unstable systems: acquisition, transfer and retention in a one-dimensional inverted pendulum task. *North American Society for the Psychology of Sport and Physical Activity Abstracts, 19,* S52.

Foo, P., Kelso, J. A. S., & DeGuzman, G. C. (1997). Learning to stabilize unstable systems: Experiment and preliminary modeling. *Society for Neuroscience Abstracts, 23,* 203.

Anderson, E., Foo, P., Greene, L., & Wallace, S.A. (1995). Visual informational constraints underlying phase shifts in reaching and grasping movements. *North American Society for the Psychology of Sport and Physical Activity Abstracts, 17,* S22.

Wallace, S.A., Foo, P. & Weeks, D.L. (1995). Identifying stable patterns of coordination in an upper extremity artificial limb. *Society for Neuroscience Abstracts, 21,* 249.

Foo, P., Greene, L., Hollander, J., Irelan, C., Riley, M., Weeks, D. and Wallace, S.A. (1994). Characterizing reaching and grasping movements using a non-linear dynamical framework. *Dynamical Neuroscience II Abstracts,* 18.

Wallace, S.A., Greene, L. S., Graese, D. M., and Foo, P. (1994). Phase transitions toward preferred reaching and grasping patterns in adult humans. *Society for Neuroscience Abstracts, 20,* 853.

McCullagh, P., Meyer K., Bealmear, S., Foo, P., Geoffrion, S., Kleinman, T. & Maller, B. (1994). *The Influence of Correct and Learning Models and Feedback on Self-Efficacy and Acquisition of a Free-Weight Squat.* Paper presented at the annual meeting of the American Alliance for Health, Physical Education, Recreation and Dance, Denver, Colorado.

Master's Thesis:

Foo, P.S. (1995). *Phase attraction towards a preferred coordination pattern in a cyclical prehension task.* Unpublished Masters Thesis, University of Colorado, Boulder, CO.

References:

Dr. J. A. S. Kelso. Center for Complex Systems and Brain Sciences, 777 Glades Road, Florida Atlantic University, Boca Raton, FL 33431.
telephone: 561-297-2231   email: kelso@walt.ccs.fau.edu

Dr. Armin Fuchs. Center for Complex Systems and Brain Sciences, 777 Glades Road, Florida Atlantic University, Boca Raton, FL 33431.
telephone: 561-297-0125   email: fuchs@walt.ccs.fau.edu

Dr. Stephen Wallace. Department of Kinesiology, 1600 Holloway Avenue, San Francisco State University, San Francisco, CA, 94132.
telephone: 415-338-6984   email: saw@sfsu.edu